CHAPTER 4

Multilayer Perceptrons

ORGANIZATION OF THE CHAPTER

In this chapter, we study the many facets of the multilayer perceptron, which stands for a neural network with one or more hidden layers. After the introductory material presented in Section 4.1, the study proceeds as follows:

1. Sections 4.2 through 4.7 discuss matters relating to back-propagation learning. We begin with some preliminaries in Section 4.2 to pave the way for the derivation of the back-propagation algorithm. This section also includes a discussion of the credit-assignment problem. In Section 4.3, we describe two methods of learning: batch and on-line. In Section 4.4, we present a detailed derivation of the back-propagation algorithm, using the chain rule of calculus; we take a traditional approach in this derivation. In Section 4.5, we illustrate the use of the back-propagation algorithm by solving the XOR problem, an interesting problem that cannot be solved by Rosenblatt's perceptron. Section 4.6 presents some heuristics and practical guidelines for making the back-propagation algorithm perform better. Section 4.7 presents a pattern-classification experiment on the multilayer perceptron trained with the back-propagation algorithm.
2. Sections 4.8 and 4.9 deal with the error surface. In Section 4.8, we discuss the fundamental role of back-propagation learning in computing partial derivatives of a network-approximating function. We then discuss computational issues relating to the Hessian of the error surface in Section 4.9. In Section 4.10, we discuss two issues: how to fulfill optimal annealing and how to make the learning-rate parameter adaptive.
3. Sections 4.11 through 4.14 focus on various matters relating to the performance of a multilayer perceptron trained with the back-propagation algorithm. In Section 4.11, we discuss the issue of generalization—the very essence of learning. Section 4.12 addresses the approximation of continuous functions by means of multiplayer perceptrons. The use of cross-validation as a statistical design tool is discussed in Section 4.13. In Section 4.14, we discuss the issue of complexity regularization, as well as network-pruning techniques.
4. Section 4.15, summarizes the advantages and limitations of back-propagation learning.
5. Having completed the study of back-propagation learning, we next take a different perspective on learning in Section 4.16 by viewing supervised learning as an optimization problem.

6. Section 4.17 describes an important neural network structure: the *convolutional multilayer perceptron*. This network has been successfully used in the solution of difficult pattern-recognition problems.
7. Section 4.18 deals with nonlinear filtering, where time plays a key role. The discussion begins with short-term memory structures, setting the stage for the universal myopic mapping theorem.
8. Section 4.19 discusses the issue of small-scale versus large-scale learning problems.

The chapter concludes with summary and discussion in Section 4.20.

4.1 INTRODUCTION

In Chapter 1, we studied Rosenblatt's perceptron, which is basically a single-layer neural network. Therein, we showed that this network is limited to the classification of linearly separable patterns. Then we studied adaptive filtering in Chapter 3, using Widrow and Hoff's LMS algorithm. This algorithm is also based on a single linear neuron with adjustable weights, which limits the computing power of the algorithm. To overcome the practical limitations of the perceptron and the LMS algorithm, we look to a neural network structure known as the *multilayer perceptron*.

The following three points highlight the basic features of multilayer perceptrons:

- The model of each neuron in the network includes a nonlinear activation function that is *differentiable*.
- The network contains one or more layers that are *hidden* from both the input and output nodes.
- The network exhibits a high degree of *connectivity*, the extent of which is determined by synaptic weights of the network.

These same characteristics, however, are also responsible for the deficiencies in our knowledge on the behavior of the network. First, the presence of a distributed form of nonlinearity and the high connectivity of the network make the theoretical analysis of a multilayer perceptron difficult to undertake. Second, the use of hidden neurons makes the learning process harder to visualize. In an implicit sense, the learning process must decide which features of the input pattern should be represented by the hidden neurons. The learning process is therefore made more difficult because the search has to be conducted in a much larger space of possible functions, and a choice has to be made between alternative representations of the input pattern.

A popular method for the training of multilayer perceptrons is the back-propagation algorithm, which includes the LMS algorithm as a special case. The training proceeds in two phases:

1. In the *forward phase*, the synaptic weights of the network are fixed and the input signal is propagated through the network, layer by layer, until it reaches the output. Thus, in this phase, changes are confined to the activation potentials and outputs of the neurons in the network.

2. In the *backward phase*, an error signal is produced by comparing the output of the network with a desired response. The resulting error signal is propagated through the network, again layer by layer, but this time the propagation is performed in the backward direction. In this second phase, successive adjustments are made to the synaptic weights of the network. Calculation of the adjustments for the output layer is straightforward, but it is much more challenging for the hidden layers.

Usage of the term "back propagation" appears to have evolved after 1985, when the term was popularized through the publication of the seminal book entitled *Parallel Distributed Processing* (Rumelhart and McClelland, 1986).

The development of the back-propagation algorithm in the mid-1980s represented a landmark in neural networks in that it provided a *computationally efficient* method for the training of multilayer perceptrons, putting to rest the pessimism about learning in multilayer perceptrons that may have been inferred from the book by Minsky and Papert (1969).

4.2 SOME PRELIMINARIES

Figure 4.1 shows the architectural graph of a multiplayer perceptron with two hidden layers and an output layer. To set the stage for a description of the multilayer perceptron in its general form, the network shown here is *fully connected*. This means that a neuron in any layer of the network is connected to all the neurons (nodes) in the previous layer. Signal flow through the network progresses in a forward direction, from left to right and on a layer-by-layer basis.

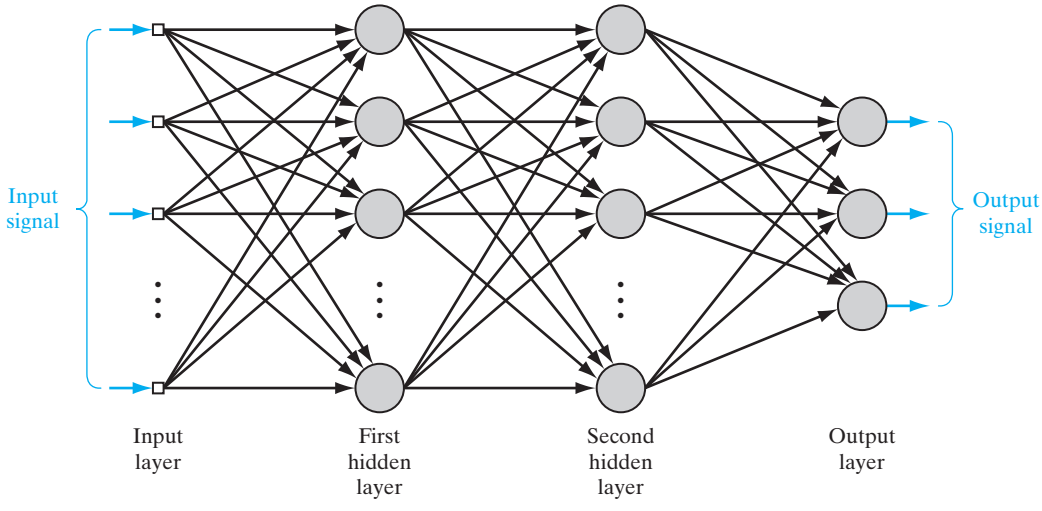

FIGURE 4.1 Architectural graph of a multilayer perceptron with two hidden layers.

Figure 4.2 depicts a portion of the multilayer perceptron. Two kinds of signals are identified in this network:

1. *Function Signals.* A function signal is an input signal (stimulus) that comes in at the input end of the network, propagates forward (neuron by neuron) through the network, and emerges at the output end of the network as an output signal. We refer to such a signal as a "function signal" for two reasons. First, it is presumed to perform a useful function at the output of the network. Second, at each neuron of the network through which a function signal passes, the signal is calculated as a function of the inputs and associated weights applied to that neuron. The function signal is also referred to as the input signal.
2. *Error Signals.* An error signal originates at an output neuron of the network and propagates backward (layer by layer) through the network. We refer to it as an "error signal" because its computation by every neuron of the network involves an error-dependent function in one form or another.

The output neurons constitute the output layer of the network. The remaining neurons constitute hidden layers of the network. Thus, the hidden units are not part of the output or input of the network—hence their designation as "hidden." The first hidden layer is fed from the input layer made up of sensory units (source nodes); the resulting outputs of the first hidden layer are in turn applied to the next hidden layer; and so on for the rest of the network.

Each hidden or output neuron of a multilayer perceptron is designed to perform two computations:

1. the computation of the function signal appearing at the output of each neuron, which is expressed as a continuous nonlinear function of the input signal and synaptic weights associated with that neuron;
2. the computation of an estimate of the gradient vector (i.e., the gradients of the error surface with respect to the weights connected to the inputs of a neuron), which is needed for the backward pass through the network.

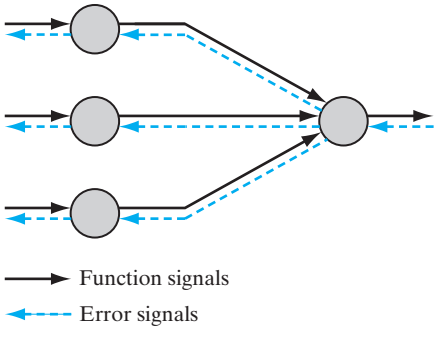

FIGURE 4.2 Illustration of the directions of two basic signal flows in a multilayer perceptron: forward propagation of function signals and back propagation of error signals.

Function of the Hidden Neurons

The hidden neurons act as *feature detectors*; as such, they play a critical role in the operation of a multilayer perceptron. As the learning process progresses across the multilayer perceptron, the hidden neurons begin to gradually "discover" the salient features that characterize the training data. They do so by performing a nonlinear transformation on the input data into a new space called the *feature space*. In this new space, the classes of interest in a pattern-classification task, for example, may be more easily separated from each other than could be the case in the original input data space. Indeed, it is the formation of this feature space through supervised learning that distinguishes the multilayer perceptron from Rosenblatt's perceptron.

Credit-Assignment Problem

When studying learning algorithms for distributed systems, exemplified by the multilayer perceptron of Figure 4.1, it is instructive to pay attention to the notion of *credit assignment.* Basically, the credit-assignment problem is the problem of assigning *credit* or *blame* for overall outcomes to each of the *internal decisions* made by the hidden computational units of the distributed learning system, recognizing that those decisions are responsible for the overall outcomes in the first place.

In a multilayer perceptron using *error-correlation learning*, the credit-assignment problem arises because the operation of each hidden neuron and of each output neuron in the network is important to the network's correct overall action on a learning task of interest. That is, in order to solve the prescribed task, the network must assign certain forms of behavior to all of its neurons through a specification of the error-correction learning algorithm. With this background, consider the multilayer perceptron depicted in Fig. 4.1. Since each output neuron is visible to the outside world, it is possible to supply a desired response to guide the behavior of such a neuron. Thus, as far as output neurons are concerned, it is a straightforward matter to adjust the synaptic weights of each output neuron in accordance with the error-correction algorithm. But how do we assign credit or blame for the action of the hidden neurons when the error-correction learning algorithm is used to adjust the respective synaptic weights of these neurons? The answer to this fundamental question requires more detailed attention than in the case of output neurons.

In what follows in this chapter, we show that the back-propagation algorithm, basic to the training of a multilayer perceptron, solves the credit-assignment problem in an elegant manner. But before proceeding to do that, we describe two basic methods of supervised learning in the next section.

4.3 BATCH LEARNING AND ON-LINE LEARNING

Consider a multilayer perceptron with an input layer of source nodes, one or more hidden layers, and an output layer consisting of one or more neurons; as illustrated in Fig. 4.1. Let

$$\mathcal{T} = \{\mathbf{x}(n), \mathbf{d}(n)\}_{n=1}^{N} \tag{4.1}$$

denote the *training sample* used to train the network in a supervised manner. Let $y_j(n)$ denote the function signal produced at the output of neuron j in the output layer by the stimulus $\mathbf{x}(n)$ applied to the input layer. Correspondingly, the *error signal* produced at the output of neuron j is defined by

$$e_j(n) = d_j(n) - y_j(n) \tag{4.2}$$

where $d_j(n)$ is the ith element of the desired-response vector $\mathbf{d}(n)$. Following the terminology of the LMS algorithm studied in Chapter 3, the *instantaneous error energy* of neuron j is defined by

$$\mathscr{E}_j(n) = \frac{1}{2}e_j^2(n) \tag{4.3}$$

Summing the error-energy contributions of all the neurons in the output layer, we express the *total instantaneous error energy* of the whole network as

$$\begin{aligned}\mathscr{E}(n) &= \sum_{j\in C}\mathscr{E}_j(n)\\ &= \frac{1}{2}\sum_{j\in C}e_j^2(n)\end{aligned} \tag{4.4}$$

where the set C includes all the neurons in the output layer. With the training sample consisting of N examples, the *error energy averaged over the training sample*, or the *empirical risk*, is defined by

$$\begin{aligned}\mathscr{E}_{\text{av}}(N) &= \frac{1}{N}\sum_{n=1}^{N}\mathscr{E}(n)\\ &= \frac{1}{2N}\sum_{n=1}^{N}\sum_{j\in C}e_j^2(n)\end{aligned} \tag{4.5}$$

Naturally, the instantaneous error energy, and therefore the average error energy, are both functions of all the adjustable synaptic weights (i.e., free parameters) of the multilayer perceptron. This functional dependence has not been included in the formulas for $\mathscr{E}(n)$ and $\mathscr{E}_{\text{av}}(N)$, merely to simplify the terminology.

Depending on how the supervised learning of the multilayer perceptron is actually performed, we may identify two different methods—namely, batch learning and on-line learning, as discussed next in the context of gradient descent.

Batch Learning

In the batch method of supervised learning, adjustments to the synaptic weights of the multilayer perceptron are performed *after* the presentation of *all* the N examples in the training sample $\mathcal{T}$ that constitute one *epoch* of training. In other words, the cost function for batch learning is defined by the average error energy $\mathscr{E}_{\text{av}}$. Adjustments to the synaptic weights of the multilayer perceptron are made on an *epoch-by-epoch basis*. Correspondingly, one realization of the learning curve is obtained by plotting $\mathscr{E}_{\text{av}}$ versus the number

of epochs, where, for each epoch of training, the examples in the training sample $\mathcal{T}$ are *randomly shuffled*. The learning curve is then computed by *ensemble averaging* a large enough number of such realizations, where each realization is performed for a *different set of initial conditions* chosen at random.

With the method of gradient descent used to perform the training, the advantages of batch learning include the following:

- *accurate estimation* of the gradient vector (i.e., the derivative of the cost function $\mathscr{E}_{\text{av}}$ with respect to the weight vector $\mathbf{w}$), thereby guaranteeing, under simple conditions, convergence of the method of steepest descent to a local minimum;
- *parallelization* of the learning process.

However, from a practical perspective, batch learning is rather demanding in terms of *storage requirements*.

In a statistical context, batch learning may be viewed as a form of *statistical inference*. It is therefore well suited for solving *nonlinear regression problems*.

On-line Learning

In the on-line method of supervised learning, adjustments to the synaptic weights of the multilayer perceptron are performed on an *example-by-example basis*. The cost function to be minimized is therefore the total instantaneous error energy $\mathscr{E}(n)$.

Consider an epoch of N training examples arranged in the order $\{\mathbf{x}(1), \mathbf{d}(1)\}, \{\mathbf{x}(2), \mathbf{d}(2)\}, ..., \{\mathbf{x}(N), \mathbf{d}(N)\}$. The first example pair $\{\mathbf{x}(1), \mathbf{d}(1)\}$ in the epoch is presented to the network, and the weight adjustments are performed using the method of gradient descent. Then the second example $\{\mathbf{x}(2), \mathbf{d}(2)\}$ in the epoch is presented to the network, which leads to further adjustments to weights in the network. This procedure is continued until the last example $\{\mathbf{x}(N), \mathbf{d}(N)\}$ is accounted for. Unfortunately, such a procedure works against the parallalization of on-line learning.

For a given set of initial conditions, a single realization of the learning curve is obtained by plotting the final value $\mathscr{E}(N)$ versus the number of epochs used in the training session, where, as before, the training examples are randomly shuffled after each epoch. As with batch learning, the learning curve for on-line learning is computed by ensemble averaging such realizations over a large enough number of initial conditions chosen at random. Naturally, for a given network structure, the learning curve obtained under on-line learning will be quite different from that under batch learning.

Given that the training examples are presented to the network in a random manner, the use of on-line learning makes the search in the multidimensional weight space *stochastic* in nature; it is for this reason that the method of on-line learning is sometimes referred to as a *stochastic method*. This stochasticity has the desirable effect of making it less likely for the learning process to be trapped in a local minimum, which is a definite advantage of on-line learning over batch learning. Another advantage of on-line learning is the fact that it requires much less storage than batch learning.

Moreover, when the training data are *redundant* (i.e., the training sample $\mathcal{T}$ contains several copies of the same example), we find that, unlike batch learning, on-line

learning is able to take advantage of this redundancy because the examples are presented one at a time.

Another useful property of on-line learning is its ability to *track small changes* in the training data, particularly when the environment responsible for generating the data is nonstationary.

To summarize, despite the disadvantages of on-line learning, it is highly popular for solving *pattern-classification problems* for two important practical reasons:

- On-line learning is simple to implement.
- It provides effective solutions to large-scale and difficult pattern-classification problems.

It is for these two reasons that much of the material presented in this chapter is devoted to on-line learning.

4.4 THE BACK-PROPAGATION ALGORITHM

The popularity of on-line learning for the supervised training of multilayer perceptrons has been further enhanced by the development of the back-propagation algorithm. To describe this algorithm, consider Fig. 4.3, which depicts neuron j being fed by a set of

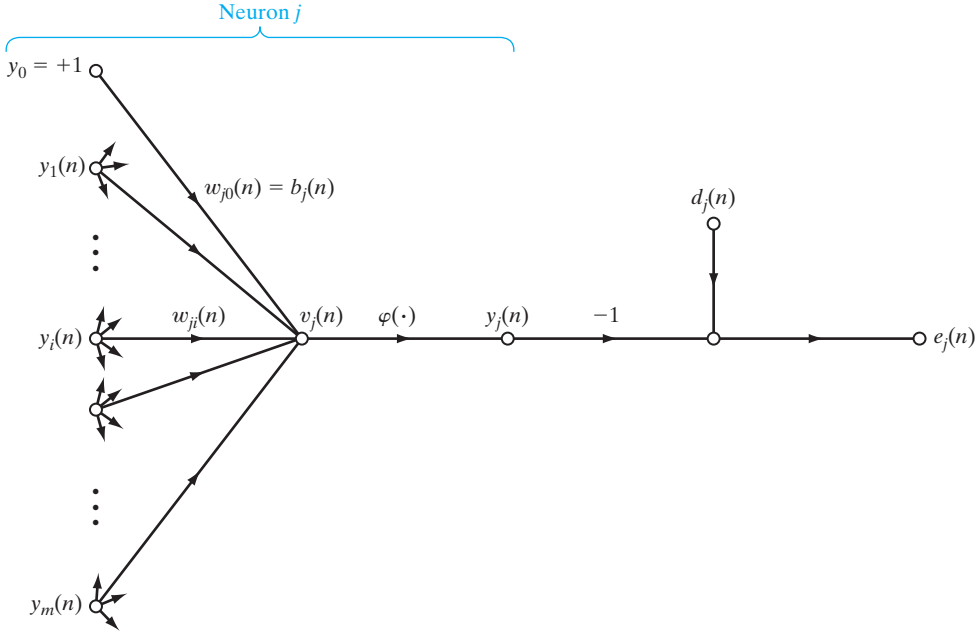

FIGURE 4.3 Signal-flow graph highlighting the details of output neuron j.

function signals produced by a layer of neurons to its left. The induced local field $v_j(n)$ produced at the input of the activation function associated with neuron j is therefore

$$v_j(n) = \sum_{i=0}^{m} w_{ji}(n) y_i(n) \tag{4.6}$$

where m is the total number of inputs (excluding the bias) applied to neuron j. The synaptic weight w_{j0} (corresponding to the fixed input $y_0 = +1$) equals the bias b_j applied to neuron j. Hence, the function signal $y_j(n)$ appearing at the output of neuron j at iteration n is

$$y_j(n) = \varphi_j(v_j(n)) \tag{4.7}$$

In a manner similar to the LMS algorithm studied in Chapter 3, the back-propagation algorithm applies a correction $\Delta w_{ji}(n)$ to the synaptic weight $w_{ji}(n)$, which is proportional to the partial derivative $\partial \mathscr{E}(n)/\partial w_{ji}(n)$. According to the *chain rule* of calculus, we may express this gradient as

$$\frac{\partial \mathscr{E}(n)}{\partial w_{ji}(n)} = \frac{\partial \mathscr{E}(n)}{\partial e_j(n)} \frac{\partial e_j(n)}{\partial y_j(n)} \frac{\partial y_j(n)}{\partial v_j(n)} \frac{\partial v_j(n)}{\partial w_{ji}(n)} \tag{4.8}$$

The partial derivative $\partial \mathscr{E}(n)/\partial w_{ji}(n)$ represents a *sensitivity factor*, determining the direction of search in weight space for the synaptic weight w_{ji}.

Differentiating both sides of Eq. (4.4) with respect to $e_j(n)$, we get

$$\frac{\partial \mathscr{E}(n)}{\partial e_j(n)} = e_j(n) \tag{4.9}$$

Differentiating both sides of Eq. (4.2) with respect to $y_j(n)$, we get

$$\frac{\partial e_j(n)}{\partial y_j(n)} = -1 \tag{4.10}$$

Next, differentiating Eq. (4.7) with respect to $v_j(n)$, we get

$$\frac{\partial y_j(n)}{\partial v_j(n)} = \varphi_j'(v_j(n)) \tag{4.11}$$

where the use of prime (on the right-hand side) signifies differentiation with respect to the argument. Finally, differentiating Eq. (4.6) with respect to $w_{ji}(n)$ yields

$$\frac{\partial v_j(n)}{\partial w_{ji}(n)} = y_i(n) \tag{4.12}$$

The use of Eqs. (4.9) to (4.12) in Eq. (4.8) yields

$$\frac{\partial \mathscr{E}(n)}{\partial w_{ji}(n)} = -e_j(n)\varphi_j'(v_j(n))y_i(n) \tag{4.13}$$

The correction $\Delta w_{ji}(n)$ applied to $w_{ji}(n)$ is defined by the *delta rule*, or

$$\Delta w_{ji}(n) = -\eta \frac{\partial \mathscr{E}(n)}{\partial w_{ji}(n)} \tag{4.14}$$

where η is the *learning-rate parameter* of the back-propagation algorithm. The use of the minus sign in Eq. (4.14) accounts for *gradient descent* in weight space (i.e., seeking a direction for weight change that reduces the value of $\mathscr{E}(n)$). Accordingly, the use of Eq. (4.13) in Eq. (4.14) yields

$$\Delta w_{ji}(n) = \eta \delta_j(n) y_i(n) \tag{4.15}$$

where the *local gradient* $\delta_j(n)$ is defined by

$$\begin{aligned} \delta_j(n) &= \frac{\partial \mathscr{E}(n)}{\partial v_j(n)} \\ &= \frac{\partial \mathscr{E}(n)}{\partial e_j(n)} \frac{\partial e_j(n)}{\partial y_j(n)} \frac{\partial y_j(n)}{\partial v_j(n)} \\ &= e_j(n) \varphi_j'(v_j(n)) \end{aligned} \tag{4.16}$$

The local gradient points to required changes in synaptic weights. According to Eq. (4.16), the local gradient $\delta_j(n)$ for output neuron j is equal to the product of the corresponding error signal $e_j(n)$ for that neuron and the derivative $\varphi_j'(v_j(n))$ of the associated activation function.

From Eqs. (4.15) and (4.16), we note that a key factor involved in the calculation of the weight adjustment $\Delta w_{ji}(n)$ is the error signal $e_j(n)$ at the output of neuron j. In this context, we may identify two distinct cases, depending on where in the network neuron j is located. In case 1, neuron j is an output node. This case is simple to handle because each output node of the network is supplied with a desired response of its own, making it a straightforward matter to calculate the associated error signal. In case 2, neuron j is a hidden node. Even though hidden neurons are not directly accessible, they share responsibility for any error made at the output of the network. The question, however, is to know how to penalize or reward hidden neurons for their share of the responsibility. This problem is the *credit-assignment problem* considered in Section 4.2.

Case 1 Neuron *j* Is an Output Node

When neuron j is located in the output layer of the network, it is supplied with a desired response of its own. We may use Eq. (4.2) to compute the error signal $e_j(n)$ associated with this neuron; see Fig. 4.3. Having determined $e_j(n)$, we find it a straightforward matter to compute the local gradient $\delta_j(n)$ by using Eq. (4.16).

Case 2 Neuron *j* Is a Hidden Node

When neuron j is located in a hidden layer of the network, there is no specified desired response for that neuron. Accordingly, the error signal for a hidden neuron would have to be determined recursively and working backwards in terms of the error signals of all the neurons to which that hidden neuron is directly connected; this is where the

development of the back-propagation algorithm gets complicated. Consider the situation in Fig. 4.4, which depicts neuron j as a hidden node of the network. According to Eq. (4.16), we may redefine the local gradient $\delta_j(n)$ for hidden neuron j as

$$\begin{aligned}\delta_j(n) &= -\frac{\partial \mathscr{E}(n)}{\partial y_j(n)}\frac{\partial y_j(n)}{\partial v_j(n)} \\ &= -\frac{\partial \mathscr{E}(n)}{\partial y_j(n)}\varphi_j'(v_j(n)), \qquad \text{neuron } j \text{ is hidden}\end{aligned} \tag{4.17}$$

where in the second line we have used Eq. (4.11). To calculate the partial derivative $\partial \mathscr{E}(n)/\partial y_j(n)$, we may proceed as follows: From Fig. 4.4, we see that

$$\mathscr{E}(n) = \frac{1}{2}\sum_{k \in C} e_k^2(n), \qquad \text{neuron } k \text{ is an output node} \tag{4.18}$$

which is Eq. (4.4) with index k used in place of index j. We have made this substitution in order to avoid confusion with the use of index j that refers to a hidden neuron under case 2. Differentiating Eq. (4.18) with respect to the function signal $y_j(n)$, we get

$$\frac{\partial \mathscr{E}(n)}{\partial y_j(n)} = \sum_k e_k \frac{\partial e_k(n)}{\partial y_j(n)} \tag{4.19}$$

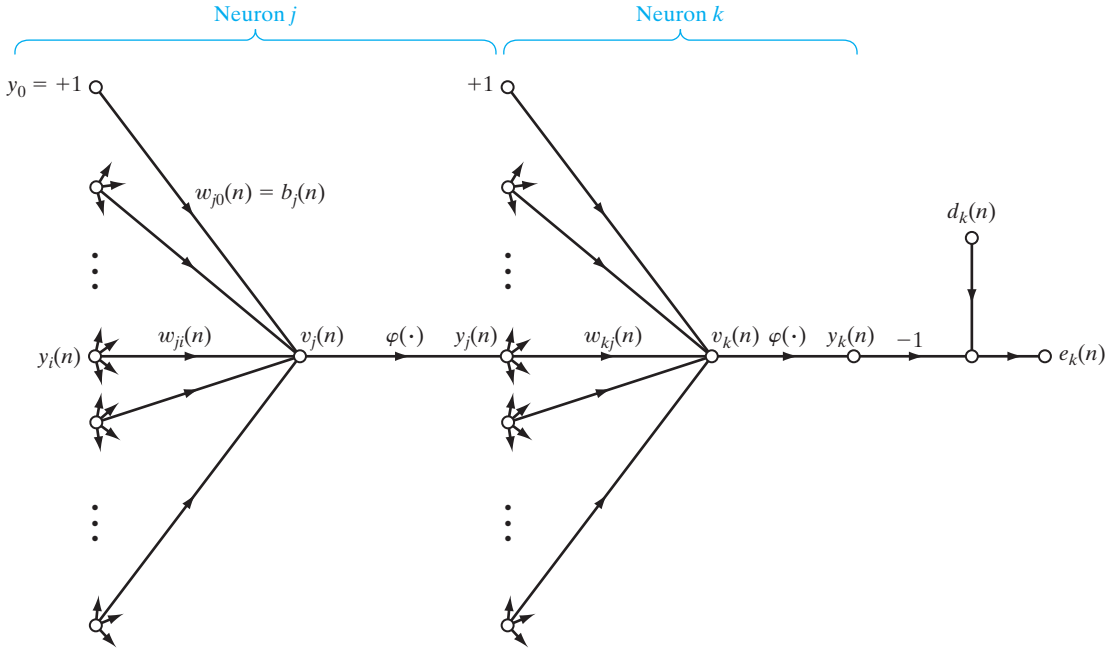

FIGURE 4.4 Signal-flow graph highlighting the details of output neuron k connected to hidden neuron j.

Next we use the chain rule for the partial derivative $\partial e_k(n)/\partial y_j(n)$ and rewrite Eq. (4.19) in the equivalent form

$$\frac{\partial \mathscr{E}(n)}{\partial y_j(n)} = \sum_k e_k(n) \frac{\partial e_k(n)}{\partial v_k(n)} \frac{\partial v_k(n)}{\partial y_j(n)} \tag{4.20}$$

However, from Fig. 4.4, we note that

$$\begin{aligned} e_k(n) &= d_k(n) - y_k(n) \\ &= d_k(n) - \varphi_k(v_k(n)), \qquad \text{neuron } k \text{ is an output node} \end{aligned} \tag{4.21}$$

Hence,

$$\frac{\partial e_k(n)}{\partial v_k(n)} = -\varphi_k'(v_k(n)) \tag{4.22}$$

We also note from Fig. 4.4 that for neuron k, the induced local field is

$$v_k(n) = \sum_{j=0}^{m} w_{kj}(n) y_j(n) \tag{4.23}$$

where m is the total number of inputs (excluding the bias) applied to neuron k. Here again, the synaptic weight $w_{k0}(n)$ is equal to the bias $b_k(n)$ applied to neuron k, and the corresponding input is fixed at the value +1. Differentiating Eq. (4.23) with respect to $y_j(n)$ yields

$$\frac{\partial v_k(n)}{\partial y_j(n)} = w_{kj}(n) \tag{4.24}$$

By using Eqs. (4.22) and (4.24) in Eq. (4.20), we get the desired partial derivative

$$\begin{aligned} \frac{\partial \mathscr{E}(n)}{\partial y_j(n)} &= -\sum_k e_k(n) \varphi_k'(v_k(n)) w_{kj}(n) \\ &= -\sum_k \delta_k(n) w_{kj}(n) \end{aligned} \tag{4.25}$$

where, in the second line, we have used the definition of the local gradient $\delta_k(n)$ given in Eq. (4.16), with the index k substituted for j.

Finally, using Eq. (4.25) in Eq. (4.17), we get the *back-propagation formula* for the local gradient $\delta_j(n)$, described by

$$\delta_j(n) = \varphi_j'(v_j(n)) \sum_k \delta_k(n) w_{kj}(n), \qquad \text{neuron } j \text{ is hidden} \tag{4.26}$$

Figure 4.5 shows the signal-flow graph representation of Eq. (4.26), assuming that the output layer consists of m_L neurons.

The outside factor $\varphi_j'(v_j(n))$ involved in the computation of the local gradient $\delta_j(n)$ in Eq. (4.26) depends solely on the activation function associated with hidden neuron j. The remaining factor involved in this computation—namely, the summation over k—depends on two sets of terms. The first set of terms, the $\delta_k(n)$, requires knowledge of the error

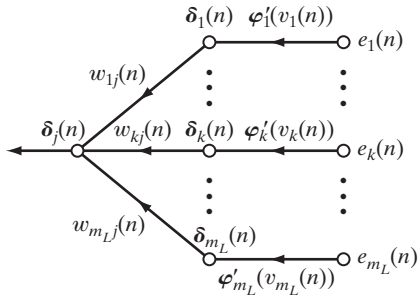

FIGURE 4.5 Signal-flow graph of a part of the adjoint system pertaining to back-propagation of error signals.

signals $e_k(n)$ for all neurons that lie in the layer to the immediate right of hidden neuron j and that are directly connected to neuron j; see Fig. 4.4. The second set of terms, the $w_{kj}(n)$, consists of the synaptic weights associated with these connections.

We now summarize the relations that we have derived for the back-propagation algorithm. First, the correction $\Delta w_{ji}(n)$ applied to the synaptic weight connecting neuron i to neuron j is defined by the delta rule:

$$\begin{pmatrix} \textit{Weight} \\ \textit{correction} \\ \Delta w_{ji}(n) \end{pmatrix} = \begin{pmatrix} \textit{learning-} \\ \textit{rate parameter} \\ \eta \end{pmatrix} \times \begin{pmatrix} \textit{local} \\ \textit{gradient} \\ \delta_j(n) \end{pmatrix} \times \begin{pmatrix} \textit{input signal} \\ \textit{of neuron } j, \\ y_i(n) \end{pmatrix} \tag{4.27}$$

Second, the local gradient $\delta_j(n)$ depends on whether neuron j is an output node or a hidden node:

1. If neuron j is an output node, $\delta_j(n)$ equals the product of the derivative $\varphi_j'(v_j(n))$ and the error signal $e_j(n)$, both of which are associated with neuron j; see Eq. (4.16).
2. If neuron j is a hidden node, $\delta_j(n)$ equals the product of the associated derivative $\varphi_j'(v_j(n))$ and the weighted sum of the δs computed for the neurons in the next hidden or output layer that are connected to neuron j; see Eq. (4.26).

The Two Passes of Computation

In the application of the back-propagation algorithm, two different passes of computation are distinguished. The first pass is referred to as the forward pass, and the second is referred to as the backward pass.

In the *forward pass*, the synaptic weights remain unaltered throughout the network, and the function signals of the network are computed on a neuron-by-neuron basis. The function signal appearing at the output of neuron j is computed as

$$y_j(n) = \varphi(v_j(n)) \tag{4.28}$$

where $v_j(n)$ is the induced local field of neuron j, defined by

$$v_j(n) = \sum_{i=0}^{m} w_{ji}(n) y_i(n) \tag{4.29}$$

where m is the total number of inputs (excluding the bias) applied to neuron j; $w_{ji}(n)$ is the synaptic weight connecting neuron i to neuron j; and $y_i(n)$ is an input signal of neuron j, or, equivalently, the function signal appearing at the output of neuron i. If neuron j is in the first hidden layer of the network, then $m = m_0$ and the index i refers to the ith input terminal of the network, for which we write

$$y_i(n) = x_i(n) \tag{4.30}$$

where $x_i(n)$ is the ith element of the input vector (pattern). If, on the other hand, neuron j is in the output layer of the network, then $m = m_L$ and the index j refers to the jth output terminal of the network, for which we write

$$y_j(n) = o_j(n) \tag{4.31}$$

where $o_j(n)$ is the jth element of the output vector of the multilayer perceptron. This output is compared with the desired response $d_j(n)$, obtaining the error signal $e_j(n)$ for the jth output neuron. Thus, the forward phase of computation begins at the first hidden layer by presenting it with the input vector and terminates at the output layer by computing the error signal for each neuron of this layer.

The backward pass, on the other hand, starts at the output layer by passing the error signals leftward through the network, layer by layer, and recursively computing the δ (i.e., the local gradient) for each neuron. This recursive process permits the synaptic weights of the network to undergo changes in accordance with the delta rule of Eq. (4.27). For a neuron located in the output layer, the δ is simply equal to the error signal of that neuron multiplied by the first derivative of its nonlinearity. Hence, we use Eq. (4.27) to compute the changes to the weights of all the connections feeding into the output layer. Given the δs for the neurons of the output layer, we next use Eq. (4.26) to compute the δs for all the neurons in the penultimate layer and therefore the changes to the weights of all connections feeding into it. The recursive computation is continued, layer by layer, by propagating the changes to all synaptic weights in the network.

Note that for the presentation of each training example, the input pattern is fixed—that is, "clamped" throughout the round-trip process, which encompasses the forward pass followed by the backward pass.

Activation Function

The computation of the δ for each neuron of the multilayer perceptron requires knowledge of the derivative of the activation function $\varphi(\cdot)$ associated with that neuron. For this derivative to exist, we require the function $\varphi(\cdot)$ to be continuous. In basic terms, *differentiability* is the only requirement that an activation function has to satisfy. An example of a continuously differentiable nonlinear activation function commonly used in multilayer perceptrons is *sigmoidal nonlinearity*,[1] two forms of which are described here:

1. *Logistic Function.* This form of sigmoidal nonlinearity, in its general form, is defined by

$$\varphi_j(v_j(n)) = \frac{1}{1 + \exp(-av_j(n))}, \qquad a > 0 \tag{4.32}$$

where $v_j(n)$ is the induced local field of neuron j and a is an adjustable positive parameter. According to this nonlinearity, the amplitude of the output lies inside the range $0 \leq y_j \leq 1$. Differentiating Eq. (4.32) with respect to $v_j(n)$, we get

$$\varphi_j'(v_j(n)) = \frac{a \exp(-av_j(n))}{[1 + \exp(-av_j(n))]^2} \tag{4.33}$$

With $y_j(n) = \varphi_j(v_j(n))$, we may eliminate the exponential term $\exp(-av_j(n))$ from Eq. (4.33) and consequently express the derivative $\varphi_j'(v_j(n))$ as

$$\varphi_j'(v_j(n)) = ay_j(n)[1 - y_j(n)] \tag{4.34}$$

For a neuron j located in the output layer, $y_j(n) = o_j(n)$. Hence, we may express the local gradient for neuron j as

$$\begin{aligned} \delta_j(n) &= e_j(n)\varphi_j'(v_j(n)) \\ &= a[d_j(n) - o_j(n)]o_j(n)[1 - o_j(n)], \qquad \text{neuron } j \text{ is an output node} \end{aligned} \tag{4.35}$$

where $o_j(n)$ is the function signal at the output of neuron j, and $d_j(n)$ is the desired response for it. On the other hand, for an arbitrary hidden neuron j, we may express the local gradient as

$$\begin{aligned} \delta_j(n) &= \varphi_j'(v_j(n)) \sum_k \delta_k(n) w_{kj}(n) \\ &= ay_j(n)[1 - y_j(n)] \sum_k \delta_k(n) w_{kj}(n), \qquad \text{neuron } j \text{ is hidden} \end{aligned} \tag{4.36}$$

Note from Eq. (4.34) that the derivative $\varphi_j'(v_j(n))$ attains its maximum value at $y_j(n) = 0.5$ and its minimum value (zero) at $y_j(n) = 0$, or $y_j(n) = 1.0$. Since the amount of change in a synaptic weight of the network is proportional to the derivative $\varphi_j'(v_j(n))$, it follows that for a sigmoid activation function, the synaptic weights are changed the most for those neurons in the network where the function signals are in their midrange. According to Rumelhart et al. (1986a), it is this feature of back-propagation learning that contributes to its stability as a learning algorithm.

2. *Hyperbolic tangent function.* Another commonly used form of sigmoidal nonlinearity is the hyperbolic tangent function, which, in its most general form, is defined by

$$\varphi_j(v_j(n)) = a \tanh(bv_j(n)) \tag{4.37}$$

where a and b are positive constants. In reality, the hyperbolic tangent function is just the logistic function rescaled and biased. Its derivative with respect to $v_j(n)$ is given by

$$\begin{aligned} \varphi_j'(v_j(n)) &= ab \operatorname{sech}^2(bv_j(n)) \\ &= ab(1 - \tanh^2(bv_j(n))) \\ &= \frac{b}{a}[a - y_j(n)][a + y_j(n)] \end{aligned} \tag{4.38}$$

For a neuron j located in the output layer, the local gradient is

$$\begin{aligned}\delta_j(n) &= e_j(n)\varphi_j'(v_j(n)) \\ &= \frac{b}{a}[d_j(n) - o_j(n)][a - o_j(n)][a + o_j(n)]\end{aligned} \tag{4.39}$$

For a neuron j in a hidden layer, we have

$$\begin{aligned}\delta_j(n) &= \varphi_j'(v_j(n)) \sum_k \delta_k(n) w_{kj}(n) \\ &= \frac{b}{a}[a - y_j(n)][a + y_j(n)] \sum_k \delta_k(n) w_{kj}(n), \qquad \text{neuron } j \text{ is hidden}\end{aligned} \tag{4.40}$$

By using Eqs. (4.35) and (4.36) for the logistic function and Eqs. (4.39) and (4.40) for the hyperbolic tangent function, we may calculate the local gradient δ_j without requiring explicit knowledge of the activation function.

Rate of Learning

The back-propagation algorithm provides an "approximation" to the trajectory in weight space computed by the method of steepest descent. The smaller we make the learning-rate parameter η, the smaller the changes to the synaptic weights in the network will be from one iteration to the next, and the smoother will be the trajectory in weight space. This improvement, however, is attained at the cost of a slower rate of learning. If, on the other hand, we make the learning-rate parameter η too large in order to speed up the rate of learning, the resulting large changes in the synaptic weights assume such a form that the network may become unstable (i.e., oscillatory). A simple method of increasing the rate of learning while avoiding the danger of instability is to modify the delta rule of Eq. (4.15) by including a momentum term, as shown by

$$\Delta w_{ji}(n) = \alpha \Delta w_{ji}(n-1) + \eta \delta_j(n) y_i(n) \tag{4.41}$$

where α is usually a positive number called the *momentum constant*. It controls the feedback loop acting around $\Delta w_{ji}(n)$, as illustrated in Fig. 4.6, where z^{-1} is the unit-time delay operator. Equation (4.41) is called the *generalized delta rule*[2]; it includes the delta rule of Eq. (4.15) as a special case (i.e., $\alpha = 0$).

In order to see the effect of the sequence of pattern presentations on the synaptic weights due to the momentum constant α, we rewrite Eq. (4.41) as a time series with index t. The index t goes from the initial time 0 to the current time n. Equation (4.41)

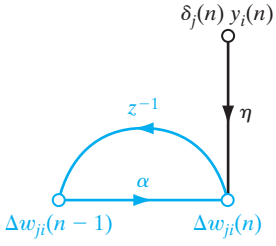

FIGURE 4.6 Signal-flow graph illustrating the effect of momentum constant α, which lies inside the feedback loop.

may be viewed as a first-order difference equation in the weight correction $\Delta w_{ji}(n)$. Solving this equation for $\Delta w_{ji}(n)$, we have

$$\Delta w_{ji}(n) = \eta \sum_{t=0}^{n} \alpha^{n-t} \delta_j(t) y_i(t) \tag{4.42}$$

which represents a time series of length $n + 1$. From Eqs. (4.13) and (4.16), we note that the product $\delta_j(n)y_i(n)$ is equal to $-\partial \mathscr{E}(n)/\partial w_{ji}(n)$. Accordingly, we may rewrite Eq. (4.42) in the equivalent form

$$\Delta w_{ji}(n) = -\eta \sum_{t=0}^{n} \alpha^{n-t} \frac{\partial \mathscr{E}(t)}{\partial w_{ji}(t)} \tag{4.43}$$

Based on this relation, we may make the following insightful observations:

1. The current adjustment $\Delta w_{ji}(n)$ represents the sum of an exponentially weighted time series. For the time series to be *convergent*, the momentum constant must be restricted to the range $0 \leq |\alpha| < 1$. When α is zero, the back-propagation algorithm operates without momentum. Also, the momentum constant α can be positive or negative, although it is unlikely that a negative α would be used in practice.

2. When the partial derivative $\partial \mathscr{E}(t)/\partial w_{ji}(t)$ has the same algebraic sign on consecutive iterations, the exponentially weighted sum $\Delta w_{ji}(n)$ grows in magnitude, and consequently the weight $w_{ji}(n)$ is adjusted by a large amount. The inclusion of momentum in the back-propagation algorithm tends to *accelerate descent* in steady downhill directions.

3. When the partial derivative $\partial \mathscr{E}(t)/\partial w_{ji}(t)$ has opposite signs on consecutive iterations, the exponentially weighted sum $\Delta w_{ji}(n)$ shrinks in magnitude, and consequently the weight $w_{ji}(n)$ is adjusted by a small amount. The inclusion of momentum in the back-propagation algorithm has a *stabilizing effect* in directions that oscillate in sign.

The incorporation of momentum in the back-propagation algorithm represents a minor modification to the weight update; however, it may have some beneficial effects on the learning behavior of the algorithm. The momentum term may also have the benefit of preventing the learning process from terminating in a shallow local minimum on the error surface.

In deriving the back-propagation algorithm, it was assumed that the learning-rate parameter is a constant denoted by η. In reality, however, it should be defined as η_{ji}; that is, the learning-rate parameter should be *connection dependent.* Indeed, many interesting things can be done by making the learning-rate parameter different for different parts of the network. We provide more detail on this issue in subsequent sections.

It is also noteworthy that in the application of the back-propagation algorithm, we may choose all the synaptic weights in the network to be adjustable, or we may constrain any number of weights in the network to remain fixed during the adaptation process. In the latter case, the error signals are back propagated through the network in the usual manner; however, the fixed synaptic weights are left unaltered. This can be done simply by making the learning-rate parameter η_{ji} for synaptic weight w_{ji} equal to zero.

Stopping Criteria

In general, the back-propagation algorithm cannot be shown to converge, and there are no well-defined criteria for stopping its operation. Rather, there are some reasonable criteria, each with its own practical merit, that may be used to terminate the weight adjustments. To formulate such a criterion, it is logical to think in terms of the unique properties of a *local* or *global minimum* of the error surface.[3] Let the weight vector $\mathbf{w}^*$ denote a minimum, be it local or global. A necessary condition for $\mathbf{w}^*$ to be a minimum is that the gradient vector $\mathbf{g}(\mathbf{w})$ (i.e., first-order partial derivative) of the error surface with respect to the weight vector $\mathbf{w}$ must be zero at $\mathbf{w} = \mathbf{w}^*$. Accordingly, we may formulate a sensible convergence criterion for back-propagation learning as follows (Kramer and Sangiovanni-Vincentelli, 1989):

> *The back-propagation algorithm is considered to have converged when the Euclidean norm of the gradient vector reaches a sufficiently small gradient threshold.*

The drawback of this convergence criterion is that, for successful trials, learning times may be long. Also, it requires the computation of the gradient vector $\mathbf{g}(\mathbf{w})$.

Another unique property of a minimum that we can use is the fact that the cost function $\mathscr{E}_{\text{av}}(\mathbf{w})$ is stationary at the point $\mathbf{w} = \mathbf{w}^*$. We may therefore suggest a different criterion of convergence:

> *The back-propagation algorithm is considered to have converged when the absolute rate of change in the average squared error per epoch is sufficiently small.*

The rate of change in the average squared error is typically considered to be small enough if it lies in the range of 0.1 to 1 percent per epoch. Sometimes a value as small as 0.01 percent per epoch is used. Unfortunately, this criterion may result in a premature termination of the learning process.

There is another useful, and theoretically supported, criterion for convergence: After each learning iteration, the network is tested for its generalization performance. The learning process is stopped when the generalization performance is adequate or when it is apparent that the generalization performance has peaked; see Section 4.13 for more details.

Summary of the Back-Propagation Algorithm

Figure 4.1 presents the architectural layout of a multilayer perceptron. The corresponding signal-flow graph for back-propagation learning, incorporating both the forward and backward phases of the computations involved in the learning process, is presented in Fig. 4.7 for the case of $L = 2$ and $m_0 = m_1 = m_2 = 3$. The top part of the signal-flow graph accounts for the forward pass. The lower part of the signal-flow graph accounts for the backward pass, which is referred to as a *sensitivity graph* for computing the local gradients in the back-propagation algorithm (Narendra and Parthasarathy, 1990).

Earlier, we mentioned that the sequential updating of weights is the preferred method for on-line implementation of the back-propagation algorithm. For this mode

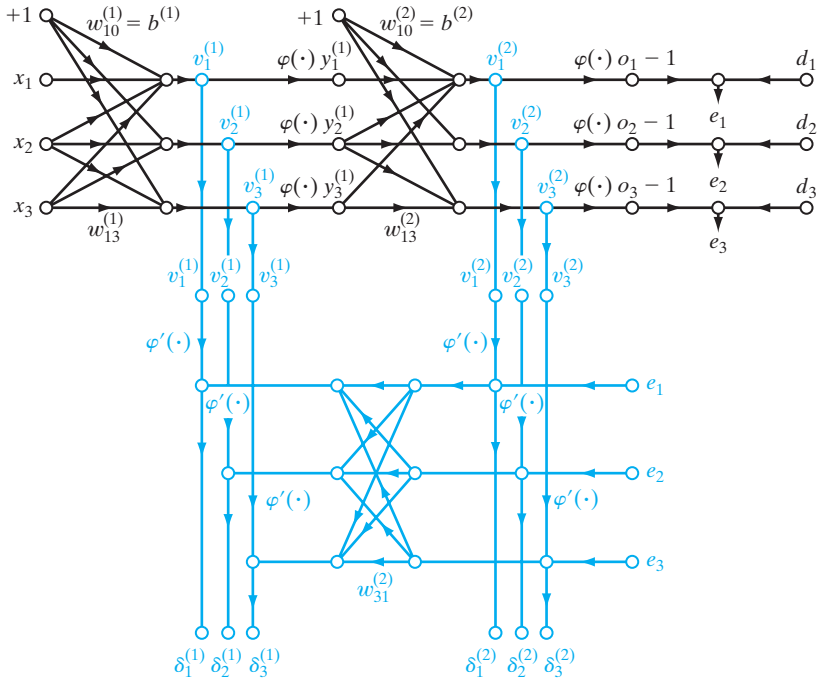

FIGURE 4.7 Signal-flow graphical summary of back-propagation learning. Top part of the graph: forward pass. Bottom part of the graph: backward pass.

of operation, the algorithm cycles through the training sample $\{(\mathbf{x}(n), \mathbf{d}(n))\}_{n=1}^{N}$ as follows:

1. *Initialization.* Assuming that no prior information is available, pick the synaptic weights and thresholds from a uniform distribution whose mean is zero and whose variance is chosen to make the standard deviation of the induced local fields of the neurons lie at the transition between the linear and standards parts of the sigmoid activation function.

2. *Presentations of Training Examples.* Present the network an epoch of training examples. For each example in the sample, ordered in some fashion, perform the sequence of forward and backward computations described under points 3 and 4, respectively.

3. *Forward Computation.* Let a training example in the epoch be denoted by $(\mathbf{x}(n), \mathbf{d}(n))$, with the input vector $\mathbf{x}(n)$ applied to the input layer of sensory nodes and the desired response vector $\mathbf{d}(n)$ presented to the output layer of computation nodes. Compute the induced local fields and function signals of the network by proceeding forward through the network, layer by layer. The induced local field $v_j^{(l)}(n)$ for neuron j in layer l is

$$v_j^{(l)}(n) = \sum_i w_{ji}^{(l)}(n) y_i^{(l-1)}(n) \tag{4.44}$$

where $y_i^{(l-1)}(n)$ is the output (function) signal of neuron i in the previous layer $l-1$ at iteration n, and $w_{ji}^{(l)}(n)$ is the synaptic weight of neuron j in layer l that is fed from neuron i in layer $l-1$. For $i = 0$, we have $y_0^{(l-1)}(n) = +1$, and $w_{j0}^{(l)}(n) = b_j^{(l)}(n)$ is the bias applied to neuron j in layer l. Assuming the use of a sigmoid function, the output signal of neuron j in layer l is

$$y_j^{(l)} = \varphi_j(v_j(n))$$

If neuron j is in the first hidden layer (i.e., $l = 1$), set

$$y_j^{(0)}(n) = x_j(n)$$

where $x_j(n)$ is the jth element of the input vector $\mathbf{x}(n)$. If neuron j is in the output layer (i.e., $l = L$, where L is referred to as the *depth* of the network), set

$$y_j^{(L)} = o_j(n)$$

Compute the error signal

$$e_j(n) = d_j(n) - o_j(n) \tag{4.45}$$

where $d_j(n)$ is the jth element of the desired response vector $\mathbf{d}(n)$.

4. *Backward Computation.* Compute the δs (i.e., local gradients) of the network, defined by

$$\delta_j^{(l)}(n) = \begin{cases} e_j^{(L)}(n)\varphi_j'(v_j^{(L)}(n)) & \text{for neuron } j \text{ in output layer } L \\ \varphi_j'(v_j^{(l)}(n)) \sum_k \delta_k^{(l+1)}(n) w^{(l+1)}_{kj}(n) & \text{for neuron } j \text{ in hidden layer } l \end{cases} \tag{4.46}$$

where the prime in $\varphi_j'(\cdot)$ denotes differentiation with respect to the argument. Adjust the synaptic weights of the network in layer l according to the generalized delta rule

$$w_{ji}^{(l)}(n+1) = w_{ji}^{(l)}(n) + \alpha[\Delta w_{ji}^{(l)}(n-1)] + \eta\delta_j^{(l)}(n) y_i^{(l-1)}(n) \tag{4.47}$$

where η is the learning-rate parameter and α is the momentum constant.

5. *Iteration.* Iterate the forward and backward computations under points 3 and 4 by presenting new epochs of training examples to the network until the chosen stopping criterion is met.

Notes: The order of presentation of training examples should be randomized from epoch to epoch. The momentum and learning-rate parameter are typically adjusted (and usually decreased) as the number of training iterations increases. Justification for these points will be presented later.

4.5 XOR PROBLEM

In Rosenblatt's single-layer perceptron, there are no hidden neurons. Consequently, it cannot classify input patterns that are not linearly separable. However, nonlinearly separable patterns commonly occur. For example, this situation arises in the *exclusive-OR (XOR) problem*, which may be viewed as a special case of a more general problem, namely, that of classifying points in the *unit hypercube*. Each point in the hypercube is in either class 0 or class 1. However, in the special case of the XOR problem, we need

consider only the four corners of a *unit square* that correspond to the input patterns (0,0), (0,1), (1,1), and (1,0), where a single bit (i.e., binary digit) changes as we move from one corner to the next. The first and third input patterns are in class 0, as shown by

$$0 \oplus 0 = 0$$

and

$$1 \oplus 1 = 0$$

where $\oplus$ denotes the exclusive-OR Boolean function operator. The input patterns (0,0) and (1,1) are at opposite corners of the unit square, yet they produce the identical output 0. On the other hand, the input patterns (0,1) and (1,0) are also at opposite corners of the square, but they are in class 1, as shown by

$$0 \oplus 1 = 1$$

and

$$1 \oplus 0 = 1$$

We first recognize that the use of a single neuron with two inputs results in a straight line for a decision boundary in the input space. For all points on one side of this line, the neuron outputs 1; for all points on the other side of the line, it outputs 0. The position and orientation of the line in the input space are determined by the synaptic weights of the neuron connected to the input nodes and the bias applied to the neuron. With the input patterns (0,0) and (1,1) located on opposite corners of the unit square, and likewise for the other two input patterns (0,1) and (1,0), it is clear that we cannot construct a straight line for a decision boundary so that (0,0) and (0,1) lie in one decision region and (0,1) and (1,0) lie in the other decision region. In other words, the single-layer perceptron cannot solve the XOR problem.

However, we may solve the XOR problem by using a single hidden layer with two neurons, as in Fig. 4.8a (Touretzky and Pomerleau, 1989). The signal-flow graph of the network is shown in Fig. 4.8b. The following assumptions are made here:

- Each neuron is represented by a McCulloch–Pitts model, which uses a threshold function for its activation function.
- Bits 0 and 1 are represented by the levels 0 and +1, respectively.

The top neuron, labeled as "Neuron 1" in the hidden layer, is characterized as

$$w_{11} = w_{12} = +1$$
$$b_1 = -\frac{3}{2}$$

The slope of the decision boundary constructed by this hidden neuron is equal to −1 and positioned as in Fig. 4.9a. The bottom neuron, labeled as "Neuron 2" in the hidden layer, is characterized as

$$w_{21} = w_{22} = +1$$
$$b_2 = -\frac{1}{2}$$

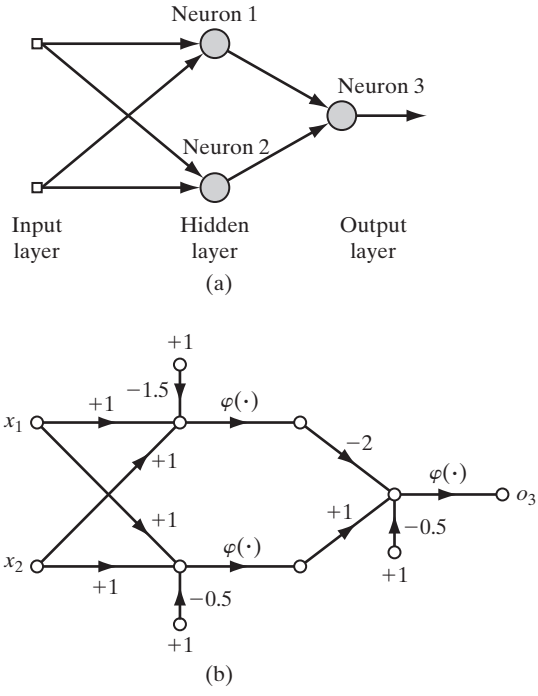

FIGURE 4.8 (a) Architectural graph of network for solving the XOR problem. (b) Signal-flow graph of the network.

The orientation and position of the decision boundary constructed by this second hidden neuron are as shown in Fig. 4.9b.

The output neuron, labeled as "Neuron 3" in Fig. 4.8a, is characterized as

$$w_{31} = -2$$
$$w_{32} = +1$$
$$b_3 = -\frac{1}{2}$$

The function of the output neuron is to construct a linear combination of the decision boundaries formed by the two hidden neurons. The result of this computation is shown in Fig. 4.9c. The bottom hidden neuron has an excitatory (positive) connection to the output neuron, whereas the top hidden neuron has an inhibitory (negative) connection to the output neuron. When both hidden neurons are off, which occurs when the input pattern is (0,0), the output neuron remains off. When both hidden neurons are on, which occurs when the input pattern is (1,1), the output neuron is switched off again because the inhibitory effect of the larger negative weight connected to the top hidden neuron overpowers the excitatory effect of the positive weight connected to the bottom hidden neuron. When the top hidden neuron is off and the bottom hidden neuron is on, which occurs when the input pattern is (0,1) or (1,0), the output neuron is switched on because of the excitatory effect of the positive weight connected to the bottom hidden neuron. Thus, the network of Fig. 4.8a does indeed solve the XOR problem.

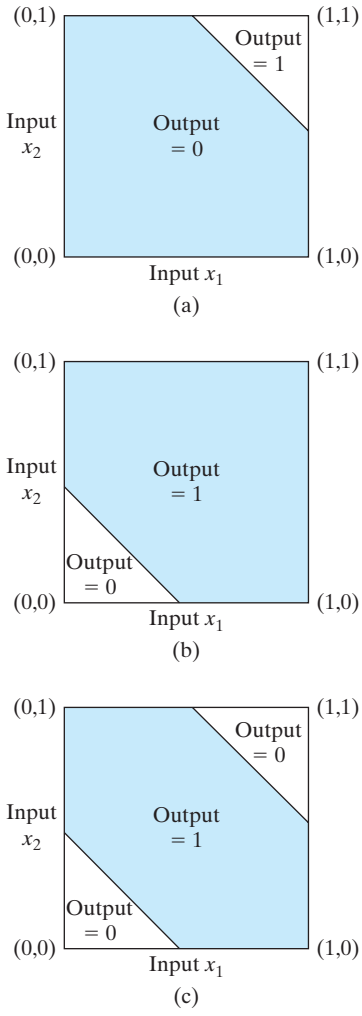

FIGURE 4.9 (a) Decision boundary constructed by hidden neuron 1 of the network in Fig. 4.8. (b) Decision boundary constructed by hidden neuron 2 of the network. (c) Decision boundaries constructed by the complete network.

4.6 HEURISTICS FOR MAKING THE BACK-PROPAGATION ALGORITHM PERFORM BETTER

It is often said that the design of a neural network using the back-propagation algorithm is more of an art than a science, in the sense that many of the factors involved in the design are the results of one's own personal experience. There is some truth in this statement. Nevertheless, there are methods that will significantly improve the back-propagation algorithm's performance, as described here:

1. *Stochastic versus batch update.* As mentioned previously, the stochastic (sequential) mode of back-propagation learning (involving pattern-by-pattern updating) is computationally faster than the batch mode. This is especially true when the

training data sample is large and highly redundant. (Highly redundant data pose computational problems for the estimation of the Jacobian required for the batch update.)

2. *Maximizing information content.* As a general rule, every training example presented to the back-propagation algorithm should be chosen on the basis that its information content is the largest possible for the task at hand (LeCun, 1993). Two ways of realizing this choice are as follows:

- Use an example that results in the largest training error.
- Use an example that is radically different from all those previously used.

These two heuristics are motivated by a desire to search more of the weight space.

In pattern-classification tasks using sequential back-propagation learning, a simple and commonly used technique is to randomize (i.e., shuffle) the order in which the examples are presented to the multilayer perceptron from one epoch to the next. Ideally, the randomization ensure that successive examples in an epoch presented to the network rarely belong to the same class.

3. *Activation function.* Insofar as the speed of learning is concerned, the preferred choice is to use a sigmoid activation function that is an *odd function of its argument*, as shown by

$$\varphi(-v) = -\varphi(v)$$

This condition is satisfied by the hyperbolic function

$$\varphi(v) = a \tanh(bv)$$

as shown in Fig. 4.10, but not the logistic function. Suitable values for the constraints a and b in the formula for $\varphi(v)$ are as follows (LeCun, 1993):

$$a = 1.7159$$

and

$$b = \frac{2}{3}$$

The hyperbolic tangent function $\varphi(v)$ of Fig. 4.10 has the following useful properties:

- $\varphi(1) = 1$ and $\varphi(-1) = -1$.
- At the origin, the slope (i.e., effective gain) of the activation function is close to unity, as shown by

$$\begin{aligned}\varphi(0) &= ab \\ &= 1.7159\left(\frac{2}{3}\right) \\ &= 1.1424\end{aligned}$$

- The second derivative of $\varphi(v)$ attains its maximum value at $v = 1$.

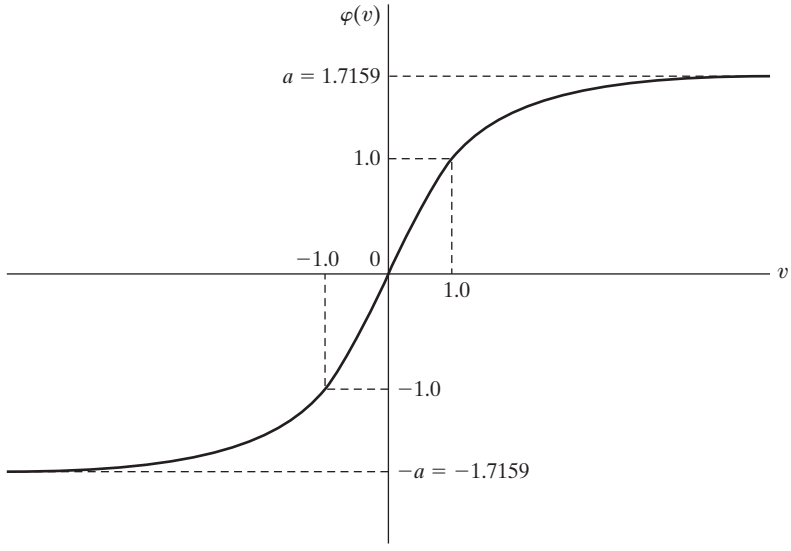

FIGURE 4.10 Graph of the hyperbolic tangent function $\varphi(v) = a\tanh(bv)$ for $a = 1.7159$ and $b = 2/3$. The recommended target values are $+1$ and -1.

4. *Target values.* It is important that the target values (desired response) be chosen within the range of the sigmoid activation function. More specifically, the desired response d_j for neuron j in the output layer of the multilayer perceptron should be *offset* by some amount ε away from the limiting value of the sigmoid activation function, depending on whether the limiting value is positive or negative. Otherwise, the back-propagation algorithm tends to drive the free parameters of the network to infinity and thereby slow down the learning process by driving the hidden neurons into saturation. To be specific, consider the hyperbolic tangent function of Fig. 4.10. For the limiting value $+a$, we set

$$d_j = a - \varepsilon$$

and for the limiting value of $-a$, we set

$$d_j = -a + \varepsilon$$

where ε is an appropriate positive constant. For the choice of $a = 1.7159$ used in Fig. 4.10, we may set $\varepsilon = 0.7159$, in which case the target value (desired response) d_j can be conveniently chosen as ± 1, as indicated in the figure.

5. *Normalizing the inputs.* Each input variable should be *preprocessed* so that its mean value, averaged over the entire training sample, is close to zero, or else it will be small compared to its standard deviation (LeCun, 1993). To appreciate the practical significance of this rule, consider the extreme case where the input variables are consistently positive. In this situation, the synaptic weights of a neuron in the first hidden layer can only increase together or decrease together. Accordingly, if the weight vector of that

neuron is to change direction, it can do so only by zigzagging its way through the error surface, which is typically slow and should therefore be avoided.

In order to accelerate the back-propagation learning process, the normalization of the inputs should also include two other measures (LeCun, 1993):

- The input variables contained in the training set should be *uncorrelated*; this can be done by using principal-components analysis, to be discussed in Chapter 8.
- The decorrelated input variables should be scaled so that their *covariances are approximately equal*, thereby ensuring that the different synaptic weights in the network learn at approximately the same speed.

Figure 4.11 illustrates the results of three normalization steps: mean removal, decorrelation, and covariance equalization, applied in that order.

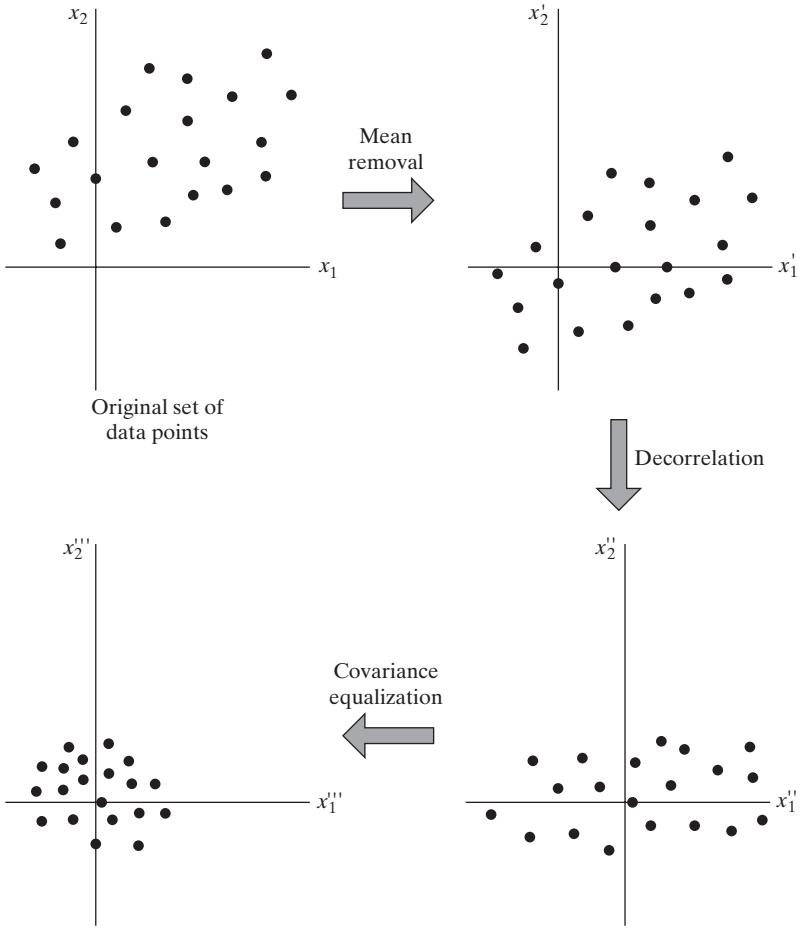

FIGURE 4.11 Illustrating the operation of mean removal, decorrelation, and covariance equalization for a two-dimensional input space.

It is also of interest to note that when the inputs are transformed in the manner illustrated in Fig. 4.11 and used in conjunction with the hyperbolic tangent function specified in Fig. 4.10, the variance of the individual neural outputs in the multilayer perceptron will be close to unity (Orr and Müller, 1998). The rationale for this statement is that the effective gain of the sigmoid function over its useful range is roughly unity.

6. *Initialization.* A good choice for the initial values of the synaptic weights and thresholds of the network can be of tremendous help in a successful network design. The key question is: What is a good choice?

When the synaptic weights are assigned large initial values, it is highly likely that the neurons in the network will be driven into saturation. If this happens, the local gradients in the back-propagation algorithm assume small values, which in turn will cause the learning process to slow down. However, if the synaptic weights are assigned small initial values, the back-propagation algorithm may operate on a very flat area around the origin of the error surface; this is particularly true in the case of sigmoid functions such as the hyperbolic tangent function. Unfortunately, the origin is a *saddle point*, which refers to a stationary point where the curvature of the error surface across the saddle is negative and the curvature along the saddle is positive. For these reasons, the use of both large and small values for initializing the synaptic weights should be avoided. The proper choice of initialization lies somewhere between these two extreme cases.

To be specific, consider a multilayer perceptron using the hyperbolic tangent function for its activation functions. Let the bias applied to each neuron in the network be set to zero. We may then express the induced local field of neuron j as

$$v_j = \sum_{i=1}^{m} w_{ji} y_i$$

Let it be assumed that the inputs applied to each neuron in the network have zero mean and unit variance, as shown by

$$\mu_y = \mathbb{E}[y_i] = 0 \qquad \text{for all } i$$

and

$$\sigma_y^2 = \mathbb{E}[(y_i - \mu_i)^2] = \mathbb{E}[y_i^2] = 1 \qquad \text{for all } i$$

Let it be further assumed that the inputs are uncorrelated, as shown by

$$\mathbb{E}[y_i y_k] = \begin{cases} 1 & \text{for } k = i \\ 0 & \text{for } k \neq i \end{cases}$$

and that the synaptic weights are drawn from a uniformly distributed set of numbers with zero mean, that is,

$$\mu_w = \mathbb{E}[w_{ji}] = 0 \qquad \text{for all } (j, i) \text{ pairs}$$

and variance

$$\sigma_w^2 = \mathbb{E}[(w_{ji} - \mu_w)^2] = \mathbb{E}[w_{ji}^2] \qquad \text{for all } (j, i) \text{ pairs}$$

Accordingly, we may express the mean and variance of the induced local field v_j as

$$\mu_v = \mathbb{E}[v_j] = \mathbb{E}\left[\sum_{i=1}^{m} w_{ji} y_i\right] = \sum_{i=1}^{m} \mathbb{E}[w_{ji}]\mathbb{E}[y_i] = 0$$

and

$$\begin{aligned}
\sigma_v^2 &= \mathbb{E}[(v_j - \mu_v)^2] = \mathbb{E}[v_j^2] \\
&= \mathbb{E}\left[\sum_{i=1}^{m}\sum_{k=1}^{m} w_{ji} w_{jk} y_i y_k\right] \\
&= \sum_{i=1}^{m}\sum_{k=1}^{m} \mathbb{E}[w_{ji} w_{jk}]\mathbb{E}[y_i y_k] \\
&= \sum_{i=1}^{m} \mathbb{E}[w_{ji}^2] \\
&= m\sigma_w^2
\end{aligned}$$

where m is the number of synaptic connections of a neuron.

In light of this result, we may now describe a good strategy for initializing the synaptic weights so that the standard deviation of the induced local field of a neuron lies in the transition area between the linear and saturated parts of its sigmoid activation function. For example, for the case of a hyperbolic tangent function with parameters a and b used in Fig. 4.10, this objective is satisfied by setting $\sigma_v = 1$ in the previous equation, in which case we obtain the following (LeCun, 1993):

$$\sigma_w = m^{-1/2} \tag{4.48}$$

Thus, it is desirable for the uniform distribution, from which the synaptic weights are selected, to have a mean of zero and a variance equal to the reciprocal of the number of synaptic connections of a neuron.

7. *Learning from hints.* Learning from a sample of training examples deals with an unknown input–output mapping function $f(\cdot)$. In effect, the learning process exploits the information contained in the examples about the function $f(\cdot)$ to *infer* an approximate implementation of it. The process of learning from examples may be generalized to *include learning from hints*, which is achieved by allowing prior information that we may have about the function $f(\cdot)$ to be included in the learning process (Abu-Mostafa, 1995). Such information may include invariance properties, symmetries, or any other knowledge about the function $f(\cdot)$ that may be used to accelerate the search for its approximate realization and, more importantly, to improve the quality of the final estimate. The use of Eq. (4.48) is an example of how this is achieved.

8. *Learning rates.* All neurons in the multilayer perceptron should ideally learn at the same rate. The last layers usually have larger local gradients than the layers at the front end of the network. Hence, the learning-rate parameter η should be assigned a

smaller value in the last layers than in the front layers of the multilayer perceptron. Neurons with many inputs should have a smaller learning-rate parameter than neurons with few inputs so as to maintain a similar learning time for all neurons in the network. In LeCun (1993), it is suggested that for a given neuron, the learning rate should be inversely proportional to the square root of synaptic connections made to that neuron.

4.7 COMPUTER EXPERIMENT: PATTERN CLASSIFICATION

In this computer experiment, we resume the sequence of pattern-classification experiments performed first in Chapter 1 using Rosenblatt's perceptron and then in Chapter 2 using the method of least squares. For both experiments, we used training and test data generated by randomly sampling the *double-moon* structure pictured in Fig. 1.8. In each of the experiments, we considered two cases, one employing linearly separable patterns and the other employing nonlinearly separable patterns. The perceptron worked perfectly fine for the linearly separable setting of $d = 1$, but the method of least squares required a larger separation between the two moons for perfect classification. In any event, they both failed the nonlinearly separable setting of $d = -4$.

The objective of the computer experiment presented herein is twofold:

1. to demonstrate that the multilayer perceptron, trained with the back-propagation algorithm, is capable of classifying nonlinearly separable test data;
2. to find a more difficult case of nonlinearly separable patterns for which the multilayer perceptron fails the double-moon classification test.

The specifications of the multilayer perceptron used in the experiment are as follows:

Size of the input layer: $m_0 = 2$
Size of the (only) hidden layer: $m_1 = 20$
Size of the output layer: $m_2 = 1$
Activation function: hyperbolic tangent function $\varphi(v) = \dfrac{1 - \exp(-2v)}{1 + \exp(-2v)}$
Threshold setting: zero
Learning-rate parameter η: annealed linearly from 10^{-1} down to 10^{-5}

The experiment is carried out in two parts, one corresponding to the vertical separation $d = -4$, and the other corresponding to $d = -5$:

(a) *Vertical separation $d = -4$.*
Figure 4.12 presents the results of the MLP experiment for the length of separation between the two moons of $d = -4$. Part (a) of the figure displays the learning curve resulting from the training session. We see that the learning curve reached convergence effectively in about 15 epochs of training. Part (b) of the figure displays the optimal nonlinear decision boundary computed by the MLP. Most important, perfect classification of the two patterns was achieved, with no classification errors. This perfect performance is attributed to the hidden layer of the MLP.

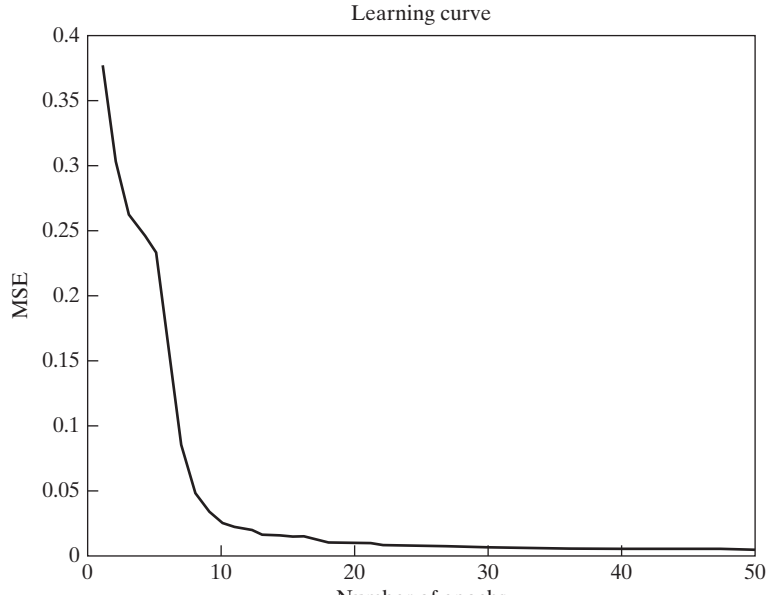

(a) Learning curve

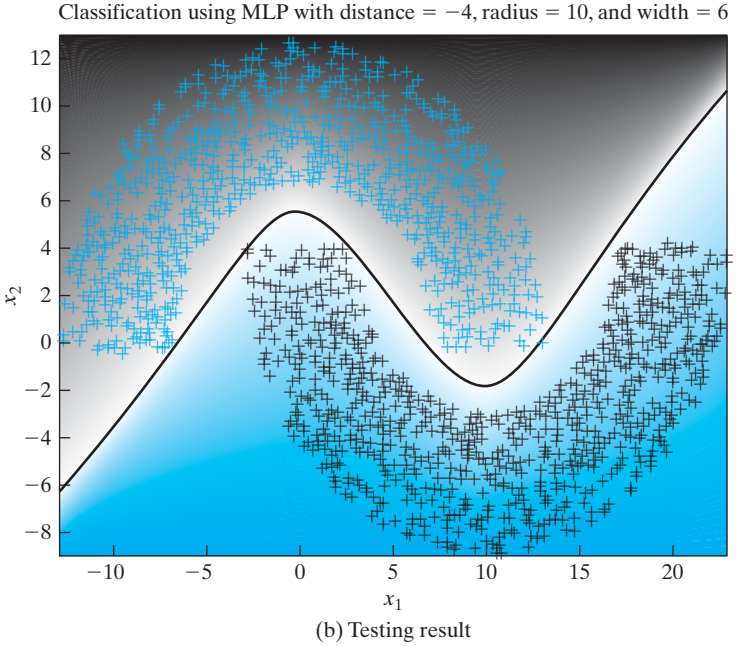

(b) Testing result

FIGURE 4.12 Results of the computer experiment on the back-propagation algorithm applied to the MLP with distance $d = -4$. MSE stands for mean-square error.

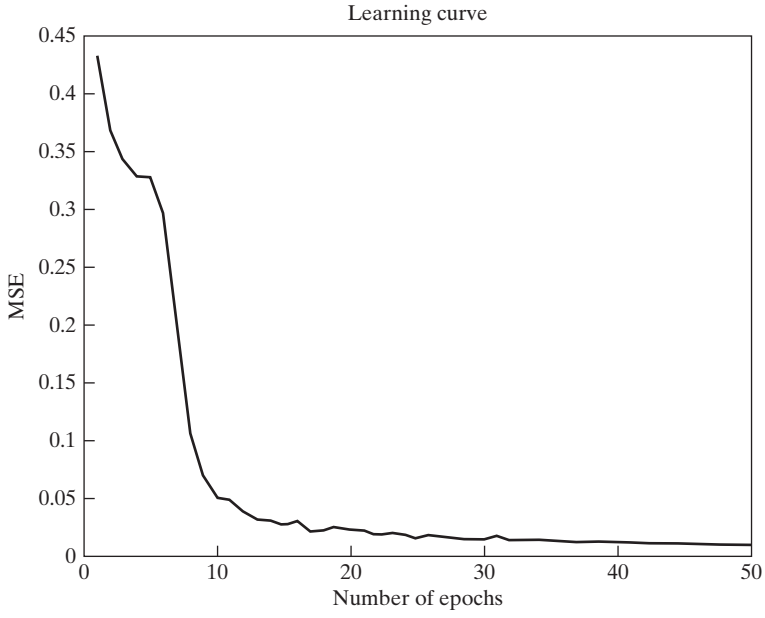

(a) Learning curve

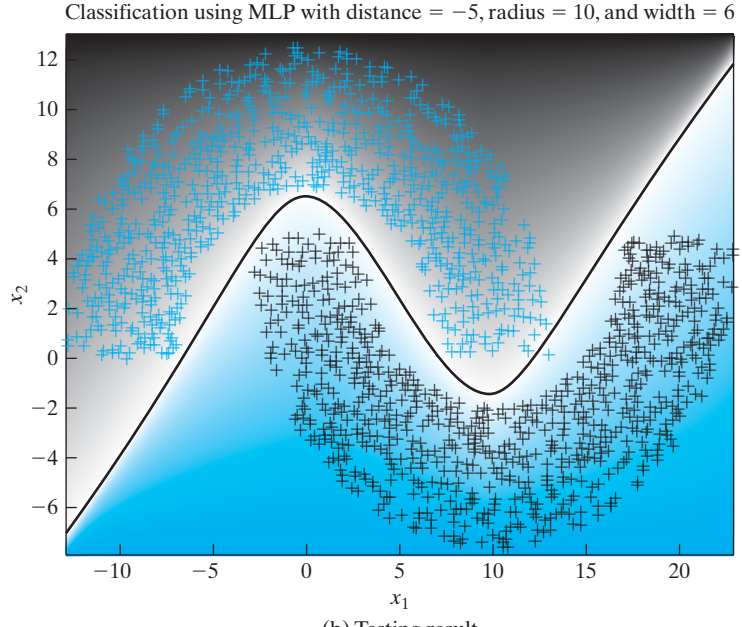

(b) Testing result

FIGURE 4.13 Results of the computer experiment on the back-propagation algorithm applied to the MLP with distance $d = -5$.

(b) *Vertical separation $d = -5$.*
To challenge the multilayer perceptron with a more difficult pattern-classification task, we reduced the vertical separation between the two moons to $d = -5$. The results of this second part of the experiment are presented in Fig. 4.13. The learning curve of the back-propagation algorithm, plotted in part (a) of the figure, shows a slower rate of convergence, roughly three times that for the easier case of $d = -4$. Moreover, the testing results plotted in part (b) of the figure reveal three classification errors in a testing set of 2,000 data points, representing an error rate of 0.15 percent.

The decision boundary is computed by finding the coordinates x_1 and x_2 pertaining to the input vector $\mathbf{x}$, for which the response of the output neuron is zero on the premise that the two classes of the experiment are equally likely. Accordingly, when a threshold of zero is exceeded, a decision is made in favor of one class; otherwise, the decision is made in favor of the other class. This procedure is followed on all the double-moon classification experiments reported in the book.

4.8 BACK PROPAGATION AND DIFFERENTIATION

Back propagation is a specific technique for implementing *gradient descent* in weight space for a multilayer perceptron. The basic idea is to efficiently compute *partial derivatives* of an approximating function $F(\mathbf{w}, \mathbf{x})$ realized by the network with respect to all the elements of the adjustable weight vector $\mathbf{w}$ for a given value of input vector $\mathbf{x}$. Herein lies the computational power of the back-propagation algorithm.[4]

To be specific, consider a multilayer perceptron with an input layer of m_0 nodes, two hidden layers, and a single output neuron, as depicted in Fig. 4.14. The elements of the weight vector $\mathbf{w}$ are ordered by layer (starting from the first hidden layer), then by neurons in a layer, and then by the number of a synapse within a neuron. Let $w_{ji}^{(l)}$ denote the synaptic weight from neuron i to neuron j in layer $l = 1, 2, \ldots$. For $l = 1$, corresponding to the first hidden layer, the index i refers to a source node rather than to a

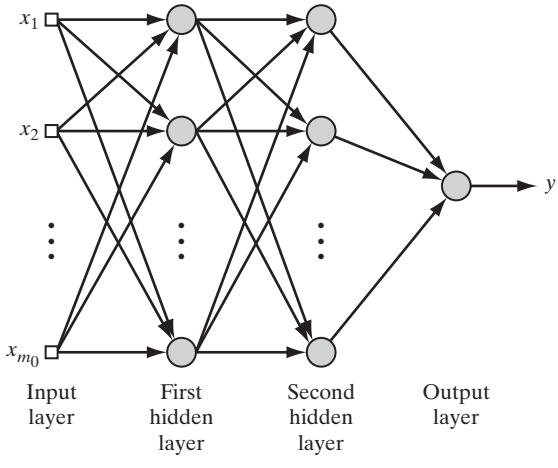

FIGURE 4.14 Multilayer perceptron with two hidden layers and one output neuron.

neuron. For $l = 3$, corresponding to the output layer in Fig. 4.14, we have $j = 1$. We wish to evaluate the derivatives of the function $F(\mathbf{w}, \mathbf{x})$ with respect to all the elements of the weight vector $\mathbf{w}$ for a specified input vector $\mathbf{x} = [x_1, x_2, ..., x_{m_0}]^T$. We have included the weight vector $\mathbf{w}$ as an argument of the function F in order to focus attention on it. For example, for $l = 2$ (i.e., a single hidden layer and a linear output layer), we have

$$F(\mathbf{w}, \mathbf{x}) = \sum_{j=0}^{m_1} w_{oj} \varphi\left(\sum_{i=0}^{m_0} w_{ji} x_i \right) \tag{4.49}$$

where $\mathbf{w}$ is the ordered weight vector and $\mathbf{x}$ is the input vector.

The multilayer perceptron of Fig. 4.14 is parameterized by an *architecture* $\mathcal{A}$ (representing a discrete parameter) and a *weight vector* $\mathbf{w}$ (made up of continuous elements). Let $\mathcal{A}_j^{(l)}$ denote that part of the architecture extending from the input layer ($l = 0$) to node j in layer $l = 1, 2, 3$. Accordingly, we may write

$$F(\mathbf{w}, \mathbf{x}) = \varphi(\mathcal{A}_1^{(3)}) \tag{4.50}$$

where φ is the activation function. However, $\mathcal{A}_1^{(3)}$ is to be interpreted merely as an architectural symbol rather than a variable. Thus, adapting Eqs. (4.2), (4.4), (4.13), and (4.25) for use in this new situation, we obtain the formulas

$$\frac{\partial F(\mathbf{w}, \mathbf{x})}{\partial w_{1k}^{(3)}} = \varphi'(\mathcal{A}_1^{(3)}) \varphi(\mathcal{A}_k^{(2)}) \tag{4.51}$$

$$\frac{\partial F(\mathbf{w}, \mathbf{x})}{\partial w_{kj}^{(2)}} = \varphi'(\mathcal{A}_1^{(3)}) \varphi'(\mathcal{A}_k^{(2)}) \varphi(\mathcal{A}_j^{(1)}) w_{1k}^{(3)} \tag{4.52}$$

$$\frac{\partial F(\mathbf{w}, \mathbf{x})}{\partial w_{ji}^{(1)}} = \varphi'(\mathcal{A}_1^{(3)}) \varphi'(\mathcal{A}_j^{(1)}) x_i \left[\sum_k w_{1k}^{(3)} \varphi'(\mathcal{A}_k^{(2)}) w_{kj}^{(2)} \right] \tag{4.53}$$

where φ' is the partial derivative of the nonlinearity φ with respect to its argument and x_i is the ith element of the input vector $\mathbf{x}$. In a similar way, we may derive the equations for the partial derivatives of a general network with more hidden layers and more neurons in the output layer.

Equations (4.51) through (4.53) provide the basis for calculating the sensitivity of the network function $F(\mathbf{w}, \mathbf{x})$ with respect to variations in the elements of the weight vector $\mathbf{w}$. Let ω denote an element of the weight vector $\mathbf{w}$. The *sensitivity* of $F(\mathbf{w}, \mathbf{x})$ with respect to ω, is formally defined by

$$S_\omega^F = \frac{\partial F / F}{\partial \omega / \omega}$$

It is for this reason that we refer to the lower part of the signal-flow graph in Fig. 4.7 as a "sensitivity graph."

The Jacobian

Let W denote the total number of free parameters (i.e., synaptic weights and biases) of a multilayer perceptron, which are ordered in a manner described to form the weight vector $\mathbf{w}$. Let N denote the total number of examples used to train the network. Using back

propagation, we may compute a set of W partial derivatives of the approximating function $F[\mathbf{w}, \mathbf{x}(n)]$ with respect to the elements of the weight vector $\mathbf{w}$ for a specific example $\mathbf{x}(n)$ in the training sample. Repeating these computations for $n = 1, 2, \ldots, N$, we end up with an N-by-W matrix of partial derivatives. This matrix is called the *Jacobian* $\mathbf{J}$ of the multilayer perceptron evaluated at $\mathbf{x}(n)$. Each row of the Jacobian corresponds to a particular example in the training sample.

There is experimental evidence to suggest that many neural network training problems are intrinsically *ill conditioned*, leading to a Jacobian $\mathbf{J}$ that is almost rank deficient (Saarinen et al., 1991). The *rank* of a matrix is equal to the number of linearly independent columns or rows in the matrix, whichever one is smallest. The Jacobian $\mathbf{J}$ is said to be *rank deficient* if its rank is less than min (N, W). Any rank deficiency in the Jacobian causes the back-propagation algorithm to obtain only partial information of the possible search directions. Rank deficiency also causes training times to be long.

4.9 THE HESSIAN AND ITS ROLE IN ON-LINE LEARNING

The *Hessian matrix*, or simply the *Hessian*, of the cost function $\mathscr{E}_{\text{av}}(\mathbf{w})$, denoted by $\mathbf{H}$, is defined as the second derivative of $\mathscr{E}_{\text{av}}(\mathbf{w})$ with respect to the weight vector $\mathbf{w}$, as shown by

$$\mathbf{H} = \frac{\partial^2 \mathscr{E}_{\text{av}}(\mathbf{w})}{\partial \mathbf{w}^2} \tag{4.54}$$

The Hessian plays an important role in the study of neural networks; specifically, we mention the following points[5]:

1. The eigenvalues of the Hessian have a profound influence on the dynamics of back-propagation learning.
2. The inverse of the Hessian provides a basis for pruning (i.e., deleting) insignificant synaptic weights from a multilayer perceptron; this issue will be discussed in Section 4.14.
3. The Hessian is basic to the formulation of second-order optimization methods as an alternative to back-propagation learning, to be discussed in Section 4.16.

In this section, we confine our attention to point 1.

In Chapter 3, we indicated that the eigenstructure of the Hessian has a profound influence on the convergence properties of the LMS algorithm. So it is also with the back-propagation algorithm, but in a much more complicated way. Typically, the Hessian of the error surface pertaining to a multilayer perceptron trained with the back-propagation algorithm has the following composition of eigenvalues (LeCun et al., 1998):

- a small number of small eigenvalues,
- a large number of medium-sized eigenvalues, and
- a small number of large eigenvalues.

There is therefore a wide spread in the eigenvalues of the Hessian.

The factors affecting the composition of the eigenvalues may be grouped as follows:

- nonzero-mean input signals or nonzero-mean induced neural output signals;
- correlations between the elements of the input signal vector and correlations between induced neural output signals;
- wide variations in the second-order derivatives of the cost function with respect to synaptic weights of neurons in the network as we proceed from one layer to the next. These derivatives are often smaller in the lower layers, with the synaptic weights in the first hidden layer learning slowly and those in the last layers learning quickly.

Avoidance of Nonzero-mean Inputs

From Chapter 3, we recall that the *learning time* of the LMS algorithm is sensitive to variations in the condition number $\lambda_{max}/\lambda_{min}$, where λ_{max} is the largest eigenvalue of the Hessian and λ_{min} is its smallest nonzero eigenvalue. Experimental results show that a similar situation holds for the back-propagation algorithm, which is a generalization of the LMS algorithm. For inputs with nonzero mean, the ratio $\lambda_{max}/\lambda_{min}$ is larger than its corresponding value for zero-mean inputs: The larger the mean of the inputs, the larger the ratio $\lambda_{max}/\lambda_{min}$ will be. This observation has a serious implication for the dynamics of back-propagation learning.

For the learning time to be minimized, the use of nonzero-mean inputs should be avoided. Now, insofar as the signal vector $\mathbf{x}$ applied to a neuron in the first hidden layer of a multilayer perceptron (i.e., the signal vector applied to the input layer) is concerned, it is easy to remove the mean from each element of $\mathbf{x}$ before its application to the network. But what about the signals applied to the neurons in the remaining hidden and output layers of the network? The answer to this question lies in the type of activation function used in the network. In the case of the logistic function, the output of each neuron is restricted to the interval $[0, 1]$. Such a choice acts as a source of *systematic bias* for those neurons located beyond the first hidden layer of the network. To overcome this problem, we need to use the hyperbolic tangent function that is odd symmetric. With this latter choice, the output of each neuron is permitted to assume both positive and negative values in the interval $[-1, 1]$, in which case it is likely for its mean to be zero. If the network connectivity is large, back-propagation learning with odd-symmetric activation functions can yield faster convergence than a similar process with nonsymmetric activation functions. This condition provides the justification for heuristic 3 described in Section 4.6.

Asymptotic Behavior of On-line Learning

For a good understanding of on-line learning, we need to know how the ensemble-averaged learning curve evolves across time. Unlike the LMS algorithm, this calculation is unfortunately much too difficult to perform. Generally speaking, the error-performance surface may have exponentially many local minima and multiple global minima because of symmetry properties of the network. Surprisingly, this characteristic of the error-performance surface may turn out to be a useful feature in the following sense: Given that an early-stopping method is used for network training (see Section 4.13) or the

network is regularized (see Section 4.14), we may nearly always find ourselves "close" to a local minimum.

In any event, due to the complicated nature of the error-performance surface, we find that in the literature, statistical analysis of the learning curve is confined to its asymptotic behavior in the neighborhood of a local minimum. In this context, we may highlight some important aspects of this asymptotic behavior, assuming a fixed learning-rate parameter, as follows (Murata, 1998):

(i) The learning curve consists of three terms:
- *minimal loss*, determined by the optimal parameter $\mathbf{w}^*$, which pertains to a local or global minimum;
- *additional loss*, caused by fluctuations in evolution of the weight-vector estimator $w(n)$ around the mean

$$\lim_{n\to\infty} \mathbb{E}[\hat{\mathbf{w}}(n)] = \mathbf{w}^*$$

- *a time-dependent term*, describing the effect of decreasing speed of error convergence on algorithmic performance.

(ii) To ensure stability of the on-line learning algorithm, the learning-rate parameter η must be assigned a value smaller than the reciprocal of the largest eigenvalue of the Hessian, $1/\lambda_{max}$. On the other hand, the speed of convergence of the algorithm is dominated by the smallest eigenvalue of the Hessian, λ_{min}.

(iii) Roughly speaking, if the learning-rate parameter η is assigned a large value, then the speed of convergence is fast, but there will be large fluctuations around the local or global minimum, even if the number of iterations, n, approaches infinity. Conversely, if η is small, then the extent of fluctuations is small, but the speed of convergence will be slow.

4.10 OPTIMAL ANNEALING AND ADAPTIVE CONTROL OF THE LEARNING RATE

In Section 4.2, we emphasized the popularity of the on-line learning algorithm for two main reasons:

(i) The algorithm is simple, in that its implementation requires a minimal amount of memory, which is used merely to store the old value of the estimated weight vector from one iteration to the next.

(ii) With each example $\{\mathbf{x}, \mathbf{d}\}$ being used only once at every time-step, the learning rate assumes a more important role in on-line learning than in batch learning, in that the on-line learning algorithm has the built-in ability to *track* statistical variations in the environment responsible for generating the training set of examples.

In Amari (1967) and, more recently, Opper (1996), it is shown that *optimally annealed* on-line learning is enabled to operate as fast as batch learning in an *asymptotic sense*. This issue is explored in what follows.

Optimal Annealing of the Learning Rate

Let $\mathbf{w}$ denote the vector of synaptic weights in the network, stacked up on top of each other in some orderly fashion. With $\hat{\mathbf{w}}(n)$ denoting the *old estimate* of the weight vector $\mathbf{w}$ at time-step n, let $\hat{\mathbf{w}}(n+1)$ denote the *updated estimate* of $\mathbf{w}$ on receipt of the "input-desired response" example $\{\mathbf{x}(n+1), \mathbf{d}(n+1)\}$. Correspondingly, let $\mathbf{F}(\mathbf{x}(n+1); \hat{\mathbf{w}}(n))$ denote the vector-valued output of the network produced in response to the input $\mathbf{x}(n+1)$; naturally the dimension of the function $\mathbf{F}$ must be the same as that of the desired response vector $\mathbf{d}(n)$. Following the defining equation of Eq. (4.3), we may express the instantaneous energy as the squared Euclidean norm of the estimation error, as shown by

$$\mathscr{E}(\mathbf{x}(n), \mathbf{d}(n); \mathbf{w}) = \frac{1}{2}\|\mathbf{d}(n) - \mathbf{F}(\mathbf{x}(n); \mathbf{w})\|^2 \tag{4.55}$$

The *mean-square error*, or *expected risk*, of the on-line learning problem is defined by

$$J(\mathbf{w}) = \mathbb{E}_{\mathbf{x},\mathbf{d}}[\mathscr{E}(\mathbf{x}, \mathbf{d}; \mathbf{w})] \tag{4.56}$$

where $\mathbb{E}_{\mathbf{x},\mathbf{d}}$ is the expectation operator performed with respect to the example $\{\mathbf{x}, \mathbf{d}\}$. The solution

$$\mathbf{w}^* = \arg\min_{\mathbf{w}}[J(\mathbf{w})] \tag{4.57}$$

defines the *optimal parameter vector*.

The instantaneous *gradient vector* of the learning process is defined by

$$\begin{aligned}\mathbf{g}(\mathbf{x}(n), \mathbf{d}(n); \mathbf{w}) &= \frac{\partial}{\partial \mathbf{w}}\mathscr{E}(\mathbf{x}(n), \mathbf{d}(n); \mathbf{w}) \\ &= -(\mathbf{d}(n) - \mathbf{F}(\mathbf{x}(n); \mathbf{w})\mathbf{F}'(\mathbf{x}(n); \mathbf{w})\end{aligned} \tag{4.58}$$

where

$$\mathbf{F}'(\mathbf{x}; \mathbf{w}) = \frac{\partial}{\partial \mathbf{w}}\mathbf{F}(\mathbf{x}; \mathbf{w}) \tag{4.59}$$

With the definition of the gradient vector just presented, we may now express the on-line learning algorithm as

$$\hat{\mathbf{w}}(n+1) = \hat{\mathbf{w}}(n) - \eta(n)\mathbf{g}(\mathbf{x}(n+1), \mathbf{d}(n+1); \hat{\mathbf{w}}(n)) \tag{4.60}$$

or, equivalently,

$$\underbrace{\hat{\mathbf{w}}(n+1)}_{\substack{\text{Updated}\\ \text{estimate}}} = \underbrace{\hat{\mathbf{w}}(n)}_{\substack{\text{Old}\\ \text{estimate}}} + \underbrace{\eta(n)}_{\substack{\text{Learning-}\\ \text{rate}\\ \text{parameter}}}\underbrace{[\mathbf{d}(n+1) - \mathbf{F}(\mathbf{x}(n+1); \hat{\mathbf{w}}(n))]}_{\text{Error signal}}\underbrace{\mathbf{F}'(\mathbf{x}(n+1); \hat{\mathbf{w}}(n))}_{\substack{\text{Partial derivative of}\\ \text{the network function } \mathbf{F}}} \tag{4.61}$$

Given this difference equation, we may go on to describe the *ensemble-averaged dynamics* of the weight vector $\mathbf{w}$ in the neighborhood of the optimal parameter $\mathbf{w}^*$ by the continuous differential equation

$$\frac{d}{dt}\hat{\mathbf{w}}(t) = -\eta(t)\mathbb{E}_{\mathbf{x},\mathbf{d}}[\mathbf{g}(\mathbf{x}(t), \mathbf{d}(t); \hat{\mathbf{w}}(t))] \tag{4.62}$$

where t denotes continuous time. Following Murata (1998), the expected value of the gradient vector is approximated by

$$\mathbb{E}_{\mathbf{x},\mathbf{d}}[\mathbf{g}(\mathbf{x}, \mathbf{d}; \hat{\mathbf{w}}(t))] \approx -\mathbf{K}^*(\mathbf{w}^* - \hat{\mathbf{w}}(t)) \tag{4.63}$$

where the ensembled-averaged matrix $\mathbf{K}^*$ is itself defined by

$$\begin{aligned}\mathbf{K}^* &= \mathbb{E}_{\mathbf{x},\mathbf{d}}\left[\frac{\partial}{\partial \mathbf{w}}\mathbf{g}(\mathbf{x}, \mathbf{d}; \mathbf{w})\right] \\ &= \mathbb{E}_{\mathbf{x},\mathbf{d}}\left[\frac{\partial^2}{\partial \mathbf{w}^2}\mathscr{E}(\mathbf{x}, \mathbf{d}; \mathbf{w})\right]\end{aligned} \tag{4.64}$$

The new Hessian $\mathbf{K}^*$ is a positive-definite matrix defined differently from the Hessian $\mathbf{H}$ of Eq. (4.54). However, if the environment responsible for generating the training examples $\{\mathbf{x}, \mathbf{d}\}$ is *ergodic*, we may then substitute the Hessian $\mathbf{H}$, based on time averaging, for the Hessian $\mathbf{K}^*$, based on ensemble-averaging. In any event, using Eq. (4.63) in Eq. (4.62), we find that the continuous differential equation describing the evolution of the estimator $\hat{\mathbf{w}}(t)$ may be approximated as

$$\frac{d}{dt}\hat{\mathbf{w}}(t) \approx -\eta(t)\mathbf{K}^*(\mathbf{w}^* - \hat{\mathbf{w}}(t)) \tag{4.65}$$

Let the vector $\mathbf{q}$ denote an eigenvector of the matrix $\mathbf{K}^*$, as shown by the defining equation

$$\mathbf{K}^*\mathbf{q} = \lambda\mathbf{q} \tag{4.66}$$

where λ is the eigenvalue associated with the eigenvector $\mathbf{q}$. We may then introduce the new function

$$\xi(t) = \mathbb{E}_{\mathbf{x},\mathbf{d}}[\mathbf{q}^T\mathbf{g}(\mathbf{x}, \mathbf{d}; \hat{\mathbf{w}}(t))] \tag{4.67}$$

which, in light of Eq. (4.63), may itself be approximated as

$$\begin{aligned}\xi(t) &\approx -\mathbf{q}^T\mathbf{K}^*(\mathbf{w}^* - \hat{\mathbf{w}}(t)) \\ &= -\lambda\mathbf{q}^T(\mathbf{w}^* - \hat{\mathbf{w}}(t))\end{aligned} \tag{4.68}$$

At each instant of time t, the function $\xi(t)$ takes on a scalar value, which may be viewed as an approximate measure of the *Euclidean distance* between two projections onto the eigenvector $\mathbf{q}$, one due to the optimal parameter $\mathbf{w}^*$ and the other due to the estimator $\hat{\mathbf{w}}(t)$. The value of $\xi(t)$ is therefore reduced to zero if, and when, the estimator $\hat{\mathbf{w}}(t)$ converges to $\mathbf{w}^*$.

From Eqs. (4.65), (4.66), and (4.68), we find that the function $\xi(t)$ is related to the time-varying learning-rate parameter $\eta(t)$ as follows:

$$\frac{d}{dt}\xi(t) = -\lambda\eta(t)\xi(t) \tag{4.69}$$

This differential equation may be solved to yield

$$\xi(t) = c\exp(-\lambda\textstyle\int\eta(t)dt) \tag{4.70}$$

where c is a positive integration constant.

Following the annealing schedule due to Darken and Moody (1991) that was discussed in Chapter 3 on the LMS algorithm, let the formula

$$\eta(t) = \frac{\tau}{t + \tau}\,\eta_0 \tag{4.71}$$

account for dependence of the learning-rate on time t, where τ and η_0 are positive *tuning parameters*. Then, substituting this formula into Eq. (4.70), we find that the corresponding formula tor the function $\xi(t)$ is

$$\xi(t) = c(t + \tau)^{-\lambda\tau\eta_0} \tag{4.72}$$

For $\xi(t)$ to vanish as time t approaches infinity, we require that the product term $\lambda\tau\eta_0$ in the exponent be large compared with unity, which may be satisfied by setting $\eta_0 = \alpha/\lambda$ for positive α.

Now, there remains only the issue of how to choose the eigenvector $\mathbf{q}$. From the previous section, we recall that the convergence speed of the learning curve is dominated by the smallest eigenvalue $\lambda_{\min}$ of the Hessian $\mathbf{H}$. With this Hessian and the new Hessian $\mathbf{K}^*$ tending to behave similarly, a clever choice is to hypothesize that for a sufficiently large number of iterations, the evolution of the estimator $\hat{\mathbf{w}}(t)$ over time t may be considered as a one-dimensional process, running "almost parallel" to the eigenvector of the Hessian $\mathbf{K}^*$ associated with the smallest eigenvalue $\lambda_{\min}$, as illustrated in Fig. 4.15. We may thus set

$$\mathbf{q} = \frac{\mathbb{E}_{\mathbf{x},\mathbf{d}}[\mathbf{g}(\mathbf{x}, \mathbf{d}; \hat{\mathbf{w}})]}{\|\mathbb{E}_{\mathbf{x},\mathbf{d}}[\mathbf{g}(\mathbf{x}, \mathbf{d}; \hat{\mathbf{w}})]\|} \tag{4.73}$$

where the normalization is introduced to make the eigenvector $\mathbf{q}$ assume unit Euclidean length. Correspondingly, the use of this formula in Eq. (4.67) yields

$$\xi(t) = \|\mathbb{E}_{\mathbf{x},\mathbf{d}}[\mathbf{g}(\mathbf{x}, \mathbf{d}; \hat{\mathbf{w}}(t))]\| \tag{4.74}$$

We may now summarize the results of the discussion presented in this section by making the following statements:

1. The choice of the annealing schedule described in Eq. (4.71) satisfies the two conditions

$$\sum_t \eta(t) \to \infty \text{ and } \sum_t \eta^2(t) > \infty, \text{ as } t \to \infty \tag{4.75}$$

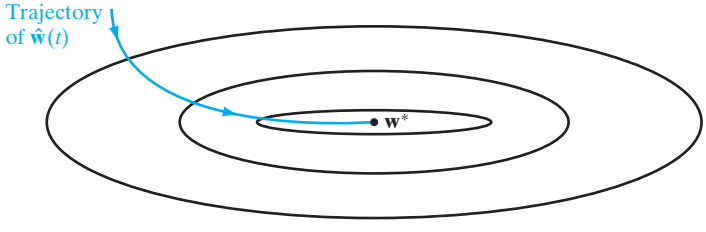

FIGURE 4.15 The evolution of the estimator $\hat{\mathbf{w}}(t)$ over time t. The ellipses represent contours of the expected risk for varying values of $\mathbf{w}$, assumed to be two-dimensional.

In other words, $\eta(t)$ satisfies the requirements of *stochastic approximation theory* (Robbins and Monro, 1951).

2. As time t approaches infinity, the function $\xi(t)$ approaches zero asymptotically. In accordance with Eq. (4.68), it follows that the estimator $\hat{\mathbf{w}}(t)$ approaches the optimal estimator $\mathbf{w}^*$ as t approaches infinity.
3. The ensemble-averaged trajectory of the estimator $\hat{\mathbf{w}}(t)$ is almost parallel to the eigenvector of the Hessian $\mathbf{K}^*$ associated with the smallest eigenvalue $\lambda_{\min}$ after a large enough number of iterations.
4. The optimally annealed on-line learning algorithm for a network characterized by the weight vector $\mathbf{w}$ is collectively described by the following set of three equations:

$$\left.\begin{aligned} &\underbrace{\hat{\mathbf{w}}(n+1)}_{\text{Updated estimate}} = \underbrace{\hat{\mathbf{w}}(n)}_{\text{Old estimate}} + \underbrace{\eta(n)}_{\text{Learning-rate parameter}}\underbrace{(\mathbf{d}(n+1) - \mathbf{F}(\mathbf{x}(n)+1;\ \hat{\mathbf{w}}(n))}_{\text{Error signal}}\underbrace{\mathbf{F}'(\mathbf{x}(n+1);\ \hat{\mathbf{w}}(n))}_{\text{Partial derivative of the network function } \mathbf{F}} \\ &\eta(n) = \frac{n_{\text{switch}}}{n + n_{\text{switch}}}\,\eta_0 \\ &\eta_0 = \frac{\alpha}{\lambda_{\min}}, \qquad \alpha = \text{positive constant} \end{aligned}\right\} \quad (4.76)$$

Here, it is assumed that the environment responsible for generating the training examples $\{\mathbf{x}, \mathbf{d}\}$ is ergodic, so that the ensemble-averaged Hessian $\mathbf{K}^*$ assumes the same value as the time-averaged Hessian $\mathbf{H}$.

5. When the learning-rate parameter η_0 is *fixed* in on-line learning based on stochastic gradient descent, stability of the algorithm requires that we choose $\eta_0 < 1/\lambda_{\max}$, where $\lambda_{\max}$ is the largest eigenvalue of the Hessian $\mathbf{H}$. On the other hand, in the case of optimally annealed stochastic gradient descent, according to the third line of Eq. (4.76), the choice is $\eta_0 < 1/\lambda_{\min}$, where $\lambda_{\min}$ is the smallest eigenvalue of $\mathbf{H}$.
6. The *time constant* n_{switch}, a positive integer, defines the *transition* from a regime of fixed η_0 to the annealing regime, where the time-varying learning-rate parameter $\eta(n)$ assumes the desired form c/n, where c is a constant, in accordance with stochastic approximation theory.

Adaptive Control of the Learning Rate

The optimal annealing schedule, described in the second line of Eq. (4.76), provides an important step in improved utilization of on-line learning. However, a practical limitation of this annealing schedule is the requirement that we know the time constant η_{switch} a priori. A practical issue of concern, then, is the fact that when the application of interest builds on the use of on-line learning in a nonstationary environment where the statistics of the training sequence change from one example to the next, the use of a prescribed time constant n_{switch} may no longer be a realistic option. In situations of this kind, which occur frequently in practice, the on-line learning algorithm needs to be equipped with a built-in mechanism for the *adaptive control* of the learning rate. Such

a mechanism was first described in the literature by Murata (1998), in which the so-called *learning of the learning algorithm* (Sompolinsky et al., 1995) was appropriately modified.

The adaptive algorithm due to Murata is configured to achieve two objectives:

1. *automatic adjustment* of the learning rate, which accounts for statistical variations in the environment responsible for generation of the training sequence of examples;
2. *generalization* of the on-line learning algorithm so that its applicability is broadened by avoiding the need for a prescribed cost function.

To be specific, the ensemble-averaged dynamics of the weight vector $\mathbf{w}$, defined in Eq. (4.62), is now rewritten as[6]

$$\frac{d}{dt}\hat{\mathbf{w}}(t) = -\eta(t)\mathbb{E}_{\mathbf{x},\mathbf{d}}[\mathbf{f}(\mathbf{x}(t), \mathbf{d}(t); \hat{\mathbf{w}}(t))] \tag{4.77}$$

where the vector-valued function $\mathbf{f}(\cdot,\cdot;\cdot)$ denotes *flow* that determines the change applied to the estimator $\hat{\mathbf{w}}(t)$ in response to the incoming example $\{\mathbf{x}(t), \mathbf{d}(t)\}$. The flow $\mathbf{f}$ is required to satisfy the condition

$$\mathbb{E}_{\mathbf{x},\mathbf{d}}[\mathbf{f}(\mathbf{x}, \mathbf{d}; \mathbf{w}^*)] = \mathbf{0} \tag{4.78}$$

where $\mathbf{w}^*$ is the optimal value of the weight vector $\mathbf{w}$, as previously defined in Eq. (4.57). In other words, the flow $\mathbf{f}$ must asymptotically converge to the optimal parameter $\mathbf{w}^*$ across time t. Moreover, for stability, we also require that the gradient of $\mathbf{f}$ should be a positive-definite matrix. The flow $\mathbf{f}$ includes the gradient vector $\mathbf{g}$ in Eq. (4.62) as a special case.

The previously defined equations of Eqs. (4.63) through (4.69) apply equally well to Murata's algorithm. Thereafter, however, the assumption made is that the evolution of the learning rate $\eta(t)$ across time t is governed by a dynamic system that comprises the pair of differential equations

$$\frac{d}{dt}\xi(t) = -\lambda\eta(t)\xi(t) \tag{4.79}$$

and

$$\frac{d}{dt}\eta(t) = \alpha\eta(t)(\beta\xi(t) - \eta(t)) \tag{4.80}$$

where it should be noted that $\xi(t)$ is always positive and α and β are positive constants. The first equation of this dynamic system is a repeat of Eq. (4.69). The second equation of the system is motivated by the corresponding differential equation in the learning of the learning algorithm described in Sompolinsky et al. (1995).[7]

As before, the λ in Eq. (4.79) is the eigenvalue associated with the eigenvector $\mathbf{q}$ of the Hessian $\mathbf{K}^*$. Moreover, it is hypothesized that $\mathbf{q}$ is chosen as the particular eigenvector associated with the smallest eigenvalue $\lambda_{\min}$. This, in turn, means that the ensemble-averaged flow $\mathbf{f}$ converges to the optimal parameter $\mathbf{w}^*$ in a manner similar to that previously described, as depicted in Fig. 4.15.

The *asymptotic behavior* of the dynamic system described in Eqs. (4.79) and (4.80) is given by the corresponding pair of equations

$$\xi(t) = \frac{1}{\beta}\left(\frac{1}{\lambda} - \frac{1}{\alpha}\right)\frac{1}{t}, \qquad \alpha > \lambda \tag{4.81}$$

and

$$\eta(t) = \frac{c}{t}, \qquad c = \lambda^{-1} \tag{4.82}$$

The important point to note here is that this new dynamic system exhibits the desired annealing of the learning rate $\eta(t)$—namely, c/t for large t—which is optimal for any estimator $\hat{\mathbf{w}}(t)$ converging to $\mathbf{w}^*$, as previously discussed.

In light of the considerations just presented, we may now formally describe the *Murata adaptive algorithm* for on-line learning in discrete time as follows (Murata, 1998; Müller et al., 1998):

$$\hat{\mathbf{w}}(n+1) = \hat{\mathbf{w}}(n) - \eta(n)\mathbf{f}(\mathbf{x}(n+1), \mathbf{d}(n+1); \hat{\mathbf{w}}(n)) \tag{4.83}$$

$$\mathbf{r}(n+1) = \mathbf{r}(n) + \delta\mathbf{f}(\mathbf{x}(n+1), \mathbf{d}(n+1); \hat{\mathbf{w}}(n)), \qquad 0 < \delta < 1 \tag{4.84}$$

$$\eta(n+1) = \eta(n) + \alpha\eta(n)(\beta\|\mathbf{r}(n+1)\| - \eta(n)) \tag{4.85}$$

The following points are noteworthy in the formulation of this discrete-time system of equations:

- Equation (4.83) is simply the instantaneous discrete-time version of the differential equation of Eq. (4.77).
- Equation (4.84) includes an *auxiliary* vector $\mathbf{r}(n)$, which has been introduced to account for the continuous-time function $\xi_\chi(t)$. Moreover, this second equation of the Murata adaptive algorithm includes a *leakage factor* whose value δ controls the running average of the flow $\mathbf{f}$.
- Equation (4.85) is a discrete-time version of the differential equation Eq. (4.80). The updated auxiliary vector $\mathbf{r}(n+1)$ included in Eq. (4.85) links it to Eq. (4.84); in so doing, allowance is made for the linkage between the continuous-time functions $\xi(t)$ and $\eta(t)$ previously defined in Eqs. (4.79) and (4.80).

Unlike the continuous-time dynamic system described in Eqs. (4.79) and (4.80), the asymptotic behavior of the learning-rate parameter $\eta(t)$ in Eq. (4.85) does not converge to zero as the number of iterations, n, approaches infinity, thereby violating the requirement for optimal annealing. Accordingly, in the neighborhood of the optimal parameter $\mathbf{w}^*$, we now find that for the Murata adaptive algorithm:

$$\lim_{n\to\infty} \hat{\mathbf{w}}(n) \neq \mathbf{w}^* \tag{4.86}$$

This asymptotic behavior is different from that of the optimally annealed on-line learning algorithm of Eq. (4.76). Basically, the deviation from optimal annealing is attributed to the use of a running average of the flow in Eq. (4.77), the inclusion of which was motivated by the need to account for the algorithm not having access to a prescribed cost

function, as was the case in deriving the optimally annealed on-line learning algorithm of Eq. (4.76).

The learning of the learning rule is useful when the optimal $\hat{\mathbf{w}}^*$ varies with time n slowly (i.e., the environment responsible for generating the examples is nonstationary) or it changes suddenly. On the other hand, the $1/n$ rule is not a good choice in such an environment, because η_n becomes very small for large n, causing the $1/n$ rule to lose its learning capability. Basically, the difference between the optimally annealed on-learning algorithm of Eq. (4.76) and the on-line learning algorithm described in Eqs. (4.83) to (4.85) is that the latter has a built-in mechanism for adaptive control of the learning rate—hence its ability to *track* variations in the optimal $\hat{\mathbf{w}}^*$.

A final comment is in order: Although the Murata adaptive algorithm is indeed *suboptimal* insofar as annealing of the learning-rate parameter is concerned, its important virtue is the broadened applicability of on-line learning in a practically implementable manner.

4.11 GENERALIZATION

In back-propagation learning, we typically start with a training sample and use the back-propagation algorithm to compute the synaptic weights of a multilayer perceptron by loading (encoding) as many of the training examples as possible into the network. The hope is that the neural network so designed will generalize well. A network is said to *generalize* well when the input–output mapping computed by the network is correct (or nearly so) for test data never used in creating or training the network; the term "generalization" is borrowed from psychology. Here, it is assumed that the test data are drawn from the same population used to generate the training data.

The learning process (i.e., training of a neural network) may be viewed as a "curve-fitting" problem. The network itself may be considered simply as a nonlinear input–output mapping. Such a viewpoint then permits us to look at generalization not as a mystical property of neural networks, but rather simply as the effect of a good nonlinear interpolation of the input data. The network performs useful interpolation primarily because multilayer perceptrons with continuous activation functions lead to output functions that are also continuous.

Figure 4.16a illustrates how generalization may occur in a hypothetical network. The nonlinear input–output mapping represented by the curve depicted in this figure is computed by the network as a result of learning the points labeled as "training data." The point marked in red on the curve as "generalization" is thus seen as the result of interpolation performed by the network.

A neural network that is designed to generalize well will produce a correct input–output mapping even when the input is slightly different from the examples used to train the network, as illustrated in the figure. When, however, a neural network learns too many input–output examples, the network may end up memorizing the training data. It may do so by finding a feature (due to noise, for example) that is present in the training data, but not true of the underlying function that is to be modeled. Such a phenomenon is referred to as *overfitting* or *overtraining*. When the network is overtrained, it loses the ability to generalize between similar input–output patterns.

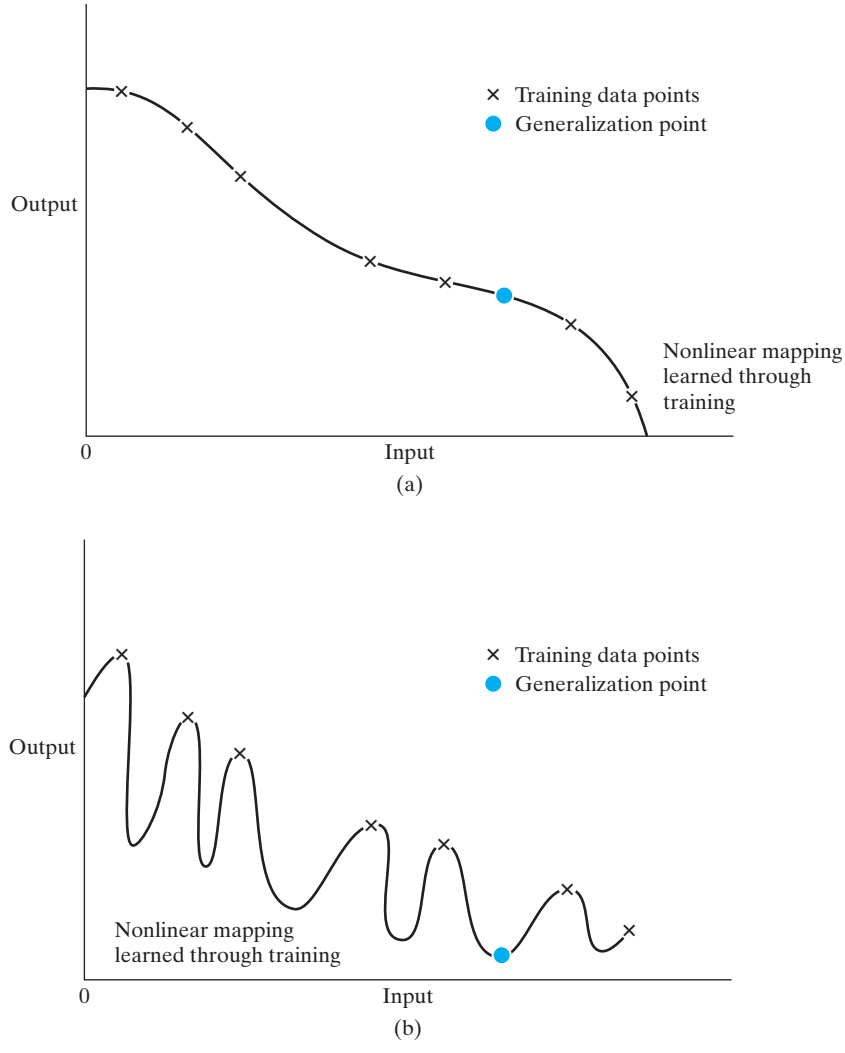

FIGURE 4.16 (a) Properly fitted nonlinear mapping with good generalization. (b) Overfitted nonlinear mapping with poor generalization.

Ordinarily, loading data into a multilayer perceptron in this way requires the use of more hidden neurons than are actually necessary, with the result that undesired contributions in the input space due to noise are stored in synaptic weights of the network. An example of how poor generalization due to memorization in a neural network may occur is illustrated in Fig. 4.16b for the same data as depicted in Fig. 4.16a. "Memorization" is essentially a "look-up table," which implies that the input–output mapping computed by the neural network is not smooth. As pointed out in Poggio and Girosi (1990a), smoothness of input–output mapping is closely related to such model-selection criteria as *Occam's*

razor, the essence of which is to select the "simplest" function in the absence of any prior knowledge to the contrary. In the context of our present discussion, the simplest function means the smoothest function that approximates the mapping for a given error criterion, because such a choice generally demands the fewest computational resources. Smoothness is also natural in many applications, depending on the scale of the phenomenon being studied. It is therefore important to seek a smooth nonlinear mapping for ill-posed input–output relationships, so that the network is able to classify novel patterns correctly with respect to the training patterns (Wieland and Leighton, 1987).

Sufficient Training-Sample Size for a Valid Generalization

Generalization is influenced by three factors: (1) the size of the training sample and how representative the training sample is of the environment of interest, (2) the architecture of the neural network, and (3) the physical complexity of the problem at hand. Clearly, we have no control over the lattermost factor. In the context of the other two factors, we may view the issue of generalization from two different perspectives:

- The architecture of the network is fixed (hopefully in accordance with the physical complexity of the underlying problem), and the issue to be resolved is that of determining the size of the training sample needed for a good generalization to occur.
- The size of the training sample is fixed, and the issue of interest is that of determining the best architecture of network for achieving good generalization.

Both of these viewpoints are valid in their own individual ways.

In practice, it seems that all we really need for a good generalization is to have the size of the training sample, N, satisfy the condition

$$N = O\left(\frac{W}{\varepsilon}\right) \tag{4.87}$$

where W is the total number of free parameters (i.e., synaptic weights and biases) in the network, ε denotes the fraction of classification errors permitted on test data (as in pattern classification), and $O(\cdot)$ denotes the order of quantity enclosed within. For example, with an error of 10 percent, the number of training examples needed should be about 10 times the number of free parameters in the network.

Equation (4.87) is in accordance with *Widrow's rule of thumb* for the LMS algorithm, which states that the settling time for adaptation in linear adaptive temporal filtering is approximately equal to the memory span of an adaptive tapped-delay-line filter divided by the misadjustment (Widrow and Stearns, 1985; Haykin, 2002). The misadjustment in the LMS algorithm plays a role somewhat analogous to the error ε in Eq. (4.87). Further justification for this empirical rule is presented in the next section.

4.12 APPROXIMATIONS OF FUNCTIONS

A multilayer perceptron trained with the back-propagation algorithm may be viewed as a practical vehicle for performing a *nonlinear input–output mapping* of a general nature. To be specific, let m_0 denote the number of input (source) nodes of a multilayer

perceptron, and let $M = m_L$ denote the number of neurons in the output layer of the network. The input–output relationship of the network defines a mapping from an m_0-dimensional Euclidean input space to an M-dimensional Euclidean output space, which is infinitely continuously differentiable when the activation function is likewise. In assessing the capability of the multilayer perceptron from this viewpoint of input–output mapping, the following fundamental question arises:

What is the minimum number of hidden layers in a multilayer perceptron with an input–output mapping that provides an approximate realization of any continuous mapping?

Universal Approximation Theorem

The answer to this question is embodied in the *universal approximation theorem*[8] for a nonlinear input–output mapping, which may be stated as follows:

Let $\varphi(\cdot)$ be a nonconstant, bounded, and monotone-increasing continuous function. Let I_{m_0} denote the m_0-dimensional unit hypercube $[0, 1]^{m_0}$. The space of continuous functions on I_{m_0} is denoted by $C(I_{m_0})$. Then, given any function $f \ni C(I_{m_0})$ and $\varepsilon > 0$, there exist an integer m_1 and sets of real constants α_i, b_i, and w_{ij}, where $i = 1, ..., m_1$ and $j = 1, ..., m_0$ such that we may define

$$F(x_1, ..., x_{m_0}) = \sum_{i=1}^{m_1} \alpha_i \varphi\left(\sum_{j=1}^{m_0} w_{ij} x_j + b_i \right) \tag{4.88}$$

as an approximate realization of the function $f(\cdot)$; that is,

$$|F(x_1, ..., x_{m_0}) - f(x_1, ..., x_{m_0})| < \varepsilon$$

for all $x_1, x_2, ..., x_{m_0}$ that lie in the input space.

The universal approximation theorem is directly applicable to multilayer perceptrons. We first note, for example, that the hyperbolic tangent function used as the nonlinearity in a neural model for the construction of a multilayer perceptron is indeed a nonconstant, bounded, and monotone-increasing function; it therefore satisfies the conditions imposed on the function $\varphi(\cdot)$ Next, we note that Eq. (4.88) represents the output of a multilayer perceptron described as follows:

1. The network has m_0 input nodes and a single hidden layer consisting of m_1 neurons; the inputs are denoted by $x_1, ..., x_{m_0}$.
2. Hidden neuron i has synaptic weights $w_{i_1}, ..., w_{m_0}$, and bias b_i.
3. The network output is a linear combination of the outputs of the hidden neurons, with $\alpha_1, ..., \alpha_{m_1}$ defining the synaptic weights of the output layer.

The universal approximation theorem is an *existence theorem* in the sense that it provides the mathematical justification for the approximation of an arbitrary continuous function as opposed to exact representation. Equation (4.88), which is the backbone of the theorem, merely generalizes approximations by finite Fourier series. In effect, the theorem states that *a single hidden layer is sufficient for a multilayer perceptron to compute a uniform ε approximation to a given training set represented by the set of inputs* $x_1, ..., x_{m_0}$ and a desired (target) output $f(x_1, ..., x_{m_0})$. However, the theorem

does not say that a single hidden layer is optimum in the sense of learning time, ease of implementation, or (more importantly) generalization.

Bounds on Approximation Errors

Barron (1993) has established the approximation properties of a multilayer perceptron, assuming that the network has a single layer of hidden neurons using sigmoid functions and a linear output neuron. The network is trained using the back-propagation algorithm and then tested with new data. During training, the network learns specific points of a target function f in accordance with the training data and thereby produces the approximating function F defined in Eq. (4.88). When the network is exposed to test data that have not been seen before, the network function F acts as an "estimator" of new points of the target function; that is, $F = \hat{f}$.

A smoothness property of the target function f is expressed in terms of its Fourier representation. In particular, the average of the norm of the frequency vector weighted by the Fourier magnitude distribution is used as a measure for the extent to which the function f oscillates. Let $\tilde{f}(\boldsymbol{\omega})$ denote the multidimensional Fourier transform of the function $f(\mathbf{x})$, $\mathbf{x} \in \mathbb{R}^{m_0}$; the m_0-by-1 vector $\boldsymbol{\omega}$ is the frequency vector. The function $f(x)$ is defined in terms of its Fourier transform $\tilde{f}(\boldsymbol{\omega})$ by the inverse formula

$$f(x) = \int_{\mathbb{R}^{m_0}} \tilde{f}(\boldsymbol{\omega}) \exp(j\boldsymbol{\omega}^T\mathbf{x})\, d\boldsymbol{\omega} \tag{4.89}$$

where $j = \sqrt{-1}$. For the complex-valued function $\tilde{f}(\boldsymbol{\omega})$ for which $\boldsymbol{\omega}\tilde{f}(\boldsymbol{\omega})$ is integrable, we define the *first absolute moment* of the Fourier magnitude distribution of the function f as

$$C_f = \int_{\mathbb{R}^{m_0}} |\tilde{f}(\boldsymbol{\omega})| \times \|\boldsymbol{\omega}\|^{1/2}\, d\boldsymbol{\omega} \tag{4.90}$$

where $\|\boldsymbol{\omega}\|$ is the Euclidean norm of $\boldsymbol{\omega}$ and $|\tilde{f}(\boldsymbol{\omega})|$ is the absolute value of $\tilde{f}(\boldsymbol{\omega})$. The first absolute moment C_f quantifies the *smoothness* of the function f.

The first absolute moment C_f provides the basis for a *bound* on the error that results from the use of a multilayer perceptron represented by the input–output mapping function $F(\mathbf{x})$ of Eq. (4.88) to approximate $f(\mathbf{x})$. The approximation error is measured by the *integrated squared error* with respect to an arbitrary probability measure μ on the ball $B_r = \{\mathbf{x}: \|\mathbf{x}\| \leq r\}$ of radius $r > 0$. On this basis, we may state the following proposition for a bound on the approximation error given by Barron (1993):

> *For every continuous function $f(\mathbf{x})$ with finite first moment C_f and every $m_1 \geq 1$, there exists a linear combination of sigmoid-based functions $F(\mathbf{x})$ of the form defined in Eq. (4.88) such that when the function $f(\mathbf{x})$ is observed at a set of values of the input vector $\mathbf{x}$ denoted by $\{\mathbf{x}_i\}_{i=1}^N$ that are restricted to lie inside the prescribed ball of radius r, the result provides the following bound on the empirical risk:*
>
> $$\mathscr{E}_{\text{av}}(N) = \frac{1}{N}\sum_{i=1}^{N} (f(\mathbf{x}_i) - F(\mathbf{x}_i))^2 \leq \frac{C_f'}{m_1} \tag{4.91}$$
>
> where $C_f' = (2rC_f)^2$.

In Barron (1992), the approximation result of Eq. (4.91) is used to express the bound on the risk $\mathscr{E}_{\text{av}}(N)$ resulting from the use of a multilayer perceptron with m_0 input nodes and m_1 hidden neurons as follows:

$$\mathscr{E}_{\text{av}}(N) \leq O\left(\frac{C_f^2}{m_1}\right) + O\left(\frac{m_0 m_1}{N} \log N\right) \tag{4.92}$$

The two terms in the bound on the risk $\mathscr{E}_{\text{av}}(N)$ express the tradeoff between two conflicting requirements on the size of the hidden layer:

1. *Accuracy of best approximation.* For this requirement to be satisfied, the size of the hidden layer, m_1, must be large in accordance with the universal approximation theorem.
2. *Accuracy of empirical fit to the approximation.* To satisfy this second requirement, we must use a small ratio m_1/N. For a fixed size of training sample, N, the size of the hidden layer, m_1, should be kept small, which is in conflict with the first requirement.

The bound on the risk $\mathscr{E}_{\text{av}}(N)$ described in Eq. (4.92) has other interesting implications. Specifically, we see that an exponentially large sample size, large in the dimensionality m_0 of the input space, is *not* required to get an accurate estimate of the target function, provided that the first absolute moment C_f remains finite. This result makes multilayer perceptrons as universal approximators even more important in practical terms.

The error between the empirical fit and the best approximation may be viewed as an *estimation error.* Let ε_0 denote the mean-square value of this estimation error. Then, ignoring the logarithmic factor $\log N$ in the second term of the bound in Eq. (4.92), we may infer that the size N of the training sample needed for a good generalization is about $m_0 m_1/\varepsilon_0$. This result has a mathematical structure similar to the empirical rule of Eq. (4.87), bearing in mind that $m_0 m_1$ is equal to the total number of free parameters W in the network. In other words, we may generally say that for good generalization, the number N of training examples should be larger than the ratio of the total number of free parameters in the network to the mean-square value of the estimation error.

Curse of Dimensionality

Another interesting result that emerges from the bounds described in (4.92) is that when the size of the hidden layer is optimized (i.e., the risk $\mathscr{E}_{\text{av}}(N)$ is minimized with respect to N) by setting

$$m_1 \simeq C_f \left(\frac{N}{m_0 \log N}\right)^{1/2}$$

then the risk $\mathscr{E}_{\text{av}}(N)$ is bounded by $O(C_f \sqrt{m_0 (\log N / N)})$. A surprising aspect of this result is that in terms of the first-order behavior of the risk $\mathscr{E}_{\text{av}}(N)$, the rate of convergence expressed as a function of the training-sample size N is of order $(1/N)^{1/2}$ (times a logarithmic factor). In contrast, for traditional smooth functions (e.g., polynomials and trigonometric

functions), we have a different behavior. Let s denote a measure of *smoothness*, defined as the number of continuous derivatives of a function of interest. Then, for traditional smooth functions, we find that the minimax rate of convergence of the total risk $\mathscr{E}_{\text{av}}(N)$ is of order $(1/N)^{2s/(2s+mo)}$. The dependence of this rate on the dimensionality of the input space, m_0, is responsible for the *curse of dimensionality*, which severely restricts the practical application of these functions. The use of a multilayer perceptron for function approximation appears to offer an advantage over the use of traditional smooth functions. This advantage is, however, subject to the condition that the first absolute moment C_f remains finite; this is a smoothness constraint.

The curse of dimensionality was introduced by Richard Bellman in his studies of adaptive control processes (Bellman, 1961). For a geometric interpretation of this notion, let $\mathbf{x}$ denote an m_0-dimensional input vector and $\{(\mathbf{x}_i, d_i)\}$, $i = 1, 2, \ldots, N$, denote the training sample. The *sampling density* is proportional to N^{1/m_0}. Let a function $f(\mathbf{x})$ represent a surface lying in the m_0-dimensional input space that passes near the data points $\{(\mathbf{x}_i, d_i)\}_{i=1}^{N}$. Now, if the function $f(\mathbf{x})$ is arbitrarily complex and (for the most part) completely unknown, we need *dense* sample (data) points to learn it well. Unfortunately, dense samples are hard to find in "high dimensions"—hence the curse of dimensionality. In particular, there is an *exponential* growth in complexity as a result of an increase in dimensionality, which, in turn, leads to the deterioration of the space-filling properties for uniformly randomly distributed points in higher-dimension spaces. The basic reason for the curse of dimensionality is as follows (Friedman, 1995):

> *A function defined in high-dimensional space is likely to be much more complex than a function defined in a lower-dimensional space, and those complications are harder to discern.*

Basically, there are only two ways of mitigating the curse-of-dimensionality problem:

1. Incorporate *prior knowledge* about the unknown function to be approximated. This knowledge is provided over and above the training data. Naturally, the acquisition of knowledge is problem dependent. In pattern classification, for example, knowledge may be acquired from understanding the pertinent classes (categories) of the input data.
2. Design the network so as to provide increasing *smoothness* of the unknown function with increasing input dimensionality.

Practical Considerations

The universal approximation theorem is important from a theoretical viewpoint because it provides the *necessary mathematical tool* for the viability of feedforward networks with a single hidden layer as a class of approximate solutions. Without such a theorem, we could conceivably be searching for a solution that cannot exist. However, the theorem is not constructive; that is, it does not actually specify how to determine a multilayer perceptron with the stated approximation properties.

The universal approximation theorem assumes that the continuous function to be approximated is given and that a hidden layer of unlimited size is available for the

approximation. Both of these assumptions are violated in most practical applications of multilayer perceptrons.

The problem with multilayer perceptrons using a single hidden layer is that the neurons therein tend to interact with each other globally. In complex situations, this interaction makes it difficult to improve the approximation at one point without worsening it at some other point. On the other hand, with two hidden layers, the approximation (curve-fitting) process becomes more manageable. In particular, we may proceed as follows (Funahashi, 1989; Chester, 1990):

1. *Local features* are extracted in the first hidden layer. Specifically, some neurons in the first hidden layer are used to partition the input space into regions, and other neurons in that layer learn the local features characterizing those regions.
2. *Global features* are extracted in the second hidden layer. Specifically, a neuron in the second hidden layer combines the outputs of neurons in the first hidden layer operating on a particular region of the input space and thereby learns the global features for that region and outputs zero elsewhere.

Further justification for the use of two hidden layers is presented in Sontag (1992) in the context of *inverse problems*.

4.13 CROSS-VALIDATION

The essence of back-propagation learning is to encode an input–output mapping (represented by a set of labeled examples) into the synaptic weights and thresholds of a multilayer perceptron. The hope is that the network becomes well trained so that it learns enough about the past to generalize to the future. From such a perspective, the learning process amounts to a choice of network parameterization for a given set of data. More specifically, we may view the network selection problem as choosing, within a set of candidate model structures (parameterizations), the "best" one according to a certain criterion.

In this context, a standard tool in statistics, known as *cross-validation*, provides an appealing guiding principle[9] (Stone, 1974, 1978). First the available data set is randomly partitioned into a training sample and a test set. The training sample is further partitioned into two disjoint subsets:

- *an estimation subset*, used to select the model;
- *a validation subset*, used to test or validate the model.

The motivation here is to validate the model on a data set different from the one used for parameter estimation. In this way, we may use the training sample to assess the performance of various candidate models and thereby choose the "best" one. There is, however, a distinct possibility that the model with the best-performing parameter values so selected may end up overfitting the validation subset. To guard against this possibility, the generalization performance of the selected model is measured on the test set, which is different from the validation subset.

The use of cross-validation is appealing particularly when we have to design a large neural network with good generalization as the goal. For example, we may use

cross-validation to determine the multilayer perceptron with the best number of hidden neurons and to figure out when it is best to stop training, as described in the next two subsections.

Model Selection

To expand on the idea of selecting a model in accordance with cross-validation, consider a nested *structure* of Boolean function classes denoted by

$$\begin{aligned} &\mathcal{F}_1 \subset \mathcal{F}_2 \subset \cdots \subset \mathcal{F}_n \\ &\mathcal{F}_k = \{F_k\} \\ &\quad = \{F(\mathbf{x}, \mathbf{w}); \mathbf{w} \in \mathcal{W}_k\}, \qquad k = 1, 2, ..., n \end{aligned} \tag{4.93}$$

In words, the kth function class $\mathcal{F}_k$ encompasses a family of multilayer perceptrons with similar architecture and weight vectors $\mathbf{w}$ drawn from a multidimensional weight space $\mathcal{W}_k$. A member of this class, characterized by the function or hypothesis $F_k = F(\mathbf{x}, \mathbf{w})$, $\mathbf{w} \in \mathcal{W}_k$, maps the input vector $\mathbf{x}$ into $\{0, 1\}$, where $\mathbf{x}$ is drawn from an input space $\mathcal{X}$ with some unknown probability P. Each multilayer perceptron in the structure described is trained with the back-propagation algorithm, which takes care of training the parameters of the multilayer perceptron. The model-selection problem is essentially that of choosing the multilayer perceptron with the best value of $\mathbf{w}$, the number of free parameters (i.e., synaptic weights and biases). More precisely, given that the scalar desired response for an input vector $\mathbf{x}$ is $d = \{0, 1\}$, we define the generalization error as the probability

$$\varepsilon_g(F) = P(F(\mathbf{x}) \neq d) \qquad \text{for } \mathbf{x} \in \mathcal{X}$$

We are given a training sample of labeled examples

$$\mathcal{T} = \{(\mathbf{x}_i, d_i)\}_{i=1}^{N}$$

The objective is to select the particular hypothesis $F(\mathbf{x}, \mathbf{w})$ that minimizes the generalization error $\varepsilon_g(F)$, which results when it is given inputs from the test set.

In what follows, we assume that the structure described by Eq. (4.93) has the property that, for any sample size N, we can always find a multilayer perceptron with a large enough number of free parameters $W_{\max}(N)$ such that the training sample $\mathcal{T}$ can be fitted adequately. This assumption is merely restating the universal approximation theorem of Section 4.12. We refer to $W_{\max}(N)$ as the *fitting number*. The significance of $W_{\max}(N)$ is that a reasonable model-selection procedure would choose a hypothesis $F(\mathbf{x}, \mathbf{w})$ that requires $W \leq W_{\max}(N)$; otherwise, the network complexity would be increased.

Let a parameter r, lying in the range between 0 and 1, determine the split of the training sample $\mathcal{T}$ between the estimation subset and validation subset. With $\mathcal{T}$ consisting of N examples, $(1 - r)N$ examples are allotted to the estimation subset, and the remaining rN examples are allotted to the validation subset. The estimation subset, denoted by $\mathcal{T}'$, is used to train a nested sequence of multilayer perceptrons, resulting in the hypotheses $\mathcal{F}_1, \mathcal{F}_2, ..., \mathcal{F}_n$ of increasing complexity. With $\mathcal{T}'$ made up of $(1-r)N$ examples, we consider values of W smaller than or equal to the corresponding fitting number $W_{\max}((1 - r)N)$.

The use of cross-validation results in the choice

$$\mathcal{F}_{cv} = \min_{k=1,2,\ldots,v} \{e_t''(\mathcal{F}_k)\} \tag{4.94}$$

where v corresponds to $W_v \leq W_{\max}((1-r)N)$, and $e_t''(\mathcal{F}_k)$ is the classification error produced by hypothesis $\mathcal{F}_k$ when it is tested on the validation subset $\mathcal{T}''$, consisting of rN examples.

The key issue is how to specify the parameter r that determines the split of the training sample $\mathcal{T}$ between the estimation subset $\mathcal{T}'$ and validation subset $\mathcal{T}''$. In a study described in Kearns (1996) involving an analytic treatment of this issue and supported with detailed computer simulations, several qualitative properties of the optimum r are identified:

- When the complexity of the target function, which defines the desired response d in terms of the input vector $\mathbf{x}$, is small compared with the sample size N, the performance of cross-validation is relatively insensitive to the choice of r.
- As the target function becomes more complex relative to the sample size N, the choice of optimum r has a more pronounced effect on cross-validation performance, and the value of the target function itself decreases.
- A single *fixed* value of r works *nearly* optimally for a wide range of target-function complexity.

On the basis of the results reported in Kearns (1996), a fixed value of r equal to 0.2 appears to be a sensible choice, which means that 80 percent of the training sample $\mathcal{T}$ is assigned to the estimation subset and the remaining 20 percent is assigned to the validation subset.

Early-Stopping Method of Training

Ordinarily, a multilayer perceptron trained with the back-propagation algorithm learns in stages, moving from the realization of fairly simple to more complex mapping functions as the training session progresses. This process is exemplified by the fact that in a typical situation, the mean-square error decreases with an increasing number of epochs used for training: It starts off at a large value, decreases rapidly, and then continues to decrease slowly as the network makes its way to a local minimum on the error surface. With good generalization as the goal, it is very difficult to figure out when it is best to stop training if we were to look at the learning curve for training all by itself. In particular, in light of what was said in Section 4.11 on generalization, it is possible for the network to end up overfitting the training data if the training session is not stopped at the right point.

We may identify the onset of overfitting through the use of cross-validation, for which the training data are split into an estimation subset and a validation subset. The estimation subset of examples is used to train the network in the usual way, except for a minor modification: The training session is stopped periodically (i.e., every so many epochs), and the network is tested on the validation subset after each period of training. More specifically, the periodic "estimation-followed-by-validation process" proceeds as follows:

- After a period of estimation (training)—every five epochs, for example—the synaptic weights and bias levels of the multilayer perceptron are all fixed, and the

network is operated in its forward mode. The validation error is thus measured for each example in the validation subset.

- When the validation phase is completed, the estimation (training) is resumed for another period, and the process is repeated.

This procedure is referred to as the *early-stopping method of training*, which is simple to understand and therefore widely used in practice.

Figure 4.17 shows conceptualized forms of two learning curves, one pertaining to measurements on the estimation subset and the other pertaining to the validation subset. Typically, the model does not do as well on the validation subset as it does on the estimation subset, on which its design was based. The *estimation learning curve* decreases monotonically for an increasing number of epochs in the usual manner. In contrast, the *validation learning curve* decreases monotonically to a minimum and then starts to increase as the training continues. When we look at the estimation learning curve, it may appear that we could do better by going beyond the minimum point on the validation learning curve. In reality, however, what the network is learning beyond this point is essentially noise contained in the training data. This heuristic suggests that the minimum point on the validation learning curve be used as a sensible criterion for stopping the training session.

However, a word of caution is in order here. In reality, the validation-sample error does *not* evolve over the number of epochs used for training as smoothly as the idealized curve shown in Fig. 4.17. Rather, the validation-sample error may exhibit few local minima of its own before it starts to increase with an increasing number of epochs. In such situations, a stopping criterion must be selected in some systematic manner. An empirical investigation on multilayer perceptrons carried out by Prechelt (1998) demonstrates experimentally that there is, in fact, a tradeoff between training time and generalization performance. Based on experimental results obtained therein on 1,296 training sessions, 12 different problems, and 24 different network architectures, it is concluded that, in the presence of two or more local minima, the selection of a "slower" stopping criterion (i.e., a criterion that stops later than other criteria) permits the attainment of a small improvement in generalization performance (typically, about 4 percent, on average) at the cost of a much longer training time (about a factor of four, on average).

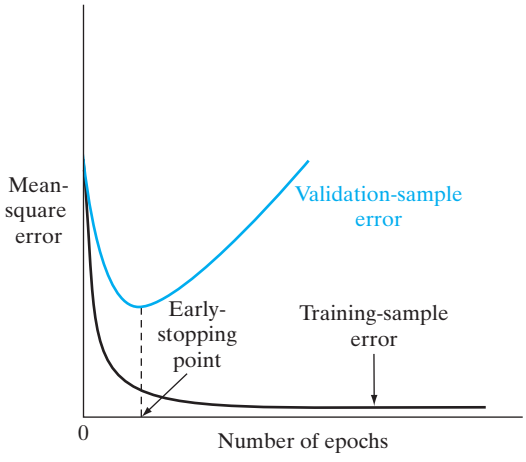

FIGURE 4.17 Illustration of the early-stopping rule based on cross-validation.

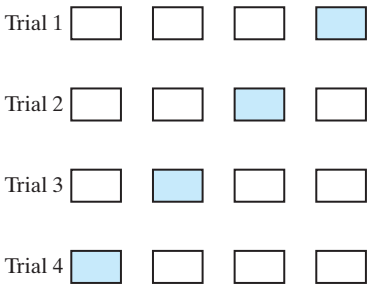

FIGURE 4.18 Illustration of the multifold method of cross-validation. For a given trial, the subset of data shaded in red is used to validate the model trained on the remaining data.

Variants of Cross-Validation

The approach to cross-validation just described is also referred to as the *holdout method.* There are other variants of cross-validation that find their own uses in practice, particularly when there is a scarcity of labeled examples. In such a situation, we may use *multifold cross-validation* by dividing the available set of N examples into K subsets, where $K > 1$; this procedure assumes that K is divisible into N. The model is trained on all the subsets except for one, and the validation error is measured by testing it on the subset that is left out. This procedure is repeated for a total of K trials, each time using a different subset for validation, as illustrated in Fig. 4.18 for $K = 4$. The performance of the model is assessed by averaging the squared error under validation over all the trials of the experiment. There is a disadvantage to multifold cross-validation: It may require an excessive amount of computation, since the model has to be trained K times, where $1 < K \leq N$.

When the available number of labeled examples, N, is severely limited, we may use the extreme form of multifold cross-validation known as the *leave-one-out method.* In this case, $N-1$ examples are used to train the model, and the model is validated by testing it on the example that is left out. The experiment is repeated for a total of N times, each time leaving out a different example for validation. The squared error under validation is then averaged over the N trials of the experiment.

4.14 COMPLEXITY REGULARIZATION AND NETWORK PRUNING

In designing a multilayer perceptron by whatever method, we are in effect building a nonlinear *model* of the physical phenomenon responsible for the generation of the input–output examples used to train the network. Insofar as the network design is statistical in nature, we need an appropriate tradeoff between reliability of the training data and goodness of the model (i.e., a method for solving the bias–variance dilemma discussed in Chapter 2). In the context of back-propagation learning, or any other supervised learning procedure for that matter, we may realize this tradeoff by minimizing the *total risk*, expressed as a function of the parameter vector $\mathbf{w}$, as follows:

$$R(\mathbf{w}) = \mathscr{E}_{\text{av}}(\mathbf{w}) + \lambda \mathscr{E}_c(\mathbf{w}) \tag{4.95}$$

The first term, $\mathscr{E}_{\text{av}}(\mathbf{w})$, is the standard *performance metric*, which depends on both the network (model) and the input data. In back-propagation learning, it is typically defined

as a mean-square error whose evaluation extends over the output neurons of the network and is carried out for all the training examples on an epoch-by-epoch basis, see Eq. (4.5). The second term, $\mathscr{E}_c(\mathbf{w})$, is the *complexity penalty*, where the notion of complexity is measured in terms of the network (weights) alone; its inclusion imposes on the solution prior knowledge that we may have on the models being considered. For the present discussion, it suffices to think of λ as a *regularization parameter*, which represents the relative importance of the complexity-penalty term with respect to the performance-metric term. When λ is zero, the back-propagation learning process is unconstrained, with the network being completely determined from the training examples. When λ is made infinitely large, on the other hand, the implication is that the constraint imposed by the complexity penalty is by itself sufficient to specify the network, which is another way of saying that the training examples are unreliable. In practical applications of complexity regularization, the regularization parameter λ is assigned a value somewhere between these two limiting cases. The subject of regularization theory is discussed in great detail in Chapter 7.

Weight-Decay Procedure

In a simplified, yet effective, form of complex regularization called the *weight-decay procedure* (Hinton, 1989), the complexity penalty term is defined as the squared norm of the weight vector $\mathbf{w}$ (i.e., all the free parameters) in the network, as shown by

$$\begin{aligned}\mathscr{E}_c(\mathbf{w}) &= \|\mathbf{w}\|^2 \\ &= \sum_{i \in \mathscr{C}_{\text{total}}} w_i^2\end{aligned} \tag{4.96}$$

where the set $\mathscr{C}_{\text{total}}$ refers to all the synaptic weights in the network. This procedure operates by forcing some of the synaptic weights in the network to take values close to zero, while permitting other weights to retain their relatively large values. Accordingly, the weights of the network are grouped roughly into two categories:

- **(i)** weights that have a significant influence on the network's performance;
- **(ii)** weights that have practically little or no influence on the network's performance.

The weights in the latter category are referred to as *excess weights*. In the absence of complexity regularization, these weights result in poor generalization by virtue of their high likelihood of taking on completely arbitrary values or causing the network to overfit the data in order to produce a slight reduction in the training error (Hush and Horne, 1993). The use of complexity regularization encourages the excess weights to assume values close to zero and thereby improve generalization.

Hessian-Based Network Pruning: Optimal Brain Surgeon

The basic idea of an analytic approach to network pruning is to use information on second-order derivatives of the error surface in order to make a trade-off between network complexity and training-error performance. In particular, a local model of the error surface is constructed for analytically predicting the effect of perturbations in synaptic weights. The starting point in the construction of such a model is the local

approximation of the cost function $\mathscr{E}_{\text{av}}$ by using a *Taylor series* about the operating point, described as

$$\mathscr{E}_{\text{av}}(\mathbf{w} + \Delta\mathbf{w}) = \mathscr{E}_{\text{av}}(\mathbf{w}) + \mathbf{g}^T(\mathbf{w})\Delta\mathbf{w} + \frac{1}{2}\Delta\mathbf{w}^T\mathbf{H}\Delta\mathbf{w} + O(\|\Delta\mathbf{w}\|^3) \tag{4.97}$$

where $\Delta\mathbf{w}$ is a perturbation applied to the operating point $\mathbf{w}$ and $\mathbf{g}(\mathbf{w})$ is the gradient vector evaluated at $\mathbf{w}$. The Hessian is also evaluated at the point $\mathbf{w}$, and therefore, to be correct, we should denote it by $\mathbf{H}(\mathbf{w})$. We have not done so in Eq. (4.97) merely to simplify the notation.

The requirement is to identify a set of parameters whose deletion from the multilayer perceptron will cause the least increase in the value of the cost function $\mathscr{E}_{\text{av}}$. To solve this problem in practical terms, we make the following approximations:

1. *Extremal Approximation.* We assume that parameters are deleted from the network only after the training process has converged (i.e., the network is fully trained). The implication of this assumption is that the parameters have a set of values corresponding to a local minimum or global minimum of the error surface. In such a case, the gradient vector $\mathbf{g}$ may be set equal to zero, and the term $\mathbf{g}^T\Delta\mathbf{w}$ on the right-hand side of Eq. (4.97) may therefore be ignored; otherwise, the saliency measures (defined later) will be invalid for the problem at hand.

2. *Quadratic Approximation.* We assume that the error surface around a local minimum or global minimum is "nearly quadratic." Hence, the higher-order terms in Eq. (4.97) may also be neglected.

Under these two assumptions, Eq. (4.97) is simplified as

$$\begin{aligned}\Delta\mathscr{E}_{\text{av}} &= \mathscr{E}(\mathbf{w} + \Delta\mathbf{w}) - \mathscr{E}(\mathbf{w}) \\ &= \frac{1}{2}\Delta\mathbf{w}^T\mathbf{H}\Delta\mathbf{w}\end{aligned} \tag{4.98}$$

Equation (4.98) provides the basis for the pruning procedure called *optimal brain surgeon* (OBS), which is due to Hassibi and Stork (1993).

The goal of OBS is to set one of the synaptic weights to zero in order to minimize the incremental increase in $\mathscr{E}_{\text{av}}$ given in Eq. (4.98). Let $w_i(n)$ denote this particular synaptic weight. The elimination of this weight is equivalent to the condition

$$\mathbf{1}_i^T\Delta\mathbf{w} + w_i = 0 \tag{4.99}$$

where $\mathbf{1}_i$ is the *unit vector* whose elements are all zero, except for the ith element, which is equal to unity. We may now restate the goal of OBS as follows:

> *Minimize the quadratic form $\frac{1}{2}\Delta\mathbf{w}^T\mathbf{H}\Delta\mathbf{w}$ with respect to the incremental change in the weight vector, $\Delta\mathbf{w}$, subject to the constraint that $\mathbf{1}_i^T\Delta\mathbf{w} + w_i$ is zero, and then minimize the result with respect to the index i.*

There are two levels of minimization going on here. One minimization is over the synaptic-weight vectors that remain after the ith weight vector is set equal to zero. The second minimization is over which particular vector is pruned.

To solve this constrained-optimization problem, we first construct the *Lagrangian*

$$S = \frac{1}{2}\Delta\mathbf{w}^T\mathbf{H}\Delta\mathbf{w} - \lambda(\mathbf{1}_i^T\Delta\mathbf{w} + w_i) \tag{4.100}$$

where λ is the *Lagrange multiplier*. Then, taking the derivative of the Lagrangian S with respect to $\Delta\mathbf{w}$, applying the constraint of Eq. (4.99), and using matrix inversion, we find that the optimum change in the weight vector $\mathbf{w}$ is given by

$$\Delta\mathbf{w} = -\frac{w_i}{[\mathbf{H}^{-1}]_{i,i}}\mathbf{H}^{-1}\mathbf{1}_i \tag{4.101}$$

and the corresponding optimum value of the Lagrangian S for element w_i is

$$S_i = \frac{w_i^2}{2[\mathbf{H}^{-1}]_{i,i}} \tag{4.102}$$

where $\mathbf{H}^{-1}$ is the inverse of the Hessian $\mathbf{H}$, and $[\mathbf{H}^{-1}]_{i,i}$ is the ii-th element of this inverse matrix. The Lagrangian S_i optimized with respect to $\Delta\mathbf{w}$, subject to the constraint that the ith synaptic weight w_i be eliminated, is called the *saliency* of w_i. In effect, the saliency S_i represents the increase in the mean-square error (performance measure) that results from the deletion of w_i. Note that the saliency S_i, is proportional to w_i^2. Thus, small weights have a small effect on the mean-square error. However, from Eq. (4.102), we see that the saliency S_i, is also inversely proportional to the diagonal elements of the inverse Hessian. Thus, if $[\mathbf{H}^{-1}]_{i,i}$ is small, then even small weights may have a substantial effect on the mean-square error.

In the OBS procedure, the weight corresponding to the smallest saliency is the one selected for deletion. Moreover, the corresponding optimal changes in the remainder of the weights are given in Eq. (4.101), which show that they should be updated along the direction of the i-th column of the inverse of the Hessian.

According to Hassibi and coworkers commenting on some benchmark problems, the OBS procedure resulted in smaller networks than those obtained using the weight-decay procedure. It is also reported that as a result of applying the OBS procedure to the NETtalk multilayer perceptron, involving a single hidden layer and well over 18,000 weights, the network was pruned to a mere 1,560 weights, a dramatic reduction in the size of the network. NETtalk, due to Sejnowski and Rosenberg (1987), is described in Section 4.18.

Computing the inverse Hessian. The inverse Hessian $\mathbf{H}^{-1}$ is fundamental to the formulation of the OBS procedure. When the number of free parameters, W, in the network is large, the problem of computing $\mathbf{H}^{-1}$ may be intractable. In what follows, we describe a manageable procedure for computing $\mathbf{H}^{-1}$, assuming that the multilayer perceptron is fully trained to a local minimum on the error surface (Hassibi and Stork, 1993).

To simplify the presentation, suppose that the multilayer perceptron has a single output neuron. Then, for a given training sample, we may redefine the cost function of Eq. (4.5) as

$$\mathscr{E}_{\text{av}}(\mathbf{w}) = \frac{1}{2N}\sum_{n=1}^{N}(d(n) - o(n))^2$$

where $o(n)$ is the actual output of the network on the presentation of the nth example, $d(n)$ is the corresponding desired response, and N is the total number of examples in the training sample. The output $o(n)$ may itself be expressed as

$$o(n) = F(\mathbf{w}, \mathbf{x})$$

where F is the input–output mapping function realized by the multilayer perceptron, $\mathbf{x}$ is the input vector, and $\mathbf{w}$ is the synaptic-weight vector of the network. The first derivative of $\mathscr{E}_{\text{av}}$ with respect to $\mathbf{w}$ is therefore

$$\frac{\partial \mathscr{E}_{\text{av}}}{\partial \mathbf{w}} = -\frac{1}{N}\sum_{n=1}^{N}\frac{\partial F(\mathbf{w}, \mathbf{x}(n))}{\partial \mathbf{w}}(d(n) - o(n)) \tag{4.103}$$

and the second derivative of $\mathscr{E}_{\text{av}}$ with respect to $\mathbf{w}$ or the Hessian is

$$\begin{aligned}\mathbf{H}(N) &= \frac{\partial^2 \mathscr{E}_{\text{av}}}{\partial \mathbf{w}^2} \\ &= \frac{1}{N}\sum_{n=1}^{N}\left\{\left(\frac{\partial F(\mathbf{w}, \mathbf{x}(n))}{\partial \mathbf{w}}\right)\left(\frac{\partial F(\mathbf{w}, \mathbf{x}(n))}{\partial \mathbf{w}}\right)^T\right. \\ &\quad \left. - \frac{\partial^2 F(\mathbf{w}, \mathbf{x}(n))}{\partial \mathbf{w}^2}(d(n) - o(n))\right\}\end{aligned} \tag{4.104}$$

where we have emphasized the dependence of the Hessian on the size of the training sample, N.

Under the assumption that the network is fully trained—that is, the cost function $\mathscr{E}_{\text{av}}$ has been adjusted to a local minimum on the error surface—it is reasonable to say that $o(n)$ is close to $d(n)$. Under this condition, we may ignore the second term and approximate Eq. (4.104) as

$$\mathbf{H}(N) \approx \frac{1}{N}\sum_{n=1}^{N}\left(\frac{\partial F(\mathbf{w}, \mathbf{x}(n))}{\partial \mathbf{w}}\right)\left(\frac{\partial F(\mathbf{w}, \mathbf{x}(n))}{\partial \mathbf{w}}\right)^T \tag{4.105}$$

To simplify the notation, define the W-by-1 vector

$$\boldsymbol{\xi}(n) = \frac{1}{\sqrt{N}}\frac{\partial F(\mathbf{w}, \mathbf{x}(n))}{\partial \mathbf{w}} \tag{4.106}$$

which may be computed using the procedure described in Section 4.8. We may then rewrite Eq. (4.105) in the form of a recursion as follows:

$$\begin{aligned}\mathbf{H}(n) &= \sum_{k=1}^{n}\boldsymbol{\xi}(k)\boldsymbol{\xi}^T(k) \\ &= \mathbf{H}(n-1) + \boldsymbol{\xi}(n)\boldsymbol{\xi}^T(n), \qquad n = 1, 2, ..., N\end{aligned} \tag{4.107}$$

This recursion is in the right form for application of the so-called *matrix inversion lemma*, also known as *Woodbury's equality*.

Let $\mathbf{A}$ and $\mathbf{B}$ denote two positive-definite matrices related by

$$\mathbf{A} = \mathbf{B}^{-1} + \mathbf{CDC}^T$$

where **C** and **D** are two other matrices. According to the matrix inversion lemma, the inverse of matrix **A** is defined by

$$\mathbf{A}^{-1} = \mathbf{B} - \mathbf{BC}(\mathbf{D} + \mathbf{C}^T\mathbf{BC})^{-1}\mathbf{C}^T\mathbf{B}$$

For the problem described in Eq. (4.107) we have

$$\begin{aligned}\mathbf{A} &= \mathbf{H}(n)\\ \mathbf{B}^{-1} &= \mathbf{H}(n-1)\\ \mathbf{C} &= \boldsymbol{\xi}(n)\\ \mathbf{D} &= 1\end{aligned}$$

Application of the matrix inversion lemma therefore yields the desired formula for recursive computation of the inverse Hessian:

$$\mathbf{H}^{-1}(n) = \mathbf{H}^{-1}(n-1) - \frac{\mathbf{H}^{-1}(n-1)\boldsymbol{\xi}(n)\boldsymbol{\xi}^T(n)\mathbf{H}^{-1}(n-1)}{1 + \boldsymbol{\xi}^T(n)\mathbf{H}^{-1}(n-1)\boldsymbol{\xi}(n)} \tag{4.108}$$

Note that the denominator in Eq. (4.108) is a scalar; it is therefore straightforward to calculate its reciprocal. Thus, given the past value of the inverse Hessian, $\mathbf{H}^{-1}(n-1)$, we may compute its updated value $\mathbf{H}^{-1}(n)$ on the presentation of the nth example, represented by the vector $\boldsymbol{\xi}(n)$. This recursive computation is continued until the entire set of N examples has been accounted for. To initialize the algorithm, we need to make $\mathbf{H}^{-1}(0)$ large, since it is being constantly reduced according to Eq. (4.108). This requirement is satisfied by setting

$$\mathbf{H}^{-1}(0) = \delta^{-1}\mathbf{I}$$

where δ is a small positive number and **I** is the identity matrix. This form of initialization assures that $\mathbf{H}^{-1}(n)$ is always positive definite. The effect of δ becomes progressively smaller as more and more examples are presented to the network.

A summary of the optimal-brain-surgeon algorithm is presented in Table 4.1.

4.15 VIRTUES AND LIMITATIONS OF BACK-PROPAGATION LEARNING

First and foremost, it should be understood that the back-propagation algorithm is *not* an algorithm intended for the optimum design of a multilayer perceptron. Rather, the correct way to describe it is to say:

> *The back-propagation algorithm is a computationally efficient technique for computing the gradients (i.e., first-order derivatives) of the cost function $\mathscr{E}(w)$, expressed as a function of the adjustable parameters (synaptic weights and bias terms) that characterize the multilayer perceptron.*

The computational power of the algorithm is derived from two distinct properties:

1. The back-propagation algorithm is *simple to compute locally.*
2. It performs *stochastic gradient descent* in weight space, when the algorithm is implemented in its on-line (sequential) mode of learning.

TABLE 4.1 Summary of the Optimal-Brain-Surgeon Algorithm

1. Train the given multilayer perceptron to minimum mean-square error.
2. Use the procedure described in Section 4.8 to compute the vector

$$\boldsymbol{\xi}(n) = \frac{1}{\sqrt{N}} \frac{\partial F(\mathbf{w}, \mathbf{x}(n))}{\partial \mathbf{w}}$$

where $F(\mathbf{w}, \mathbf{x}(n))$ is the input–output mapping realized by the multilayer perceptron with an overall weight vector $\mathbf{w}$, and $\mathbf{x}(n)$ is the input vector.

3. Use the recursion in Eq. (4.108) to compute the inverse Hessian $\mathbf{H}^{-1}$.
4. Find the i that corresponds to the smallest saliency

$$S_i = \frac{w_i^2}{2[\mathbf{H}^{-1}]_{i,i}}$$

where $[\mathbf{H}^{-1}]_{i,i}$ is the (i, i)th element of $\mathbf{H}^{-1}$. If the saliency S_i is much smaller than the mean-square error $\mathscr{E}_{\text{av}}$, then delete the synaptic weight w_i and proceed to step 5. Otherwise, go to step 6.

5. Update all the synaptic weights in the network by applying the adjustment

$$\Delta \mathbf{w} = -\frac{w_i}{[\mathbf{H}^{-1}]_{i,i}} \mathbf{H}^{-1} \mathbf{1}_i$$

Go to step 2.

6. Stop the computation when no more weights can be deleted from the network without a large increase in the mean-square error. (It may be desirable to retrain the network at this point).

Connectionism

The back-propagation algorithm is an example of a *connectionist paradigm* that relies on local computations to discover the information-processing capabilities of neural networks. This form of computational restriction is referred to as the *locality constraint*, in the sense that the computation performed by each neuron in the network is influenced solely by those other neurons that are in physical contact with it. The use of local computations in the design of (artificial) neural networks is usually advocated for three principal reasons:

1. Neural networks that perform local computations are often held up as *metaphors* for biological neural networks.
2. The use of local computations permits a graceful degradation in performance caused by hardware errors and therefore provides the basis for a *fault-tolerant* network design.
3. Local computations favor the use of *parallel architectures* as an efficient method for the implementation of neural networks.

Replicator (Identity) Mapping

The hidden neurons of a multilayer perceptron trained with the back-propagation algorithm play a critical role as feature detectors. A novel way in which this important property of the multilayer perceptron can be exploited is in its use as a *replicator* or *identity map* (Rumelhart et al., 1986b; Cottrel et al., 1987). Figure 4.19 illustrates

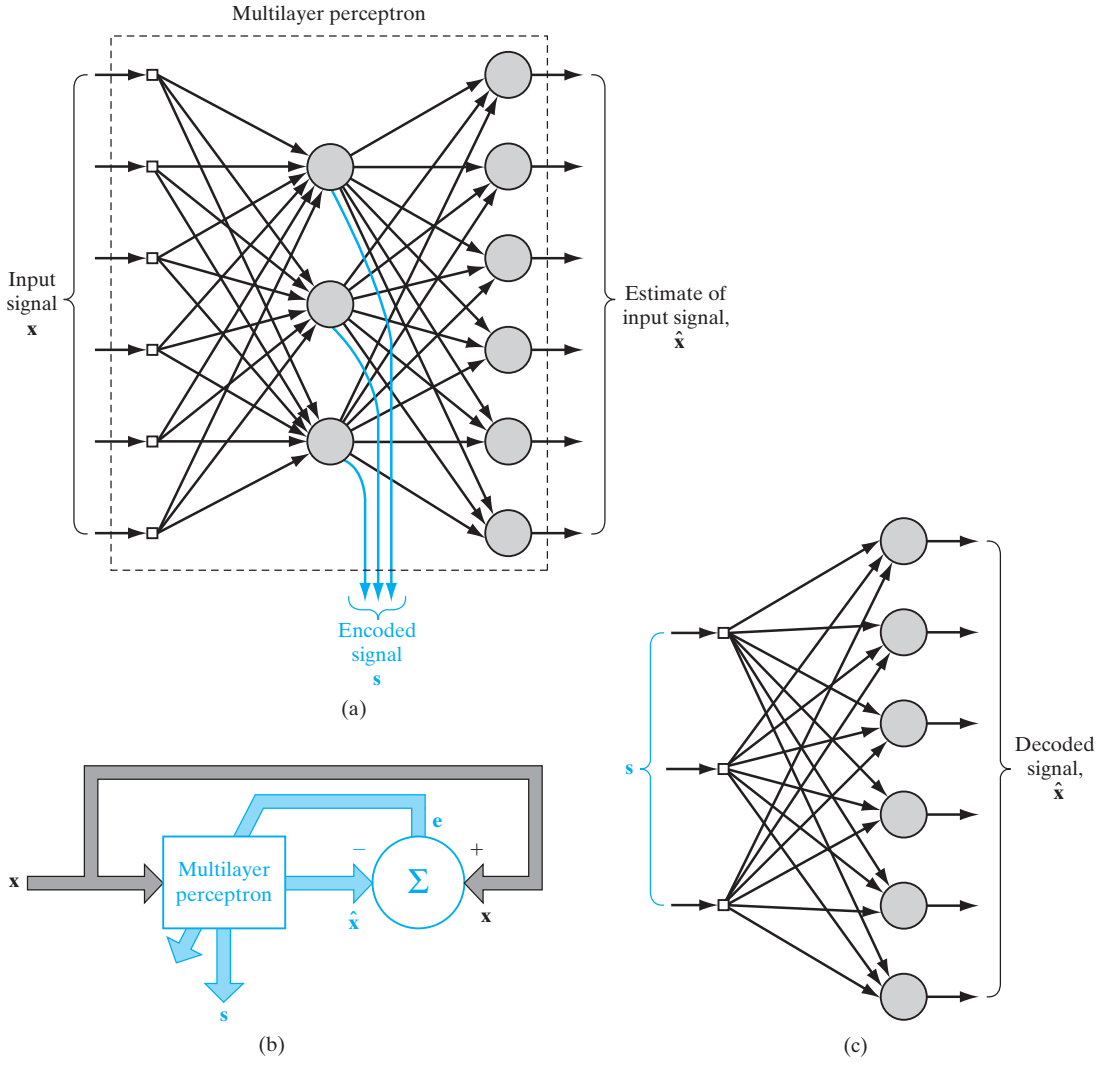

FIGURE 4.19 (a) Replicator network (identity map) with a single hidden layer used as an encoder. (b) Block diagram for the supervised training of the replicator network. (c) Part of the replicator network used as a decoder.

how this can be accomplished for the case of a multilayer perceptron using a single hidden layer. The network layout satisfies the following structural requirements, as illustrated in Fig. 4.19a:

- The input and output layers have the same size, m.
- The size of the hidden layer, M, is smaller than m.
- The network is fully connected.

A given pattern $\mathbf{x}$ is simultaneously applied to the input layer as the stimulus and to the output layer as the desired response. The actual response of the output layer, $\hat{\mathbf{x}}$, is

intended to be an "estimate" of $\mathbf{x}$. The network is trained using the back-propagation algorithm in the usual way, with the estimation error vector $(\mathbf{x} - \hat{\mathbf{x}})$ treated as the error signal, as illustrated in Fig. 4.19b. The training is performed in an *unsupervised* manner (i.e., without the need for a teacher). By virtue of the special structure built into the design of the multilayer perceptron, the network is *constrained* to perform identity mapping through its hidden layer. An *encoded* version of the input pattern, denoted by $\mathbf{s}$, is produced at the output of the hidden layer, as indicated in Fig. 4.19a. In effect, the fully trained multilayer perceptron performs the role of an "encoder." To reconstruct an estimate $\hat{\mathbf{x}}$ of the original input pattern $\mathbf{x}$ (i.e., to perform *decoding*), we apply the encoded signal to the hidden layer of the replicator network, as illustrated in Fig. 4.19c. In effect, this latter network performs the role of a "decoder." The smaller we make the size M of the hidden layer compared with the size m of the input–output layer, the more effective the configuration of Fig. 4.19a will be as a *data-compression system*.[10]

Function Approximation

A multilayer perceptron trained with the back-propagation algorithm manifests itself as a *nested sigmoidal structure*, written for the case of a single output in the compact form

$$F(\mathbf{x}, \mathbf{w}) = \varphi\left(\sum_k w_{ok}\varphi\left(\sum_j w_{kj}\varphi\left(\cdots\varphi\left(\sum_i w_{li}x_i\right)\right)\right)\right) \tag{4.109}$$

where $\varphi(\cdot)$ is a sigmoid activation function; w_{ok} is the synaptic weight from neuron k in the last hidden layer to the single output neuron o, and so on for the other synaptic weights; and x_i is the ith element of the input vector $\mathbf{x}$. The weight vector $\mathbf{w}$ denotes the entire set of synaptic weights ordered by layer, then neurons in a layer, and then synapses in a neuron. The scheme of nested nonlinear functions described in Eq. (4.109) is unusual in classical approximation theory. It is a *universal approximator*, as discussed in Section 4.12.

Computational Efficiency

The *computational complexity* of an algorithm is usually measured in terms of the number of multiplications, additions, and storage requirement involved in its implementation. A learning algorithm is said to be *computationally efficient* when its computational complexity is *polynomial* in the number of adjustable parameters that are to be updated from one iteration to the next. On this basis, it can be said that the back-propagation algorithm is computationally efficient, as stated in the summarizing description at the beginning of this section. Specifically, in using the algorithm to train a multilayer perceptron containing a total of W synaptic weights (including biases), its computational complexity is linear in W. This important property of the back-propagation algorithm can be readily verified by examining the computations involved in performing the forward and backward passes summarized in Section 4.4. In the forward pass, the only computations involving the synaptic weights are those that pertain to the induced local fields of the various neurons in the network. Here, we see from Eq. (4.44) that these computations are all linear in the synaptic weights of the network. In the backward pass, the only computations involving the synaptic weights are those that pertain to (1) the local gradients of the hidden neurons, and (2) the updating of the synaptic weights themselves, as shown in Eqs. (4.46) and (4.47), respectively. Here again, we also see that these computations are

all linear in the synaptic weights of the network. The conclusion is therefore that the computational complexity of the back-propagation algorithm is *linear* in W; that is, it is $O(W)$.

Sensitivity Analysis

Another computational benefit gained from the use of back-propagation learning is the efficient manner in which we can carry out a sensitivity analysis of the input–output mapping realized by the algorithm. The *sensitivity* of an input–output mapping function F with respect to a parameter of the function, denoted by ω, is defined by

$$S_{\omega}^{F} = \frac{\partial F/F}{\partial \omega/\omega} \tag{4.110}$$

Consider then a multilayer perceptron trained with the back-propagation algorithm. Let the function $F(\mathbf{w})$ be the input–output mapping realized by this network; $\mathbf{w}$ denotes the vector of all synaptic weights (including biases) contained in the network. In Section 4.8, we showed that the partial derivatives of the function $F(\mathbf{w})$ with respect to all the elements of the weight vector $\mathbf{w}$ can be computed efficiently. In particular, we see that the complexity involved in computing each of these partial derivatives is linear in W, the total number of weights contained in the network. This linearity holds regardless of where the synaptic weight in question appears in the chain of computations.

Robustness

In Chapter 3, we pointed out that the LMS algorithm is robust in the sense that disturbances with small energy can give rise only to small estimation errors. If the underlying observation model is linear, the LMS algorithm is an H^{∞}-optimal filter (Hassibi et al., 1993, 1996). What this means is that the LMS algorithm minimizes the *maximum energy gain* from the disturbances to the estimation errors.

If, on the other hand, the underlying observation model is nonlinear, Hassibi and Kailath (1995) have shown that the back-propagation algorithm is a *locally* H^{∞}-optimal filter. The term "local" means that the initial value of the weight vector used in the back-propagation algorithm is sufficiently close to the optimum value $\mathbf{w}^*$ of the weight vector to ensure that the algorithm does not get trapped in a poor local minimum. In conceptual terms, it is satisfying to see that the LMS and back-propagation algorithms belong to the same class of H^{∞}-optimal filters.

Convergence

The back-propagation algorithm uses an "instantaneous estimate" for the gradient of the error surface in weight space. The algorithm is therefore *stochastic* in nature; that is, it has a tendency to zigzag its way about the true direction to a minimum on the error surface. Indeed, back-propagation learning is an application of a statistical method known as *stochastic approximation* that was originally proposed by Robbins and Monro (1951). Consequently, it tends to converge slowly. We may identify two fundamental causes for this property (Jacobs, 1988):

1. The error surface is fairly flat along a weight dimension, which means that the derivative of the error surface with respect to that weight is small in magnitude. In such

a situation, the adjustment applied to the weight is small, and consequently many iterations of the algorithm may be required to produce a significant reduction in the error performance of the network. Alternatively, the error surface is highly curved along a weight dimension, in which case the derivative of the error surface with respect to that weight is large in magnitude. In this second situation, the adjustment applied to the weight is large, which may cause the algorithm to overshoot the minimum of the error surface.

2. The direction of the negative gradient vector (i.e., the negative derivative of the cost function with respect to the vector of weights) may point away from the minimum of the error surface: hence, the adjustments applied to the weights may induce the algorithm to move in the wrong direction.

To avoid the slow rate of convergence of the back-propagation algorithm used to train a multilayer perceptron, we may opt for the optimally annealed on-line learning algorithm described in Section 4.10.

Local Minima

Another peculiarity of the error surface that affects the performance of the back-propagation algorithm is the presence of *local minima* (i.e., isolated valleys) in addition to global minima; in general, it is difficult to determine the numbers of local and global minima. Since back-propagation learning is basically a hill-climbing technique, it runs the risk of being trapped in a local minimum where every small change in synaptic weights increases the cost function. But somewhere else in the weight space, there exists another set of synaptic weights for which the cost function is smaller than the local minimum in which the network is stuck. It is clearly undesirable to have the learning process terminate at a local minimum, especially if it is located far above a global minimum.

Scaling

In principle, neural networks such as multilayer perceptrons trained with the back-propagation algorithm have the potential to be universal computing machines. However, for that potential to be fully realized, we have to overcome the *scaling problem*, which addresses the issue of how well the network behaves (e.g., as measured by the time required for training or the best generalization performance attainable) as the computational task increases in size and complexity. Among the many possible ways of measuring the size or complexity of a computational task, the predicate order defined by Minsky and Papert (1969, 1988) provides the most useful and important measure.

To explain what we mean by a predicate, let $\psi(X)$ denote a function that can have only two values. Ordinarily, we think of the two values of $\psi(X)$ as 0 and 1. But by taking the values to be FALSE or TRUE, we may think of $\psi(X)$ as a *predicate*—that is, a variable statement whose falsity or truth depends on the choice of argument X. For example, we may write

$$\psi_{\text{CIRCLE}}(X) = \begin{cases} 1 & \text{if the figure } X \text{ is a circle} \\ 0 & \text{if the figure } X \text{ is not a circle} \end{cases}$$

Using the idea of a predicate, Tesauro and Janssens (1988) performed an empirical study involving the use of a multilayer perceptron trained with the back-propagation

algorithm to learn to compute the parity function. The *parity function* is a Boolean predicate defined by

$$\psi_{\text{PARITY}}(X) = \begin{cases} 1 & \text{if } |X| \text{ is an odd number} \\ 0 & \text{otherwise} \end{cases}$$

and whose order is equal to the number of inputs. The experiments performed by Tesauro and Janssens appear to show that the time required for the network to learn to compute the parity function scales exponentially with the number of inputs (i.e., the predicate order of the computation), and that projections of the use of the back-propagation algorithm to learn arbitrarily complicated functions may be overly optimistic.

It is generally agreed that it is inadvisable for a multilayer perceptron to be fully connected. In this context, we may therefore raise the following question: Given that a multilayer perceptron should not be fully connected, how should the synaptic connections of the network be allocated? This question is of no major concern in the case of small-scale applications, but it is certainly crucial to the successful application of back-propagation learning for solving large-scale, real-world problems.

One effective method of alleviating the scaling problem is to develop insight into the problem at hand (possibly through neurobiological analogy) and use it to put ingenuity into the architectural design of the multilayer perceptron. Specifically, the network architecture and the constraints imposed on synaptic weights of the network should be designed so as to incorporate prior information about the task into the makeup of the network. This design strategy is illustrated in Section 4.17 for the optical character recognition problem.

4.16 SUPERVISED LEARNING VIEWED AS AN OPTIMIZATION PROBLEM

In this section, we take a viewpoint on supervised learning that is quite different from that pursued in previous sections of the chapter. Specifically, we view the supervised training of a multilayer perceptron as a problem in *numerical optimization*. In this context, we first point out that the error surface of a multilayer perceptron with supervised learning is a nonlinear function of a weight vector $\mathbf{w}$; in the case of a multilayer perceptron, $\mathbf{w}$ represents the synaptic weight of the network arranged in some orderly fashion. Let $\mathscr{E}_{\text{av}}(\mathbf{w})$ denote the cost function, averaged over the training sample. Using the Taylor series, we may expand $\mathscr{E}_{\text{av}}(\mathbf{w})$ about the current operating point on the error surface as in Eq. (4.97), reproduced here in the form:

$$\begin{aligned}\mathscr{E}_{\text{av}}(\mathbf{w}(n) + \Delta\mathbf{w}(n)) = \mathscr{E}_{\text{av}}(\mathbf{w}(n)) + \mathbf{g}^T(n)\Delta\mathbf{w}(n) + \frac{1}{2}\Delta\mathbf{w}^T(n)\mathbf{H}(n)\Delta\mathbf{w}(n) \\ + \text{(third- and higher-order terms)}\end{aligned} \tag{4.111}$$

where $\mathbf{g}(n)$ is the local *gradient vector*, defined by

$$\mathbf{g}(n) = \left.\frac{\partial \mathscr{E}_{\text{av}}(\mathbf{w})}{\partial \mathbf{w}}\right|_{\mathbf{w}=\mathbf{w}(n)} \tag{4.112}$$

The matrix $\mathbf{H}(n)$ is the local *Hessian* representing "curvature" of the error performance surface, defined by

$$\mathbf{H}(n) = \left.\frac{\partial^2 \mathscr{E}_{\text{av}}(\mathbf{w})}{\partial \mathbf{w}^2}\right|_{\mathbf{w}=\mathbf{w}(n)} \tag{4.113}$$

The use of an ensemble-averaged cost function $\mathscr{E}_{\text{av}}(\mathbf{w})$ presumes a *batch* mode of learning.

In the steepest-descent method, exemplified by the back-propagation algorithm, the adjustment $\Delta\mathbf{w}(n)$ applied to the synaptic weight vector $\mathbf{w}(n)$ is defined by

$$\Delta\mathbf{w}(n) = -\eta\mathbf{g}(n) \tag{4.114}$$

where η is a fixed learning-rate parameter. In effect, the steepest-descent method operates on the basis of a *liner approximation* of the cost function in the local neighborhood of the operating point $\mathbf{w}(n)$. In so doing, it relies on the gradient vector $\mathbf{g}(n)$ as the only source of local *first-order* information about the error surface. This restriction has a beneficial effect: simplicity of implementation. Unfortunately, it also has a detrimental effect: a slow rate of convergence, which can be excruciating, particularly in the case of large-scale problems. The inclusion of the momentum term in the update equation for the synaptic weight vector is a crude attempt at using second-order information about the error surface, which is of some help. However, its use makes the training process more delicate to manage by adding one more item to the list of parameters that have to be "tuned" by the designer.

In order to produce a significant improvement in the convergence performance of a multilayer perceptron (compared with back-propagation learning), we have to use *higher-order information* in the training process. We may do so by invoking a *quadratic approximation* of the error surface around the current point $\mathbf{w}(n)$. We then find from Eq. (4.111) that the optimum value of the adjustment $\Delta\mathbf{w}(n)$ applied to the synaptic weight vector $\mathbf{w}(n)$ is given by

$$\Delta\mathbf{w}^*(n) = \mathbf{H}^{-1}(n)\mathbf{g}(n) \tag{4.115}$$

where $\mathbf{H}^{-1}(n)$ is the inverse of the Hessian $\mathbf{H}(n)$, assuming that it exists. Equation (4.115) is the essence of *Newton's method*. If the cost function $\mathscr{E}_{\text{av}}(\mathbf{w})$ is quadratic (i.e., the third- and higher-order terms in Eq. (4.109) are zero), Newton's method converges to the optimum solution in one iteration. However, the practical application of Newton's method to the supervised training of a multilayer perceptron is handicapped by three factors:

- **(i)** Newton's method requires calculation of the inverse Hessian $\mathbf{H}^{-1}(n)$, which can be computationally expensive.
- **(ii)** For $\mathbf{H}^{-1}(n)$ to be computable, $\mathbf{H}(n)$ has to be nonsingular. In the case where $\mathbf{H}(n)$ is positive definite, the error surface around the current point $\mathbf{w}(n)$ is describable by a "convex bowl." Unfortunately, there is no guarantee that the Hessian of the error surface of a multilayer perceptron will always fit this description. Moreover, there is the potential problem of the Hessian being rank deficient (i.e., not all the

columns of **H** are linearly independent), which results from the intrinsically ill-conditioned nature of supervised-learning problems (Saarinen et al., 1992); this factor only makes the computational task more difficult.

(iii) When the cost function $\mathscr{E}_{av}(\mathbf{w})$ is nonquadratic, there is no guarantee for convergence of Newton's method, which makes it unsuitable for the training of a multilayer perceptron.

To overcome some of these difficulties, we may use a *quasi-Newton method*, which requires only an estimate of the gradient vector **g**. This modification of Newton's method maintains a positive-definite estimate of the inverse matrix $\mathbf{H}^{-1}$ directly without matrix inversion. By using such an estimate, a quasi-Newton method is assured of going downhill on the error surface. However, we still have a computational complexity that is $O(W^2)$, where W is the size of weight vector **w**. Quasi-Newton methods are therefore computationally impractical, except for in the training of very small-scale neural networks. A description of quasi-Newton methods is presented later in the section.

Another class of second-order optimization methods includes the conjugate-gradient method, which may be regarded as being somewhat intermediate between the method of steepest descent and Newton's method. Use of the conjugate-gradient method is motivated by the desire to accelerate the typically slow rate of convergence experienced with the method of steepest descent, while avoiding the computational requirements associated with the evaluation, storage, and inversion of the Hessian in Newton's method.

Conjugate-Gradient Method[11]

The conjugate-gradient method belongs to a class of second-order optimization methods known collectively as *conjugate-direction methods*. We begin the discussion of these methods by considering the minimization of the *quadratic function*

$$f(\mathbf{x}) = \frac{1}{2}\mathbf{x}^T\mathbf{A}\mathbf{x} - \mathbf{b}^T\mathbf{x} + c \tag{4.116}$$

where **x** is a W-by-1 parameter vector; **A** is a W-by-W symmetric, positive-definite matrix; **b** is a W-by-1 vector; and c is a scalar. Minimization of the quadratic function $f(\mathbf{x})$ is achieved by assigning to **x** the unique value

$$\mathbf{x}^* = \mathbf{A}^{-1}\mathbf{b} \tag{4.117}$$

Thus, minimizing $f(\mathbf{x})$ and solving the linear system of equations $\mathbf{A}\mathbf{x}^* = \mathbf{b}$ are equivalent problems.

Given the matrix **A**, we say that a set of nonzero vectors $\mathbf{s}(0), \mathbf{s}(1), \ldots, \mathbf{s}(W-1)$ is **A**-*conjugate* (i.e., noninterfering with each other in the context of matrix **A**) if the following condition is satisfied:

$$\mathbf{s}^T(n)\mathbf{A}\mathbf{s}(j) = 0 \qquad \text{for all } n \text{ and } j \text{ such that } n \neq j \tag{4.118}$$

If **A** is equal to the identity matrix, conjugacy is equivalent to the usual notion of orthogonality.

EXAMPLE 1 Interpretation of A-conjugate vectors

For an interpretation of **A**-conjugate vectors, consider the situation described in Fig. 4.20a, pertaining to a two-dimensional problem. The elliptic locus shown in this figure corresponds to a plot of Eq. (4.116) for

$$\mathbf{x} = [x_0, x_1]^T$$

at some constant value assigned to the quadratic function $f(\mathbf{x})$. Figure 4.20a also includes a pair of direction vectors that are conjugate with respect to the matrix **A**. Suppose that we define a new parameter vector **v** related to **x** by the transformation

$$\mathbf{v} = \mathbf{A}^{1/2}\mathbf{x}$$

where $\mathbf{A}^{1/2}$ is the square root of **A**. Then the elliptic locus of Fig. 4.20a is transformed into a circular locus, as shown in Fig. 4.20b. Correspondingly, the pair of **A**-conjugate direction vectors in Fig. 4.20a is transformed into a pair of orthogonal direction vectors in Fig. 4.20b. ■

An important property of **A**-conjugate vectors is that they are *linearly independent.* We prove this property by contradiction. Let one of these vectors—say, $\mathbf{s}(0)$—be expressed as a linear combination of the remaining $W-1$ vectors as follows:

$$\mathbf{s}(0) = \sum_{j=1}^{W-1} \alpha_j \mathbf{s}(j)$$

Multiplying by **A** and then taking the inner product of $\mathbf{As}(0)$ with $\mathbf{s}(0)$ yields

$$\mathbf{s}^T(0)\mathbf{As}(0) = \sum_{j=1}^{W-1} \alpha_j \mathbf{s}^T(0)\mathbf{As}(j) = 0$$

However, it is impossible for the quadratic form $\mathbf{s}^T(0)\mathbf{As}(0)$ to be zero, for two reasons: The matrix **A** is positive definite by assumption, and the vector $\mathbf{s}(0)$ is nonzero by definition. It follows therefore that the **A**-conjugate vectors $\mathbf{s}(0), \mathbf{s}(1), \ldots, \mathbf{s}(W-1)$ cannot be linearly dependent; that is, they must be linearly independent.

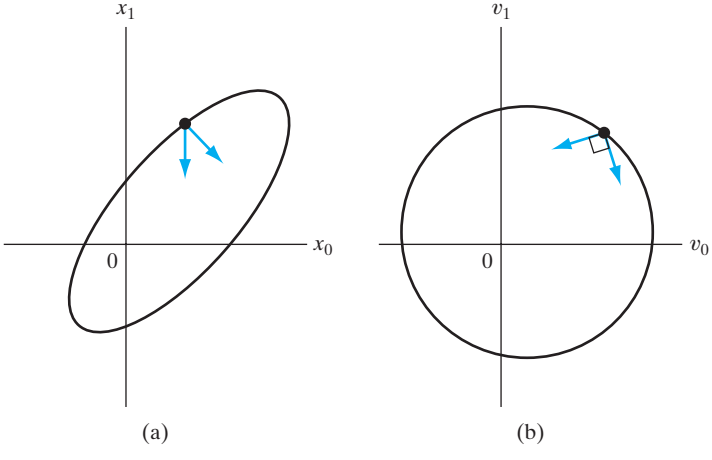

FIGURE 4.20 Interpretation of **A**-conjugate vectors. (a) Elliptic locus in two-dimensional weight space. (b) Transformation of the elliptic locus into a circular locus.

For a given set of **A**-conjugate vectors $\mathbf{s}(0), \mathbf{s}(1), ..., \mathbf{s}(W-1)$, the corresponding *conjugate-direction method* for unconstrained minimization of the quadratic error function $f(\mathbf{x})$ is defined by

$$\mathbf{x}(n+1) = \mathbf{x}(n) + \eta(n)\mathbf{s}(n), \qquad n = 0, 1, ..., W-1 \tag{4.119}$$

where $\mathbf{x}(0)$ is an arbitrary starting vector and $\eta(n)$ is a scalar defined by

$$f(\mathbf{x}(n) + \eta(n)\mathbf{s}(n)) = \min_{\eta} f(\mathbf{x}(n) + \eta\mathbf{s}(n)) \tag{4.120}$$

(Fletcher, 1987; Bertsekas, 1995). The procedure of choosing η so as to minimize the function $f(\mathbf{x}(n) + \eta\mathbf{s}(n))$ for some fixed n is referred to as a *line search*, which represents a one-dimensional minimization problem.

In light of Eqs. (4.118), (4.119) and (4.120), we now offer some observations:

1. Since the **A**-conjugate vectors $\mathbf{s}(0), \mathbf{s}(1), ..., \mathbf{s}(W-1)$ are linearly independent, they form a basis that spans the vector space of $\mathbf{w}$.
2. The update equation (4.119) and the line minimization of Eq. (4.120) lead to the same formula for the learning-rate parameter, namely,

$$\eta(n) = -\frac{\mathbf{s}^T(n)\mathbf{A}\mathbf{e}(n)}{\mathbf{s}^T(n)\mathbf{A}\mathbf{s}(n)}, \qquad n = 0, 1, ..., W-1 \tag{4.121}$$

   where $\mathbf{e}(n)$ is the *error vector* defined by

$$\mathbf{e}(n) = \mathbf{x}(n) - \mathbf{x}^* \tag{4.122}$$

3. Starting from an arbitrary point $\mathbf{x}(0)$, the conjugate-direction method is guaranteed to find the optimum solution $\mathbf{x}^*$ of the quadratic equation $f(\mathbf{x}) = 0$ in at most W iterations.

The principal property of the conjugate-direction method is described in the following statement (Fletcher, 1987; Bertsekas, 1995):

> *At successive iterations, the conjugate-direction method minimizes the quadratic function $f(\mathbf{x})$ over a progressively expanding linear vector space that eventually includes the global minimum of $f(\mathbf{x})$.*

In particular, for each iteration n, the iterate $\mathbf{x}(n+1)$ minimizes the function $f(\mathbf{x})$ over a linear vector space $\mathcal{D}_n$ that passes through some arbitrary point $\mathbf{x}(0)$ and is spanned by the **A**-conjugate vectors $\mathbf{s}(0), \mathbf{s}(1), ..., \mathbf{s}(n)$, as shown by

$$\mathbf{x}(n+1) = \arg\min_{\mathbf{x} \in \mathcal{D}_n} f(\mathbf{x}) \tag{4.123}$$

where the space $\mathcal{D}_n$ is defined by

$$\mathcal{D}_n = \left\{ \mathbf{x}(n) \,|\, \mathbf{x}(n) = \mathbf{x}(0) + \sum_{j=0}^{n} \eta(j)\mathbf{s}(j) \right\} \tag{4.124}$$

For the conjugate-direction method to work, we require the availability of a set of **A**-conjugate vectors $\mathbf{s}(0), \mathbf{s}(1), ..., \mathbf{s}(W-1)$. In a special form of this method known as the *scaled conjugate-gradient method*,[12] the successive direction vectors are generated as **A**-conjugate versions of the successive gradient vectors of the quadratic function $f(\mathbf{x})$ as the method progresses—hence the name of the method. Thus, except for $n = 0$, the set of direction vectors $\{\mathbf{s}(n)\}$ is not specified beforehand, but rather it is determined in a sequential manner at successive steps of the method.

First, we define the *residual* as the steepest-descent direction:

$$\mathbf{r}(n) = \mathbf{b} - \mathbf{A}\mathbf{x}(n) \tag{4.125}$$

Then, to proceed, we use a linear combination of $\mathbf{r}(n)$ and $\mathbf{s}(n-1)$, as shown by

$$\mathbf{s}(n) = \mathbf{r}(n) + \beta(n)\mathbf{s}(n-1), \qquad n = 1, 2, ..., W-1 \tag{4.126}$$

where $\beta(n)$ is a scaling factor to be determined. Multiplying this equation by **A**, taking the inner product of the resulting expression with $\mathbf{s}(n-1)$, invoking the **A**-conjugate property of the direction vectors, and then solving the resulting expression for $\beta(n)$, we get

$$\beta(n) = -\frac{\mathbf{s}^T(n-1)\mathbf{A}\mathbf{r}(n)}{\mathbf{s}^T(n-1)\mathbf{A}\mathbf{s}(n-1)} \tag{4.127}$$

Using Eqs. (4.126) and (4.127), we find that the vectors $\mathbf{s}(0), \mathbf{s}(1), ..., \mathbf{s}(W-1)$ so generated are indeed **A**-conjugate.

Generation of the direction vectors in accordance with the recursive equation (4.126) depends on the coefficient $\beta(n)$. The formula of Eq. (4.127) for evaluating $\beta(n)$, as it presently stands, requires knowledge of matrix **A**. For computational reasons, it would be desirable to evaluate $\beta(n)$ without explicit knowledge of **A**. This evaluation can be achieved by using one of two formulas (Fletcher, 1987):

1. *the Polak–Ribière formula*, for which $\beta(n)$ is defined by

$$\beta(n) = \frac{\mathbf{r}^T(n)(\mathbf{r}(n) - \mathbf{r}(n-1))}{\mathbf{r}^T(n-1)\mathbf{r}(n-1)} \tag{4.128}$$

2. *the Fletcher–Reeves formula*, for which $\beta(n)$ is defined by

$$\beta(n) = \frac{\mathbf{r}^T(n)\mathbf{r}(n)}{\mathbf{r}^T(n-1)\mathbf{r}(n-1)} \tag{4.129}$$

To use the conjugate-gradient method to attack the unconstrained minimization of the cost function $\mathscr{E}_{\text{av}}(\mathbf{w})$ pertaining to the unsupervised training of multilayer perceptron, we do two things:

- Approximate the cost function $\mathscr{E}_{\text{av}}(\mathbf{w})$ by a quadratic function. That is, the third- and higher-order terms in Eq. (4.111) are ignored, which means that we are operating close to a local minimum on the error surface. On this basis, comparing Eqs. (4.111) and (4.116), we can make the associations indicated in Table 4.2.
- Formulate the computation of coefficients $\beta(n)$ and $\eta(n)$ in the conjugate-gradient algorithm so as to require only gradient information.

TABLE 4.2 Correspondence Between $f(\mathbf{x})$ and $\mathscr{E}_{av}(\mathbf{w})$

Quadratic function $f(\mathbf{x})$	Cost function $\mathscr{E}_{av}(\mathbf{w})$
Parameter vector $\mathbf{x}(n)$	Synaptic weight vector $\mathbf{w}(n)$
Gradient vector $\partial f(\mathbf{x})/\partial \mathbf{x}$	Gradient vector $\mathbf{g} = \partial \mathscr{E}_{av}/\partial \mathbf{w}$
Matrix $\mathbf{A}$	Hessian matrix $\mathbf{H}$

The latter point is particularly important in the context of multilayer perceptrons because it avoids using the Hessian $\mathbf{H}(n)$, the evaluation of which is plagued with computational difficulties.

To compute the coefficient $\beta(n)$ that determines the search direction $\mathbf{s}(n)$ without explicit knowledge of the Hessian $\mathbf{H}(n)$, we can use the Polak–Ribière formula of Eq. (4.128) or the Fletcher–Reeves formula of Eq. (4.129). Both of these formulas involve the use of residuals only. In the linear form of the conjugate-gradient method, assuming a quadratic function, the Polak–Ribière and Fletcher–Reeves formulas are equivalent. On the other hand, in the case of a nonquadratic cost function, they are not.

For nonquadratic optimization problems, the Polak–Ribière form of the conjugate-gradient algorithm is typically superior to the Fletcher–Reeves form of the algorithm, for which we offer the following heuristic explanation (Bertsekas, 1995): Due to the presence of third- and higher-order terms in the cost function $\mathscr{E}_{av}(\mathbf{w})$ and possible inaccuracies in the line search, conjugacy of the generated search directions is progressively lost. This condition may in turn cause the algorithm to "jam" in the sense that the generated direction vector $\mathbf{s}(n)$ is nearly orthogonal to the residual $\mathbf{r}(n)$. When this phenomenon occurs, we have $\mathbf{r}(n) = \mathbf{r}(n-1)$, in which case the scalar $\beta(n)$ will be nearly zero. Correspondingly, the direction vector $\mathbf{s}(n)$ will be close to $\mathbf{r}(n)$, thereby breaking the jam. In contrast, when the Fletcher–Reeves formula is used, the conjugate-gradient algorithm typically continues to jam under similar conditions.

In rare cases, however, the Polak–Ribière method can cycle indefinitely without converging. Fortunately, convergence of the Polak–Ribière method can be guaranteed by choosing

$$\beta = \max\{\beta_{PR}, 0\} \tag{4.130}$$

where β_{PR} is the value defined by the Polak–Ribière formula of Eq. (4.128) (Shewchuk, 1994). Using the value of β defined in Eq. (4.130) is equivalent to restarting the conjugate gradient algorithm if $\beta_{PR} < 0$. To restart the algorithm is equivalent to forgetting the last search direction and starting it anew in the direction of steepest descent.

Consider next the issue of computing the parameter $\eta(n)$, which determines the learning rate of the conjugate-gradient algorithm. As with $\beta(n)$, the preferred method for computing $\eta(n)$ is one that avoids having to use the Hessian $\mathbf{H}(n)$. We recall that the line minimization based on Eq. (4.120) leads to the same formula for $\eta(n)$ as that derived from the update equation Eq. (4.119). We therefore need a *line search*,[12] the purpose of which is to minimize the function $\mathscr{E}_{av}(\mathbf{w} + \eta\mathbf{s})$ with respect to η. That is, given fixed values of the vectors $\mathbf{w}$ and $\mathbf{s}$, the problem is to vary η such that this function is minimized. As η varies, the argument $\mathbf{w} + \eta\mathbf{s}$ traces a line in the W-dimensional

vector space of $\mathbf{w}$—hence the name "line search." A *line-search algorithm* is an iterative procedure that generates a sequence of estimates $\{\eta(n)\}$ for each iteration of the conjugate-gradient algorithm. The line search is terminated when a satisfactory solution is found. The computation of a line search must be performed along each search direction.

Several line-search algorithms have been proposed in the literature, and a good choice is important because it has a profound impact on the performance of the conjugate-gradient algorithm in which it is embedded. There are two phases to any line-search algorithm (Fletcher, 1987):

- *the bracketing phase*, which searches for a *bracket* (that is, a nontrivial interval that is known to contain a minimum), and
- *the sectioning phase*, in which the bracket is *sectioned* (i.e., divided), thereby generating a sequence of brackets whose length is progressively reduced.

We now describe a *curve-fitting procedure* that takes care of these two phases in a straightforward manner.

Let $\mathscr{E}_{\text{av}}(\eta)$ denote the cost function of the multilayer perceptron, expressed as a function of η. It is assumed that $\mathscr{E}_{\text{av}}(\eta)$ is strictly *unimodal* (i.e., it has a single minimum in the neighborhood of the current point $\mathbf{w}(n)$) and is twice continuously differentiable. We initiate the search procedure by searching along the line until we find three points η_1, η_2, and η_3 such that the following condition is satisfied, as illustrated in Fig. 4.21:

$$\mathscr{E}_{\text{av}}(\eta_1) \geq \mathscr{E}_{\text{av}}(\eta_3) \geq \mathscr{E}_{\text{av}}(\eta_2) \qquad \text{for } \eta_1 < \eta_2 < \eta_3 \tag{4.131}$$

Since $\mathscr{E}_{\text{av}}(\eta)$ is a continuous function of η, the choice described in Eq. (4.131) ensures that the bracket $[\eta_1, \eta_3]$ contains a minimum of the function $\mathscr{E}_{\text{av}}(\eta)$. Provided that the function $\mathscr{E}_{\text{av}}(\eta)$ is sufficiently smooth, we may consider this function to be parabolic in the immediate neighborhood of the minimum. Accordingly, we may use *inverse parabolic interpolation* to do the sectioning (Press et al., 1988). Specifically, a parabolic function is fitted through the three original points η_1, η_2, and η_3, as illustrated in Fig. 4.22, where the solid line corresponds to $\mathscr{E}_{\text{av}}(\eta)$ and the dashed line corresponds to the first iteration

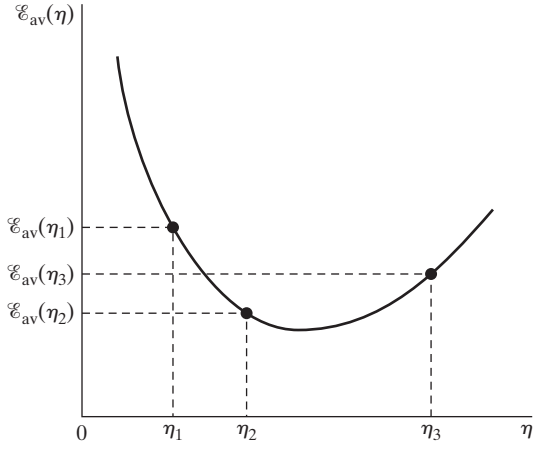

FIGURE 4.21 Illustration of the line search.

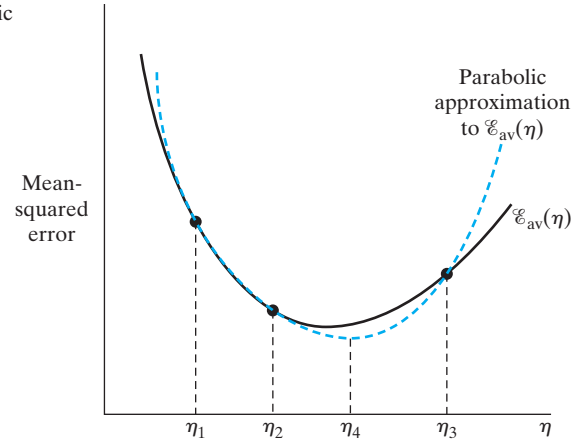

FIGURE 4.22 Inverse parabolic interpolation.

of the sectioning procedure. Let the minimum of the parabola passing through the three points η_1, η_2, and η_3 be denoted by η_4. In the example illustrated in Fig. 4.22, we have $\mathscr{E}_{av}(\eta_4) < \mathscr{E}_{av}(\eta_2)$ and $\mathscr{E}_{av}(\eta_4) < \mathscr{E}_{av}(\eta_1)$. Point η_3 is replaced in favor of η_4, making $[\eta_1, \eta_4]$ the new bracket. The process is repeated by constructing a new parabola through the points η_1, η_2, and η_4. The bracketing-followed-by-sectioning procedure, as illustrated in Fig. 4.22, is repeated several times until a point close enough to the minimum of $\mathscr{E}_{av}(\eta)$ is located, at which time the line search is terminated.

Brent's method constitutes a highly refined version of the three-point curve-fitting procedure just described (Press et al., 1988). At any particular stage of the computation, Brent's method keeps track of six points on the function $\mathscr{E}_{av}(\eta)$, which may not all be necessarily distinct. As before, parabolic interpolation is attempted through three of these points. For the interpolation to be acceptable, certain criteria involving the remaining three points must be satisfied. The net result is a robust line-search algorithm.

Summary of the Nonlinear Conjugate-Gradient Algorithm

All the ingredients we need to formally describe the nonlinear (nonquadratic) form of the conjugate-gradient algorithm for the supervised training of a multilayer perceptron are now in place. A summary of the algorithm is presented in Table 4.3.

Quasi-Newton Methods

Resuming the discussion on quasi-Newton methods, we find that these are basically gradient methods described by the update equation

$$\mathbf{w}(n+1) = \mathbf{w}(n) + \eta(n)\mathbf{s}(n) \tag{4.132}$$

where the direction vector $\mathbf{s}(n)$ is defined in terms of the gradient vector $\mathbf{g}(n)$ by

$$\mathbf{s}(n) = -\mathbf{S}(n)\mathbf{g}(n) \tag{4.133}$$

TABLE 4.3 Summary of the Nonlinear Conjugate-Gradient Algorithm for the Supervised Training of a Multilayer Perceptron

Initialization

Unless prior knowledge on the weight vector $\mathbf{w}$ is available, choose the initial value $\mathbf{w}(0)$ by using a procedure similar to that described for the back-propagation algorithm.

Computation

1. For $\mathbf{w}(0)$, use back propagation to compute the gradient vector $\mathbf{g}(0)$.

2. Set $\mathbf{s}(0) = \mathbf{r}(0) = -\mathbf{g}(0)$.

3. At time-step n, use a line search to find $\eta(n)$ that minimizes $\mathscr{E}_{\text{av}}(\eta)$ sufficiently, representing the cost function $\mathscr{E}_{\text{av}}$ expressed as a function of η for fixed values of $\mathbf{w}$ and $\mathbf{s}$.

4. Test to determine whether the Euclidean norm of the residual $\mathbf{r}(n)$ has fallen below a specified value, that is, a small fraction of the initial value $\|\mathbf{r}(0)\|$.

5. Update the weight vector:

$$\mathbf{w}(n+1) = \mathbf{w}(n) + \eta(n)\mathbf{s}(n)$$

6. For $\mathbf{w}(n+1)$, use back propagation to compute the updated gradient vector $\mathbf{g}(n+1)$.

7. Set $\mathbf{r}(n+1) = -\mathbf{g}(n+1)$.

8. Use the Polak–Ribière method to calculate:

$$\beta(n+1) = \max\left\{\frac{\mathbf{r}^T(n+1)(\mathbf{r}(n+1) - \mathbf{r}(n))}{\mathbf{r}^T(n)\mathbf{r}(n)}, 0\right\}$$

9. Update the direction vector:

$$\mathbf{s}(n+1) = \mathbf{r}(n+1) + \beta(n+1)\mathbf{s}(n)$$

10. Set $n = n + 1$, and go back to step 3.

Stopping criterion. Terminate the algorithm when the condition

$$\|\mathbf{r}(n)\| \leq \varepsilon\|\mathbf{r}(0)\|$$

is satisfied, where ε is a prescribed small number.

The matrix $\mathbf{S}(n)$ is a positive-definite matrix that is adjusted from one iteration to the next. This is done in order to make the direction vector $\mathbf{s}(n)$ approximate the *Newton direction*, namely,

$$-(\partial^2\mathscr{E}_{\text{av}}/\partial\mathbf{w}^2)^{-1}\,(\partial\mathscr{E}_{\text{av}}/\partial\mathbf{w})$$

Quasi-Newton methods use second-order (curvature) information about the error surface without actually requiring knowledge of the Hessian. They do so by using two successive iterates $\mathbf{w}(n)$ and $\mathbf{w}(n+1)$, together with the respective gradient vectors $\mathbf{g}(n)$ and $\mathbf{g}(n+1)$. Let

$$\mathbf{q}(n) = \mathbf{g}(n+1) - \mathbf{g}(n) \tag{4.134}$$

and

$$\Delta\mathbf{w}(n) = \mathbf{w}(n+1) - \mathbf{w}(n) \tag{4.135}$$

We may then derive curvature information by using the approximate formula

$$\mathbf{q}(n) \simeq \left(\frac{\partial}{\partial \mathbf{w}} \mathbf{g}(n) \right) \Delta \mathbf{w}(n) \tag{4.136}$$

In particular, given W linearly independent weight increments $\Delta\mathbf{w}(0), \Delta\mathbf{w}(1), ..., \Delta\mathbf{w}(W-1)$ and the respective gradient increments $\mathbf{q}(0), \mathbf{q}(1), ..., \mathbf{q}(W-1)$, we may approximate the Hessian as

$$\mathbf{H} \simeq [\mathbf{q}(0), \mathbf{q}(1), ..., \mathbf{q}(W-1)] [\Delta\mathbf{w}(0), \Delta\mathbf{w}(1), ..., \Delta\mathbf{w}(W-1)]^{-1} \tag{4.137}$$

We may also approximate the inverse Hessian as follows[13]:

$$\mathbf{H}^{-1} \simeq [\Delta\mathbf{w}(0), \Delta\mathbf{w}(1), ..., \Delta\mathbf{w}(W-1)] [\mathbf{q}(0), \mathbf{q}(1), ..., \mathbf{q}(W-1)]^{-1} \tag{4.138}$$

When the cost function $\mathscr{E}_{av}(\mathbf{w})$ is quadratic, Eqs. (4.137) and (4.138) are exact.

In the most popular class of quasi-Newton methods, the updated matrix $\mathbf{S}(n+1)$ is obtained from its previous value $\mathbf{S}(n)$, the vectors $\Delta\mathbf{w}(n)$ and $\mathbf{q}(n)$, by using the following recursion (Fletcher, 1987; Bertsekas, 1995):

$$\begin{aligned} \mathbf{S}(n+1) = \mathbf{S}(n) &+ \frac{\Delta\mathbf{w}(n)\Delta\mathbf{w}^T(n)}{\mathbf{q}^T(n)\mathbf{q}(n)} - \frac{\mathbf{S}(n)\mathbf{q}(n)\mathbf{q}^T(n)\mathbf{S}(n)}{\mathbf{q}^T(n)\mathbf{S}(n)\mathbf{q}(n)} \\ &+ \xi(n)[\mathbf{q}^T(n)\mathbf{S}(n)\mathbf{q}(n)]\,[\mathbf{v}(n)\mathbf{v}^T(n)] \end{aligned} \tag{4.139}$$

where

$$\mathbf{v}(n) = \frac{\Delta\mathbf{w}(n)}{\Delta\mathbf{w}^T(n)\Delta\mathbf{w}(n)} - \frac{\mathbf{S}(n)\mathbf{q}(n)}{\mathbf{q}^T(n)\mathbf{S}(n)\mathbf{q}(n)} \tag{4.140}$$

and

$$0 \le \xi(n) \le 1 \qquad \text{for all } n \tag{4.141}$$

The algorithm is initiated with some arbitrary positive- definite matrix $\mathbf{S}(0)$. The particular form of the quasi-Newton method is parameterized by how the scalar $\xi(n)$ is defined, as indicated by the following two points (Fletcher, 1987):

1. For $\xi(n) = 0$ for all n, we obtain the *Davidon–Fletcher–Powell (DFP) algorithm*, which is historically the first quasi-Newton method.
2. For $\xi(n) = 1$ for all n, we obtain the *Broyden–Fletcher–Goldfarb–Shanno (BFGS) algorithm*, which is considered to be the best form of quasi-Newton methods currently known.

Comparison of Quasi-Newton Methods with Conjugate-Gradient Methods

We conclude this brief discussion of quasi-Newton methods by comparing them with conjugate-gradient methods in the context of nonquadratic optimization problems (Bertsekas, 1995):

- Both quasi-Newton and conjugate-gradient methods avoid the need to use the Hessian. However, quasi-Newton methods go one step further by generating an

approximation to the inverse Hessian. Accordingly, when the line search is accurate and we are in close proximity to a local minimum with a positive-definite Hessian, a quasi-Newton method tends to approximate Newton's method, thereby attaining faster convergence than would be possible with the conjugate-gradient method.

- Quasi-Newton methods are not as sensitive to accuracy in the line-search stage of the optimization as the conjugate-gradient method.
- Quasi-Newton methods require storage of the matrix $\mathbf{S}(n)$, in addition to the matrix-vector multiplication overhead associated with the computation of the direction vector $\mathbf{s}(n)$. The net result is that the computational complexity of quasi-Newton methods is $O(W^2)$. In contrast, the computational complexity of the conjugate-gradient method is $O(W)$. Thus, when the dimension W (i.e., size of the weight vector $\mathbf{w}$) is large, conjugate-gradient methods are preferable to quasi-Newton methods in computational terms.

It is because of the lattermost point that the use of quasi-Newton methods is restricted, in practice, to the design of small-scale neural networks.

Levenberg–Marquardt Method

The Levenberg–Marquardt method, due to Levenberg (1994) and Marquardt (1963), is a compromise between the following two methods:

- Newton's method, which converges rapidly near a local or global minimum, but may also diverge;
- Gradient descent, which is assured of convergence through a proper selection of the step-size parameter, but converges slowly.

To be specific, consider the optimization of a second-order function $F(\mathbf{w})$, and let $\mathbf{g}$ be its gradient vector and $\mathbf{H}$ be its Hessian. According to the Levenberg–Marquardt method, the optimum adjustment $\Delta\mathbf{w}$ applied to the parameter vector $\mathbf{w}$ is defined by

$$\Delta\mathbf{w} = [\mathbf{H} + \lambda\mathbf{I}]^{-1}\mathbf{g} \tag{4.142}$$

where $\mathbf{I}$ is the identity matrix of the same dimensions as $\mathbf{H}$ and λ is a *regularizing*, or *loading*, *parameter* that forces the sum matrix $(\mathbf{H} + \lambda\mathbf{I})$ to be positive definite and safely well conditioned throughout the computation. Note also that the adjustment $\Delta\mathbf{w}$ of Eq. (4.142) is a minor modification of the formula defined in Eq. (4.115).

With this background, consider a multilayer perceptron with a single output neuron. The network is trained by minimizing the cost function

$$\mathscr{E}_{\text{av}}(\mathbf{w}) = \frac{1}{2N}\sum_{i=1}^{N}[d(i) - F(\mathbf{x}(i); \mathbf{w})]^2 \tag{4.143}$$

where $\{\mathbf{x}(i), d(i)\}_{i=1}^{N}$ is the training sample and $F(\mathbf{x}(i); \mathbf{w})$ is the approximating function realized by the network; the synaptic weights of the network are arranged in some orderly manner to form the weight vector $\mathbf{w}$. The gradient and the Hessian of the cost function $\mathscr{E}_{\text{av}}(\mathbf{w})$ are respectively defined by

$$\mathbf{g}(\mathbf{w}) = \frac{\partial \mathscr{E}_{\text{av}}(\mathbf{w})}{\partial \mathbf{w}} = -\frac{1}{N}\sum_{i=1}^{N}[d(i) - F(\mathbf{x}(i); \mathbf{w})]\frac{\partial F(\mathbf{x}(i); \mathbf{w})}{\partial \mathbf{w}} \tag{4.144}$$

and

$$\mathbf{H}(\mathbf{w}) = \frac{\partial^2 \mathscr{E}_{\text{av}}(\mathbf{w})}{\partial \mathbf{w}^2} = \frac{1}{N}\sum_{i=1}^{N}\left[\frac{\partial F(\mathbf{x}(i); \mathbf{w})}{\partial \mathbf{w}}\right]\left[\frac{\partial F(\mathbf{x}(i); \mathbf{w})}{\partial \mathbf{w}}\right]^T - \frac{1}{N}\sum_{i=1}^{N}[d(i) - F(\mathbf{x}(i); \mathbf{w})]\frac{\partial^2 F(\mathbf{x}(i); \mathbf{w})}{\partial \mathbf{w}^2} \tag{4.145}$$

Thus, substituting Eqs. (4.144) and (4.145) into Eq. (4.142), the desired adjustment $\Delta\mathbf{w}$ is computed for each iteration of the Levenberg-Marquardt algorithm.

However, from a practical perspective, the computational complexity of Eq. (4.145) can be demanding, particularly when the dimensionality of the weight vector $\mathbf{w}$ is high; the computational difficulty is attributed to the complex nature of the Hessian $\mathbf{H}(\mathbf{w})$. To mitigate this difficulty, the recommended procedure is to ignore the second term on the right-hand side of Eq. (4.145), thereby approximating the Hessian simply as

$$\mathbf{H}(\mathbf{w}) \approx \frac{1}{N}\sum_{i=1}^{N}\left[\frac{\partial F(\mathbf{x}(i); \mathbf{w})}{\partial \mathbf{w}}\right]\left[\frac{\partial F(\mathbf{x}(i); \mathbf{w})}{\partial \mathbf{w}}\right]^T \tag{4.146}$$

This approximation is recognized as the outer product of the partial derivative $\partial F(\mathbf{w}, \mathbf{x}(i))/\partial \mathbf{w}$ with itself, averaged over the training sample; accordingly, it is referred to as the *outer-product approximation* of the Hessian. The use of this approximation is justified when the Levenberg-Marquardt algorithm is operating in the neighborhood of a local or global minimum.

Clearly, the approximate version of the Levenberg–Marquardt algorithm, based on the gradient vector of Eq. (4.144) and the Hessian of Eq. (4.146), is a first-order method of optimization that is well suited for nonlinear least-squares estimation problems. Moreover, because of the fact that both of these equations involve averaging over the training sample, the algorithm is of a batch form.

The regularizing parameter λ plays a critical role in the way the Levenberg-Marquardt algorithm functions. If we set λ equal to zero, then the formula of Eq. (4.142) reduces to Newton's method. On the other hand, if we assign a large value to λ such that $\lambda\mathbf{I}$ overpowers the Hessian $\mathbf{H}$, the Levenberg-Marquardt algorithm functions effectively as a gradient descent method. From these two observations, it follows that at each iteration of the algorithm, the value assigned to λ should be just large enough to maintain the sum matrix $(\mathbf{H} + \lambda\mathbf{I})$ in its positive-definite form. In specific terms, the recommended *Marquardt recipe* for the selection of λ is as follows (Press et al.,) 1988:

1. Compute $\mathscr{E}_{\text{av}}(\mathbf{w})$ at iteration $n - 1$.
2. Choose a modest value for λ, say $\lambda = 10^{-3}$.

3. Solve Eq. (4.142) for the adjustment $\Delta\mathbf{w}$ at iteration n and evaluate $\mathscr{E}_{av}(\mathbf{w} + \Delta\mathbf{w})$.
4. If $\mathscr{E}_{av}(\mathbf{w} + \Delta\mathbf{w}) \geq \mathscr{E}_{av}(\mathbf{w})$, increase λ by a factor of 10 (or any other substantial factor) and go back to step 3.
5. If, on the other hand, $\mathscr{E}_{av}(\mathbf{w} + \Delta\mathbf{w}) < \mathscr{E}_{av}(w)$, decrease λ by a factor of 10, update the trial solution $\mathbf{w} \rightarrow \mathbf{w} + \Delta\mathbf{w}$, and go back to step 3.

For obvious reasons, a rule for stopping the iterative process is necessary. In Press et al. (1998), it is pointed out that an adjustment in the parameter vector $\mathbf{w}$ that changes $\mathscr{E}_{av}(\mathbf{w})$ by an incrementally small amount is *never* statistically meaningful. We may therefore use this insightful comment as a basis for the stopping rule.

One last comment is in order: To evaluate the partial derivative $\partial F(\mathbf{x}; \mathbf{w})/\partial\mathbf{w}$ at each iteration of the algorithm, we may use back-propagation in the manner described in Section 4.8.

Second-Order Stochastic Gradient Descent for On-line Learning

Up to this point, this section has focused on second-order optimization techniques for batch learning. Hereafter, we turn our attention to second-order stochastic gradient-descent methods for on-line learning. Although these two families of techniques are entirely different, they do share a common purpose:

The second-order information contained in the Hessian (curvature) of the cost function is used to improve the performance of supervised-learning algorithms.

A simple way of expanding on the performance of the optimally annealed on-line learning algorithm considered in Section 4.10 is to replace the learning-rate parameter $\eta(n)$ in Eq. (4.60) with the scaled inverse of the Hessian $\mathbf{H}$, as shown by

$$\underbrace{\hat{\mathbf{w}}(n+1)}_{\text{Updated estimate}} = \underbrace{\hat{\mathbf{w}}(n)}_{\text{Old estimate}} - \underbrace{\frac{1}{n}\mathbf{H}^{-1}}_{\substack{\text{Annealed inverse} \\ \text{of the} \\ \text{Hessian } \mathbf{H}}} \underbrace{\mathbf{g}(\mathbf{x}(n+1), \mathbf{d}(n+1); \hat{\mathbf{w}}(n))}_{\substack{\text{Gradient vector} \\ \mathbf{g}}} \tag{4.147}$$

The replacement of $\eta(n)$ with the new term $\frac{1}{n}\mathbf{H}^{-1}$ is intended to accelerate the speed of convergence of the on-line algorithm in an optimally annealed fashion. It is assumed that the Hessian $\mathbf{H}$ is known a priori and its inverse $\mathbf{H}^{-1}$ can therefore be precomputed.

Recognizing the fact that "there is no such thing as a free lunch," the price paid for the accelerated convergence is summarized as follows (Bottou, 2007):

(i) Whereas in the stochastic gradient descent of Eq. (4.60), the computation cost per iteration of the algorithm is $O(W)$, where W is the dimension of the weight vector $\mathbf{w}$ being estimated, the corresponding computation cost per iteration of the second-order stochastic gradient-descent algorithm in Eq. (4.147) is $O(W^2)$.

(ii) For each training example $(\mathbf{x}, \mathbf{d})$ processed by the algorithm of Eq. (4.147), the algorithm requires multiplication of the W-by-l gradient vector $\mathbf{g}$ and the W-by-W inverse matrix $\mathbf{H}^{-1}$ and storage of the product.

(iii) In a general context, whenever some form of *sparsity* exists in the training sample, the natural move is to exploit the sparsity for the purpose of improved algorithmic performance. Unfortunately, the Hessian $\mathbf{H}$ is typically a full matrix and therefore not sparse, which rules out the possibility of exploiting training-sample sparsity.

To overcome these limitations, we may resort to one of the following *approximation procedures*:

(i) *Diagonal approximation:* (Becker and LeCun, 1989). In this procedure, only the diagonal elements of the Hessian are retained, which means that the inverse matrix $\mathbf{H}^{-1}$ will likewise be a diagonal matrix. Matrix theory teaches us that the matrix product $\mathbf{H}^{-1}\mathbf{g}$ will consist of a sum of terms of the form $h_{ii}^{-1}g_i$, where h_{ii} is the ith diagonal element of the Hessian $\mathbf{H}$ and g_i is the corresponding element of the gradient $\mathbf{g}$ for $i = 1, 2, ..., W$. With the gradient vector $\mathbf{g}$ being linear in the weights, it follows that the computational complexity of the approximated second-order on-line learning algorithm is $O(W)$.

(ii) *Low-rank approximation:* (LeCun et al., 1998). By definition, the rank of a matrix equals the number of algebraically independent columns of the matrix. Given a Hessian $\mathbf{H}$, the use of *singular value decomposition* (SVD) provides an important procedure for the low-rank approximation of the Hessian $\mathbf{H}$. Let the rank of $\mathbf{H}$ be denoted by p and a rank r approximation of $\mathbf{H}$ be denoted by $\mathbf{H}_r$, where $r < p$. The squared error between the Hessian and its approximation is defined by the *Frobenius norm*

$$e^2 = \text{tr}[(\mathbf{H} - \mathbf{H}_r)^T(\mathbf{H} - \mathbf{H}_r)] \tag{4.148}$$

where tr[·] denotes the *trace* (i.e., sum of the diagonal components) of the square matrix enclosed inside the square brackets. Applying the SVD to the matrices $\mathbf{H}$ and $\mathbf{H}_r$, we write

$$\mathbf{H} = \mathbf{V}\Sigma\mathbf{U}^T \tag{4.149}$$

and

$$\mathbf{H}_r = \mathbf{V}\Sigma_r\mathbf{U}^T \tag{4.150}$$

where the orthogonal matrices $\mathbf{U}$ and $\mathbf{V}$ define the common *right* and *left singular vectors*, respectively, and the rectangular matrix

$$\Sigma_r = \text{diag}[\lambda_1, \lambda_2, ..., \lambda_r, 0 ..., 0] \tag{4.151}$$

defines the *singular values* of the low-rank approximation $\mathbf{H}_r$. The new square matrix

$$\mathbf{H}_r = \mathbf{U}\Sigma_r\mathbf{V}^T \tag{4.152}$$

provides the *least-squares*, *rank r approximation* to the Hessian $\mathbf{H}$ (Scharf, 1991). Correspondingly, the use of the new matrix $\mathbf{H}_r$ in place of the Hessian $\mathbf{H}$ in the on-line learning algorithm of Eq. (4.147) reduces the computational complexity of the algorithm to somewhere between $O(W)$ and $O(W^2)$.

(iii) *BFGS approximation:* (Schraudolph et al., 2007). As pointed out previously in this section, the BFGS algorithm is considered to be the best form of a quasi-Newton

method. In the 2007 paper by Schraudolph et al., the BFGS algorithm is modified in both its full and limited versions of memory such that it becomes usable for the stochastic aproximation of gradients. The modified algorithm appears to provide a fast, scalable, stochastic quasi-Newton procedure for on-line convex optimization. In Yu et al. (2008), the BFGS quasi-Newton method and its limited-memory variant are extended to deal with non-smooth convex objective functions.

4.17 CONVOLUTIONAL NETWORKS

Up to this point, we have been concerned with the algorithmic design of multilayer perceptrons and related issues. In this section, we focus on the structural layout of the multilayer perceptron itself. In particular, we describe a special class of multilayer perceptrons known collectively as *convolutional networks*, which are well suited for pattern classification. The idea behind the development of these networks is neurobiologically motivated, going back to the pioneering work of Hubel and Wiesel (1962, 1977) on locally sensitive and orientation-selective neurons of the visual cortex of a cat.

A *convolutional network* is a multilayer perceptron designed specifically to recognize two-dimensional shapes with a high degree of invariance to translation, scaling, skewing, and other forms of distortion. This difficult task is learned in a supervised manner by means of a network whose structure includes the following forms of *constraints* (LeCun and Bengio, 2003):

1. *Feature extraction.* Each neuron takes its synaptic inputs from a local *receptive field* in the previous layer, thereby forcing it to extract local features. Once a feature has been extracted, its exact location becomes less important, so long as its position relative to other features is approximately preserved.

2. *Feature mapping.* Each computational layer of the network is composed of multiple *feature maps*, with each feature map being in the form of a plane within which the individual neurons are *constrained* to share the same set of synaptic weights. This second form of structural constraint has the following beneficial effects:

- *shift invariance*, forced into the operation of a feature map through the use of *convolution* with a kernel of small size, followed by a sigmoid function;
- *reduction in the number of free parameters*, accomplished through the use of *weight sharing*.

3. *Subsampling.* Each convolutional layer is followed by a computational layer that performs *local averaging* and *subsampling*, whereby the resolution of the feature map is reduced. This operation has the effect of reducing the sensitivity of the feature map's output to shifts and other forms of distortion.

We emphasize that all weights in all layers of a convolutional network are learned through training. Moreover, the network learns to extract its own features automatically.

Figure 4.23 shows the architectural layout of a convolutional network made up of an input layer, four hidden layers, and an output layer. This network is designed to perform *image processing* (e.g., recognition of handwritten characters). The input layer, made up of 28×28 sensory nodes, receives the images of different characters that have

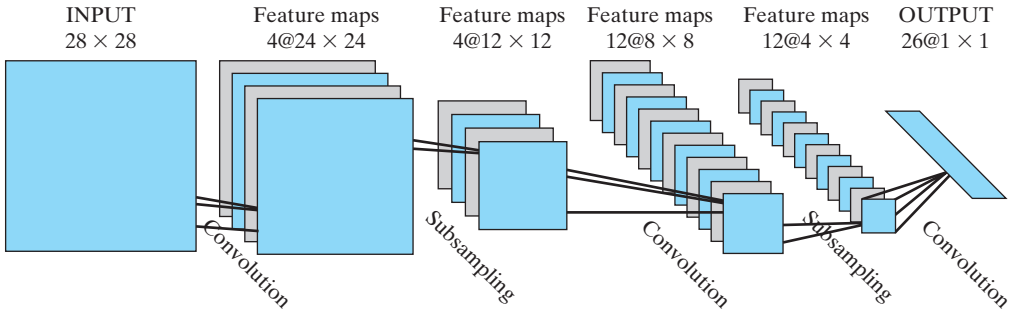

FIGURE 4.23 Convolutional network for image processing such as handwriting recognition. (Reproduced with permission of MIT Press.)

been approximately centered and normalized in size. Thereafter, the computational layouts alternate between convolution and subsampling:

1. The first hidden layer performs convolution. It consists of four feature maps, with each feature map consisting of 24×24 neurons. Each neuron is assigned a receptive field of size 5×5.
2. The second hidden layer performs subsampling and local averaging. It also consists of four feature maps, but each feature map is now made up of 12×12 neurons. Each neuron has a receptive field of size 2×2, a trainable coefficient, a trainable bias, and a sigmoid activation function. The trainable coefficient and bias control the operating point of the neuron; for example, if the coefficient is small, the neuron operates in a quasilinear mode.
3. The third hidden layer performs a second convolution. It consists of 12 feature maps, with each feature map consisting of 8×8 neurons. Each neuron in this hidden layer may have synaptic connections from several feature maps in the previous hidden layer. Otherwise, it operates in a manner similar to the first convolutional layer.
4. The fourth hidden layer performs a second subsampling and local averaging. It consists of 12 feature maps, but with each feature map consisting of 4×4 neurons. Otherwise, it operates in a manner similar to the first subsampling layer.
5. The output layer performs one final stage of convolution. It consists of 26 neurons, with each neuron assigned to one of 26 possible characters. As before, each neuron is assigned a receptive field of size 4×4.

With the successive computational layers alternating between convolution and subsampling, we get a "bipyramidal" effect. That is, at each convolutional or subsampling layer, the number of feature maps is increased while the spatial resolution is reduced, compared with the corresponding previous layer. The idea of convolution followed by subsampling is inspired by the notion of "simple" cells followed by "complex" cells[14] that was first described in Hubel and Wiesel (1962).

The multilayer perceptron described in Fig. 4.23 contains approximately 100,000 synaptic connections, but only about 2,600 free parameters. This dramatic reduction in

the number of free parameters is achieved through the use of weight sharing. The capacity of the learning machine is thereby reduced, which in turn improves the machine's generalization ability. What is even more remarkable is the fact that the adjustments to the free parameters of the network are made by using the stochastic mode of back-propagation learning.

Another noteworthy point is that the use of weight sharing makes it possible to implement the convolutional network in parallel form. This is another advantage of the convolutional network over a fully connected multilayer perceptron.

The lesson to be learned from the convolutional network of Fig. 4.23 is twofold. First, a multilayer perceptron of manageable size is able to learn a complex, high-dimensional, nonlinear mapping by *constraining* its design through the incorporation of prior knowledge about the task at hand. Second, the synaptic weights and bias levels can be learned by cycling the simple back-propagation algorithm through the training sample.

4.18 NONLINEAR FILTERING

The prototypical use of a static neural network, exemplified by the multilayer perceptron, is in *structural pattern recognition*; insofar as applications are concerned, much of the material presented in this chapter has focused on structural pattern recognition. In contrast, in *temporal pattern recognition*, or *nonlinear filtering*, the requirement is to process patterns that evolve over time, with the response at a particular instant of time depending not only on the present value of the input signal, but also on past values. Simply put, *time* is an ordered quantity that constitutes an important ingredient of the learning process in temporal-pattern-recognition tasks.

For a neural network to be dynamic, it must be given *short-term memory* in one form or another. A simple way of accomplishing this modification is through the use of *time delays*, which can be implemented at the synaptic level inside the network or externally at the input layer of the network. Indeed, the use of time delays in neural networks is neurobiologically motivated, since it is well known that signal delays are omnipresent in the brain and play an important role in neurobiological information processing (Braitenberg, 1967, 1977, 1986; Miller, 1987). Time may therefore be built into the operation of a neural network in two basic ways:

- *Implicit representation.* Time is represented by the effect it has on signal processing in an implicit manner. For example, in a digital implementation of the neural network, the input signal is *uniformly sampled*, and the sequence of synaptic weights of each neuron connected to the input layer of the network is convolved with a different sequence of input samples. In so doing, the temporal structure of the input signal is embedded in the spatial structure of the network.
- *Explicit representation.* Time is given its own particular representation inside the network structure. For example, the echolocation system of a bat operates by emitting a short frequency-modulated (FM) signal, so that the same intensity level is maintained for each frequency channel restricted to a very short period within the

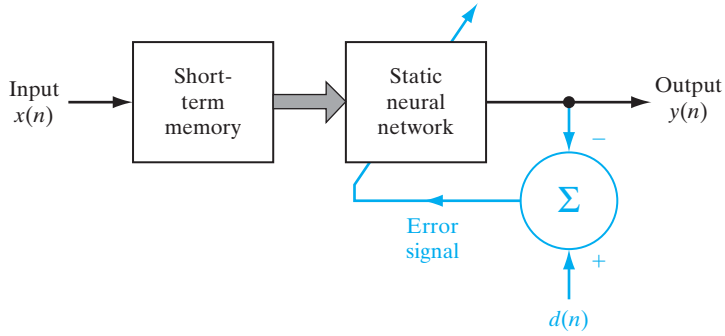

FIGURE 4.24 Nonlinear filter built on a static neural network.

FM sweep. Multiple comparisons between several different frequencies encoded by an array of auditory receptors are made for the purpose of extracting accurate distance (range) information about a target (Suga and Kanwal, 1995). When an echo is received from the target with an unknown delay, a neuron (in the auditory system) with a matching delay line responds, thereby providing an estimate of the range to the target.

In this section, we are concerned with the implicit representation of time, whereby a static neural network (e.g., multilayer perceptron) is provided with *dynamic* properties by external means.

Figure 4.24 shows the block diagram of a *nonlinear filter* consisting of the cascade connection of two subsystems: short-term memory and a static neural network (e.g., multilayer perceptron). This structure provides for a clear-cut separation of processing roles: The static network accounts for nonlinearity, and the memory accounts for time. To be specific, suppose we are given a multilayer perceptron with an input layer of size m. Then, in a corresponding way, the memory is a *single-input*, *multiple-output* (SIMO) structure providing m differently delayed versions of the input signal for stimulating the neural network.

Short-Term Memory Structures

Figure 4.25 shows the block diagram of a *discrete-time memory structure* consisting of p identical sections connected in cascade. Each section is characterized by an impulse response, denoted by $h(n)$, where n denotes discrete time. The number of sections, p, is

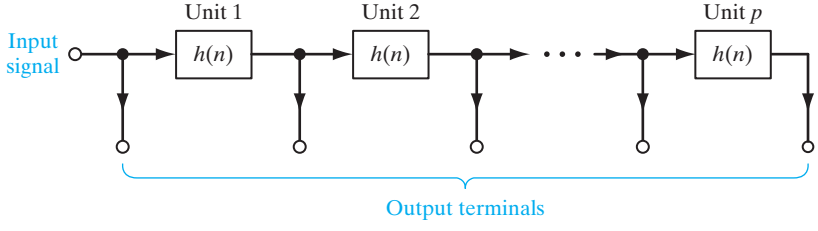

FIGURE 4.25 Generalized tapped-delay-line memory of order p.

called the *order of the memory.* Correspondingly, the number of output terminals (i.e., taps) provided by the memory is $p + 1$, which includes the direct connection from the input to the output. Thus, with m denoting the size of the input layer of the static neural network, we may set

$$m = p + 1$$

The impulse response of each delay section of the memory satisfies two properties:

- *causality*, which means that $h(n)$ is zero for $n < 0$;
- *normalization*, which means that $\sum_{n=0}^{\infty} |h(n)| = 1$.

On this basis, we may refer to $h(n)$ as the *generating kernel* of the discrete-time memory.

The attributes of a memory structure are measured in terms of depth and resolution (deVries and Principe, 1992). Let $h_{\text{overall}}(n)$ denote the overall impulse response of the memory. With p memory sections, it follows that $h_{\text{overall}}(n)$ is defined by p successive convolutions of the impulse response $h(n)$. Accordingly, the *memory depth* D is defined as the *first time moment* of $h_{\text{overall}}(n)$, namely,

$$D = \sum_{n=0}^{\infty} n h_{\text{overall}}(n) \tag{4.153}$$

A memory of low depth D holds information content for a relatively short time interval, whereas a high-depth memory holds it much further into the past. *Memory resolution* R is defined as *the number of taps in the memory structure per unit of time.* A memory of high resolution is therefore able to hold information about the input sequence at a fine level, whereas a low-resolution memory can do so only at a coarser level. For a fixed memory order p, the product of memory depth D and memory resolution R is a constant that turns out to be equal to p.

Naturally, different choices of the generating kernel $h(n)$ result in different values for the depth D and memory resolution R, as illustrated by the following two memory structures:

1. *Tapped-delay-line memory*, for which the generating kernel is simply defined by the unit impulse $\delta(n)$; that is,

$$h(n) = \delta(n) = \begin{cases} 1, & n = 0 \\ 0, & n \neq 0 \end{cases} \tag{4.154}$$

Correspondingly, the overall impulse response is

$$h_{\text{overall}}(n) = \delta(n - p) = \begin{cases} 1, & n = p \\ 0, & n \neq p \end{cases} \tag{4.155}$$

Substituting Eq. (4.155) into Eq. (4.153) yields the memory depth $D = p$, which is intuitively satisfying. Moreover, since there is only one tap per time unit, it follows that the resolution $R = 1$, yielding a depth-resolution product equal to p.

2. *Gamma memory*, for which the generating kernel is defined by

$$h(n) = \mu(1 - \mu)^{n-1}, \qquad n \geq 1 \tag{4.156}$$

where μ is an adjustable parameter (deVries and Principe, 1992). For $h(n)$ to be convergent (i.e., for the short-term memory to be stable), we require that

$$0 < \mu < 2$$

Correspondingly, the overall impulse response of the gamma memory is

$$h_{\text{overall}}(n) = \binom{n-1}{p-1}\mu^p(1 - \mu)^{n-p}, \qquad n \geq p \tag{4.157}$$

where $\binom{\cdot}{\cdot}$ is a binomial coefficient. The impulse response $h_{\text{overall}}(n)$ for varying p represents a discrete version of the integrand of the gamma function (deVries and Principe, 1992)—hence the name "gamma memory." Figure 4.26 plots the impulse response $h_{\text{overall}}(n)$, normalized with respect to μ, for varying memory order $p = 1, 2, 3, 4$ and $\mu = 0.7$. Note also that the time axis has been scaled by the parameter μ, which has the effect of positioning the peak value of $h_{\text{overall}}(n)$ at $n = p - 1$.

It turns out that the depth of gamma memory is (p/μ) and the resolution is μ, again producing a depth-resolution product equal to p. Accordingly, by choosing μ to be less than unity, the gamma memory produces improvement in depth at the expense of resolution. For the special case of $\mu = 1$, the gamma memory reduces to an ordinary tapped-delay-line memory where each section consists simply of a unit-time delay operator.

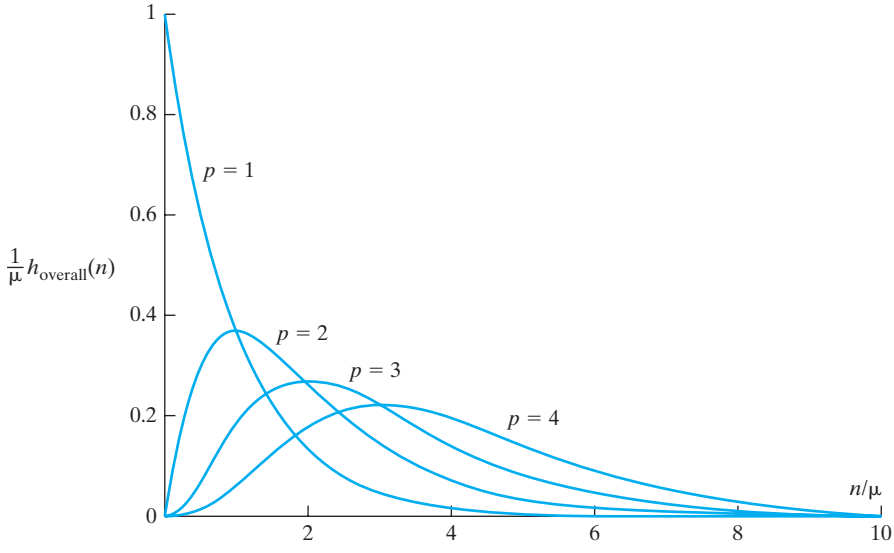

FIGURE 4.26 Family of impulse responses of the gamma memory for order $p = 1, 2, 3, 4$ and $\mu = 0.7$.

Universal Myopic Mapping Theorem

The nonlinear filter of Fig. 4.24 may be generalized to that shown in Fig. 4.27. This generic dynamic structure consists of two functional blocks. The block labeled $\{h_j\}_{j=1}^{L}$ represents *multiple convolutions* in the time domain, that is, a bank of *linear filters* operating in parallel. The h_j are drawn from a large set of real-valued kernels, each one of which represents the impulse response of a linear filter. The block labeled $\mathcal{N}$ represents a static (i.e., memoryless) nonlinear feedforward network such as the multilayer perceptron. The structure of Fig. 4.27 is a *universal dynamic mapper.* In Sandberg and Xu (1997a), it is shown that any shift-invariant *myopic map* can be uniformly approximated arbitrarily well by a structure of the form depicted in Fig. 4.27 under mild conditions. The requirement that a map be myopic is equivalent to "uniformly fading memory"; it is assumed here that the map is *causal*, which means that an output signal is produced by the map at time $n \geq 0$ only when the input signal is applied at time $n = 0$. By "shift invariant," we mean the following: If $y(n)$ is the output of the map generated by an input $x(n)$, then the output of the map generated by the shifted input $x(n - n_0)$ is $y(n - n_0)$, where the time shift n_0 is an integer. In Sandberg and Xu (1997b), it is further shown that for any single-variable, shift-invariant, causal, uniformly fading memory map, there is a gamma memory and static neural network, the combination of which approximates the map uniformly and arbitrarily well.

We may now formally state the *universal myopic mapping theorem*[15] as follows (Sandberg and Xu, 1997a, 1997b):

> *Any shift-invariant myopic dynamic map can be uniformly approximated arbitrarily well by a structure consisting of two functional blocks: a bank of linear filters feeding a static neural network.*

As already mentioned, a multilayer perceptron may serve the role of the static network. It is also noteworthy that this theorem holds when the input and output signals are functions of a finite number of variables, as in image processing, for example.

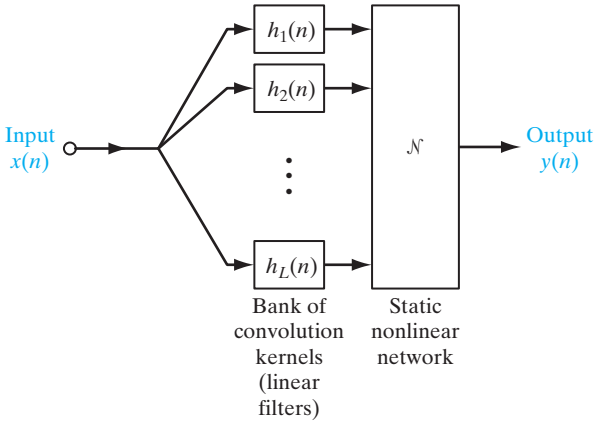

FIGURE 4.27 Generic structure for universal myopic mapping theorem.

Practical Implications of the Theorem

The universal myopic mapping theorem has profound practical implications:

1. The theorem provides justification for *NETtalk*, which was the first demonstration of a massively parallel distributed network that converts English speech to phonemes; a *phoneme* is a basic linguistic unit (Sejnowski and Rosenberg, 1987). Figure 4.28 shows a schematic diagram of the NETtalk system, based on a multilayer perceptron with an input layer of 203 sensory (source) nodes, a hidden layer of 80 neurons, and an output layer of 26 neurons. All the neurons used sigmoid (logistic) activation functions. The synaptic connections in the network were specified by a total of 18,629 weights, including a variable threshold for each neuron; threshold is the negative of bias. The standard back-propagation algorithm was used to train the network. The network had seven groups of nodes in the input layer, with each group encoding one letter of the input text. Strings of seven letters were thus presented to the input layer at any one time. The desired response for the training process was specified as the correct phoneme associated with the center (i.e., fourth) letter in the seven-letter window. The other six letters (three on either side of the center letter) provided a partial *context* for each decision made by the network. The text was stepped through the window on a letter-by-letter basis. At each step in the process, the network computed a phoneme, and after each word the synaptic weights of the network were adjusted according to how closely the computed pronunciation matched the correct one.

   The performance of NETtalk exhibited some similarities with observed human performance, as summarized here (Sejnowski and Rosenberg, 1987):

   - The training followed a power law.
   - The more words the network learned, the better it was at generalizing and correctly pronouncing new words.
   - The performance of the network degraded very slowly as synaptic connections in the network were purposely damaged.
   - Relearning after damage to the network was much faster than learning during the original training.

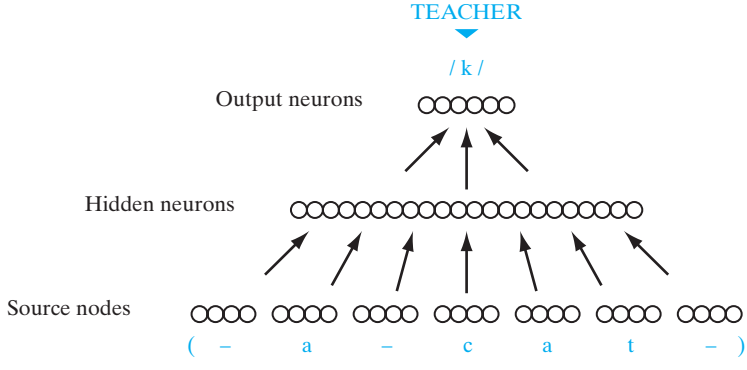

FIGURE 4.28 Schematic diagram of the NETtalk network architecture.

NETtalk was a brilliant illustration in miniature of many aspects of learning, starting out with considerable "innate" knowledge of its input patterns and then gradually acquiring competence at converting English speech to phonemes through practice.

2. The universal myopic theorem lays down the framework for the design of more elaborate models of nonlinear systems. The multiple convolutions at the front end of the structure in Fig. 4.27 may be implemented using linear filters with a finite-duration impulse response (FIR) or infinite-duration impulse response (IIR). Most importantly, the structure of Fig. 4.27 is *inherently stable*, provided that the linear filters are themselves stable. We thus have a clear-cut separation of roles as to how to take care of short-term memory and memoryless nonlinearity in building a stable dynamic system.
3. Given a stationary time series $x(1), x(2), ..., x(n)$, we may use the universal myopic mapping structure of Fig. 4.27 to build a predictive model of the underlying nonlinear physical laws responsible for generating the time series by setting $y(n) = x(n + 1)$, no matter how complex the laws are. In effect, the future sample $x(n + 1)$ plays the role of desired response. When a multilayer perceptron is used as the static network in Fig. 4.27 for such an application, it is advisable to provide a linear neuron for the output unit in the network. This provision will ensure that no amplitude limitation is placed on the dynamic range of the predictive model.

4.19 SMALL-SCALE VERSUS LARGE-SCALE LEARNING PROBLEMS

At various points along the way in this chapter and other parts of the book, we have made references to small-scale and large-scale learning problems. However, we did not elaborate rigorously on the meaning of these two kinds of supervised learning. The purpose of this section is to sharpen the statistical and computational issues that distinguish them from each other.

We begin the discussion with structural risk minimization (SRM), which is entirely statistical in nature; SRM is adequate for dealing with small-scale learning problems. Then we broaden the discussion by considering computational issues that assume a prominent role in dealing with large-scale learning problems.

Structural Risk Minimization

The feasibility of supervised learning depends on the following key question:

Does a training sample consisting of N independent and identically distributed examples

$$(\mathbf{x}_1, d_1), (\mathbf{x}_2, d_2), ..., (\mathbf{x}_N, d_N)$$

contain sufficient information to construct a learning machine capable of good generalization performance?

The answer to this fundamental question lies in the method of *structural risk minimization*, described by Vapnik (1982, 1998).

To describe what we mean by this method, let the natural source or environment responsible for generating the training sample be represented by the *nonlinear* regression model

$$d = f(\mathbf{x}) + \varepsilon \tag{4.158}$$

where, following the terminology introduced in Chapter 2, the vector $\mathbf{x}$ is the regressor, the scalar d is the response, and ε is the explanational (modeling) error. The function f is the unknown, and the objective is to estimate it. To do this estimation, we define the expected risk (i.e., the ensemble-averaged cost function) as

$$J_{\text{actual}}(f) = \mathbb{E}_{\mathbf{x},d}\left[\frac{1}{2}(d - f(\mathbf{x}))^2\right] \tag{4.159}$$

where the expectation is performed jointly with respect to the regressor–response pair $(\mathbf{x}, d)$. In Chapter 5, we will show that the *conditional mean estimator*

$$\hat{f}^* = \mathbb{E}[d|\mathbf{x}] \tag{4.160}$$

is the minimizer of the cost function $J_{\text{actual}}(f)$. Correspondingly, we write $J_{\text{actual}}(\hat{f}^*)$ as the minimum value of the cost function defined in Eq. (4.159); it serves as the *absolute optimum* that is achievable.

Determination of the conditional mean estimator $\hat{f}^*$ requires knowledge of the underlying joint probability distribution of the regressor $\mathbf{x}$ and the response d. Typically, however, we find that this knowledge is not available. To circumvent this difficulty, we look to machine learning for a viable solution. Suppose, for example, we choose a single-layer multilayer perceptron to do the machine learning. Let the function $F(\mathbf{x}; \mathbf{w})$ denote the input–output relationship of the neural network parameterized by the weight vector $\mathbf{w}$. We then make our *first approximation* by setting

$$f(\mathbf{x}) = F(\mathbf{x}; \mathbf{w}) \tag{4.161}$$

Correspondingly, we formulate the model's cost function as

$$J(\mathbf{w}) = \mathbb{E}_{\mathbf{x},d}\left[\frac{1}{2}(d - F(\mathbf{x}; \mathbf{w}))^2\right] \tag{4.162}$$

where, as before, the expectation is performed jointly with respect to the pair $(\mathbf{x}, d)$. This second cost function is naturally formulated differently from the cost function $J_{\text{actual}}(f)$ pertaining to the source—hence the use of different symbols for them. In imposing the equality of Eq. (4.161) on the neural network, we have in effect restricted the choice of the approximating function $F(\mathbf{x}; \mathbf{w})$.

Let

$$\hat{\mathbf{w}}^* = \arg\min_{\mathbf{w}} J(\mathbf{w}) \tag{4.163}$$

be the minimizer of the cost function $J(\mathbf{w})$. The reality, however, is that even if we can find the minimizer $\hat{\mathbf{w}}^*$, it is highly likely that the resulting cost function $J(\hat{\mathbf{w}}^*)$ will be worse than the minimized cost function $J_{\text{actual}}(\hat{f}^*)$. In any event, we cannot do better than $J_{\text{actual}}(\hat{f}^*)$, and thus we write

$$J(\hat{\mathbf{w}}^*) > J_{\text{actual}}(\hat{f}^*) \tag{4.164}$$

Unfortunately, we are still faced with the same practical problem as before in that we may not know the underlying joint probability distribution of the pair $(\mathbf{x}, d)$. To alleviate this difficulty, we make our *second approximation* by using the empirical risk (i.e., the time-averaged energy function)

$$\mathscr{E}_{\text{av}}(N; \mathbf{w}) = \frac{1}{2N} \sum_{n=1}^{N} (d(n) - F(\mathbf{x}(n); \mathbf{w}))^2 \tag{4.165}$$

whose minimizer is defined by

$$\hat{\mathbf{w}}_N = \arg\min_{\mathbf{w}} \mathscr{E}_{\text{av}}(N; \mathbf{w}) \tag{4.166}$$

Clearly, the minimized cost function $J(\hat{\mathbf{w}}_N)$ cannot be smaller than $J(\hat{\mathbf{w}}^*)$. Indeed, it is highly likely to find that

$$J(\hat{\mathbf{w}}_N) > J(\hat{\mathbf{w}}^*) > J_{\text{actual}}(\hat{f}^*) \tag{4.167}$$

With the two approximations that have been made, we may wonder why we should compute the minimum $\hat{\mathbf{w}}_N$ exactly. Before addressing this question, let us examine what happens when the example multilayer perceptron is changed by enlarging the size of the hidden layer.

From Section 4.12, we recall that the multilayer perceptron is a universal approximator of the unknown function $f(\mathbf{x})$. In theory, the parameterized function $F(\mathbf{x}; \mathbf{w})$ approximates the unknown function $f(\mathbf{x})$ with any desired accuracy provided that the size of the hidden layer is large enough. This, in turn, means that $J(\hat{\mathbf{w}}^*)$ becomes closer to the absolute optimum $J_{\text{actual}}(\hat{f}^*)$. However, by enlarging the size of the hidden layer, we may compromise the generalization capability of the multilayer perceptron. In particular, it is possible for the error $(J(\hat{\mathbf{w}}^*) - J_{\text{actual}}(\hat{f}^*))$ to increase as a result of enlarging the hidden layer, unless the size of the training sample, N, is correspondingly increased. The issue just discussed is the essence of Vapnik's *structural risk minimization*, which manifests itself in the "approximation–estimation trade-off."

To elaborate further on this trade-off, let the *excess error* $(J(\hat{\mathbf{w}}_N) - J_{\text{actual}}(\hat{f}^*))$ be decomposed into two terms as follows:

$$\underbrace{J(\hat{\mathbf{w}}_N) - J_{\text{actual}}(\hat{f}^*)}_{\text{Excess error}} = \underbrace{J(\hat{\mathbf{w}}_N) - J(\hat{\mathbf{w}}^*)}_{\text{Estimation error}} + \underbrace{J(\hat{\mathbf{w}}^*) - J_{\text{actual}}(\hat{f}^*)}_{\text{Approximation error}} \tag{4.168}$$

In this classical decomposition of errors, the following points are noteworthy:

(i) The *estimation error* provides a measure of how much performance is lost as a result of using a training sample of some prescribed size N. Moreover, with $\hat{\mathbf{w}}_N$ being dependent on the training sample, the approximation error is therefore relevant in the assessment of network training.

(ii) The *approximation error* provides a measure of how much performance is lost by choosing a model characterized by the approximating function $F(\mathbf{x}, \mathbf{w})$. Moreover, with $\hat{f}^*$ being a conditional estimator of the response d given the regressor $\mathbf{x}$, the estimation error is therefore relevant in the assessment of network testing.

In Vapnik's theoretical framework, the approximation and estimation errors are formulated in terms of the *VC dimension,* commonly denoted by h. This new parameter, short for the *Vapnik– Chervonenkis dimension* (Vapnik and Chervonenkis, 1971), is a measure of the *capacity*, or *expressive power*, of a family of binary classification functions realized by the learning machine.[16] For the example of a single-layer multilayer perceptron, the VC dimension is determined by the size of the hidden layer; the larger this size is, the larger the VC dimension h will be.

To put Vapnik's theory in a practical context, consider a family of *nested* approximating network functions denoted by

$$\mathcal{F}_k = \{F(\mathbf{x}; \mathbf{w})(\mathbf{w} \in \mathcal{W}_k)\}, \qquad k = 1, 2, ..., K \tag{4.169}$$

such that we have

$$\mathcal{F}_1 \subset \mathcal{F}_2 \subset \cdots \subset \mathcal{F}_K$$

where the symbol $\subset$ means "is contained in." Correspondingly, the VC dimensions of the individual subsets of $\mathcal{F}_K$ satisfy the condition

$$h_1 < h_2 < \cdots < h_K$$

In effect, the size of $\mathcal{F}_K$ is a measure of the machine capacity. Hereafter, we use the definition of Eq. (4.169) in place of the VC dimension.

Figure 4.29 plots variations of the approximation and estimation errors versus the size K of the family of approximating network functions $\mathcal{F}_K$. For the example of a single-layer multilayer perceptron, the optimum size of the hidden layer is determined by the point at which the approximation error and the estimation error assume a common value. Before the optimum condition is reached, the learning problem is *overdetermined*, which means that the machine capacity is too small for the amount of detail contained in the training sample. Beyond the minimum point, the learning problem is *underdetermined*, which means that the machine capacity is too large for the training sample.

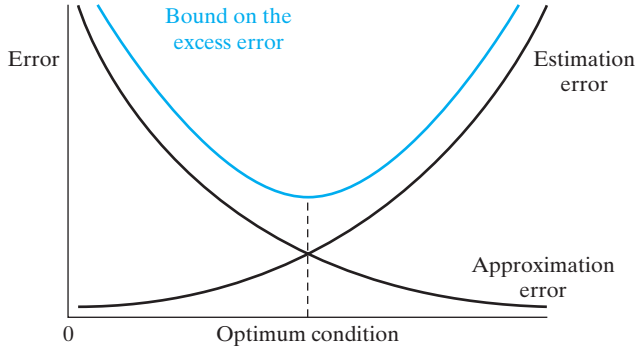

FIGURE 4.29 Variations of the approximation and estimation errors with the size K.

Computational Considerations

The neural network model (e.g., the single-layer multilayer perceptron) must be a *controlled variable*, so that it can be freely adjusted to achieve the best test performance on data not seen before. Another controlled variable is the number of examples to do the training. In order to add practical realism to the supervised-training process, Bottou (2007) has introduced the cost of computation by considering a new controlled variable: *optimization accuracy*.

In practice, it is possible to find that the task of computing the minimizer $\hat{\mathbf{w}}_N$ is rather *costly*. Moreover, in the course of coming up with a satisfactory network design, we usually make many approximations. Suppose, then, we settle on a network model characterized by the weight vector $\tilde{\mathbf{w}}_N$, which is different from $\hat{\mathbf{w}}_N$; in so doing, we will have made our *third*, *and final*, *approximation*. For example, the on-line learning algorithm could be stopped long before convergence has been reached, due to limited computing time. In any event, $\tilde{\mathbf{w}}_N$ is a suboptimal solution that satisfies the condition

$$\mathscr{E}_{\text{av}}(N; \tilde{\mathbf{w}}_N) \leq \mathscr{E}_{\text{av}}(N; \hat{\mathbf{w}}_N) + \rho \tag{4.170}$$

where ρ constitutes a new controlled variable; it provides a measure of *computational accuracy*.

In light of this new practicality, we now have a more complicated problem than that encountered in the method of structural risk minimization. Specifically, we must now adjust three variables:

- the network model (for instance, through the number of hidden neurons in a multilayer perceptron),
- the number of training examples, and
- the optimization accuracy (for instance by prematurely terminating computation of the minimizer $\hat{\mathbf{w}}_N$ and settling on the suboptimal solution $\tilde{\mathbf{w}}_N$).

In order to hit the best test performance, we have to satisfy *budget constraints*, which define the maximum number of training examples that we can use and the maximum computing time that we can afford. In a practical context, we are therefore confronted with a trade-off that is rather complicated. In solving this *constrained-optimization problem*, the trade-off will depend on whether we first hit a limit on the number of examples or impose a limit on the computing time. Which of these two limits is the active budget constraint depends on whether the supervised-learning process is of a small-scale or large-scale kind, as discussed next.

Definitions

According to Bottou (2007), small-scale and large-scale learning problems are respectively defined as follows:

Definition I. Small-scale learning

A supervised-learning problem is said to be of a small-scale kind when the *size of the training sample* (i.e., the number of examples) is the active budget constraint imposed on the learning process.

Definition II. Large-scale learning

A supervised-learning problem is said to be of a large-scale kind when the *computing time* is the active budget constraint imposed on the learning process.

In other words, it is the *active budget constraint* that distinguishes one learning problem from the other.

For an illustrative example of a small-scale learning problem, we may mention the design of an *adaptive equalizer*, the purpose of which is to compensate for the inevitable distortion of information-bearing data transmitted over a communication channel. The LMS algorithm, rooted in stochastic gradient descent and discussed in Chapter 3, is widely used for solving this on-line learning problem (Haykin, 2002).

For an illustrative example of a large-scale learning problem, we may mention the design of a check reader where the training examples consist of joint pairs, each of which describes a particular {*image*, *amount*} pair, where "image" pertains to a check and "amount" pertains to the amount of money inscribed in the check. Such a learning problem has strong structure that is complicated by the following issues (Bottou, 2007):

- field segmentation;
- character segmentation;
- character recognition;
- syntactical interpretation.

The *convolutional network*, embodying differentiable modules as described in Section 4.17 and trained with a stochastic gradient algorithm for a few weeks, is widely used for solving this challenging learning problem (LeCun et al., 1998). Indeed, this novel network has been deployed in industry since 1996, running billions of checks.

Small-Scale Learning Problems

Insofar as small-scale learning problems are concerned, there are three variables available to the designer of a learning machine:

- the number of training examples, N;
- the permissible size K of the family of approximating network functions $\mathcal{F}$;
- the computational error ρ introduced in Eq. (4.170).

With the active budget constraint being the number of examples, the design options in learning problems of the first kind are as follows (Bottou, 2007):

- Reduce the estimation error by making N as large as the budget permits.
- Reduce the optimization error by setting the computational error $\rho = 0$, which means setting $\tilde{\mathbf{w}}_N = \hat{\mathbf{w}}_N$.
- Adjust the size of $\mathcal{F}$ to the extent deemed to be reasonable.

With $\rho = 0$, the method of structural risk minimization, involving the approximation–estimation tradeoff illustrated in Fig. 4.29, is adequate for dealing with small-scale learning problems.

Large-Scale Learning Problems

As pointed out previously, the active budget constraint in large-scale learning problems is the computing time. In tackling learning problems of this second kind, we face *more complicated trade-offs* because we now have to account for the computing time T.

In large-scale learning problems, the excess error is defined by the difference $(J(\tilde{\mathbf{w}}_N) - J_{\text{actual}}(\hat{f}^*))$, which is decomposed into three terms, as shown by the following (Bottou, 2007):

$$\underbrace{J(\tilde{\mathbf{w}}_N) - J_{\text{actual}}(\hat{f}^*)}_{\text{Excess error}} = \underbrace{J(\tilde{\mathbf{w}}_N) - J(\hat{\mathbf{w}}_N)}_{\text{Optimization error}} + \underbrace{J(\hat{\mathbf{w}}_N) - J(\hat{\mathbf{w}}^*)}_{\text{Estimation error}} + \underbrace{J(\hat{\mathbf{w}}^*) - J_{\text{actual}}(\hat{f}^*)}_{\text{Approximation error}} \tag{4.171}$$

The last two terms, constituting the approximation and estimation errors, are common to both small-scale and large-scale learning problems. It is the first term in Eq. (4.171) that distinguishes large-scale learning problems from small-scale ones. This new term, called the *optimization error*, is obviously related to the computational error ρ.

Computation of the *bound* on the approximation error, depicted in Fig. 4.29, is reasonably well understood (in terms of the VC theory) for small-scale learning problems. Unfortunately, the constants involved in the formula for this bound are quite bad when the formula is applied to large-scale learning problems. In these more difficult situations, it is therefore more productive to analyze Eq. (4.171) in terms of convergence rates rather than bounds.

The requirement is to minimize the sum of the three terms in Eq. (4.171) by adjusting the available variables:

- the number of examples, N;
- the permissible size K of approximating network functions, $\mathcal{F}_K$;
- the computational error ρ, which is no longer zero.

Doing this minimization analytically is extremely difficult, due to the fact that the computing time T is actually dependent on all three variables N, $\mathcal{F}$, and ρ. To illustrate the consequences of this dependence, suppose we assign a small value to the error ρ so as to reduce the optimization error. To realize this reduction, unfortunately, we must also increase N, $\mathcal{F}$, or both, any of which would have undesirable effects on the approximation and estimation errors.

Nevertheless, in some cases, it is possible to compute the exponents with respect to which the three errors tend to decrease when ρ decreases and both $\mathcal{F}$ and N increase. Similarly, it is possible to identify the exponents with respect to which the computing time T increases when ρ decreases and both $\mathcal{F}$ and N increase. Putting these pieces together, we have the elements for an approximate solution to trade-offs in tackling large-scale

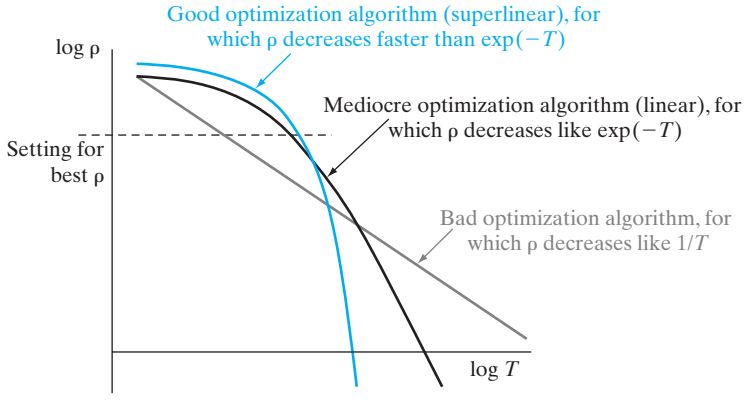

FIGURE 4.30 Variations of the computational error ρ versus the computation time T for three classes of optimization algorithm: bad, mediocre, and good. (This figure is reproduced with the permission of Dr. Leon Bottou.)

learning problems. Most importantly, in the final analysis, the trade-offs depend on the choice of the optimization algorithm.

Figure 4.30 illustrates how a plot of log ρ versus log T is affected by the type of optimization algorithm used to solve a large-scale learning problem. Three categories of optimization algorithms are identified in this figure—namely, *bad*, *mediocre*, and *good*—examples of which respectively include stochastic gradient descent (i.e., on-line learning), gradient descent (i.e., batch learning), and second-order gradient descent (e.g., quasi-Newton optimization algorithm of the BFGS kind or its extension). Table 4.4 summarizes the distinguishing features of these three categories of optimization algorithms.

TABLE 4.4 Summary of Statistical Characteristics of Three Optimization Algorithms*

Algorithm	Cost per iteration	Time to reach ρ
1. Stochastic gradient descent (on-line learning)	$O(m)$	$O\left(\frac{1}{\rho}\right)$
2. Gradient descent (batch learning)	$O(Nm)$	$O\left(\log\frac{1}{\rho}\right)$
3. Second-order gradient descent (on-line learning)	$O(m(m+N))$	$O\left(\log\left(\log\frac{1}{\rho}\right)\right)$

m : dimension of input vector $\mathbf{x}$
N : number of examples used in training
ρ : computational error

*This table is compiled from Bottou (2007).

The message to take from the material presented in this section on supervised learning may now be summed up as follows:

Whereas the study of small-scale learning problems is well-developed, the study of large-scale learning problems is in its early stages of development.

4.20 SUMMARY AND DISCUSSION

The back-propagation algorithm has established itself as a computationally efficient and useful algorithm for the training of multilayer perceptrons. The algorithm derives its name from the fact that the partial derivatives of the cost function (performance measure) with respect to the free parameters (synaptic weights and biases) of the network are determined by back-propagating the error signals (computed by the output neurons) through the network, layer by layer. In so doing, the algorithm solves the credit-assignment problem in a most elegant fashion. The computing power of the algorithm lies in its two main attributes:

- the *local* method, for updating the synaptic weights and biases of the multilayer perceptron;
- the *efficient* method, for computing *all* the partial derivatives of the cost function with respect to these free parameters.

Stochastic and Batch Methods of Training

For a given epoch of training data, the back-propagation algorithm operates in one of two modes: stochastic or batch. In the stochastic mode, the synaptic weights of all neurons in the network are adjusted in a sequential manner, pattern by pattern. Consequently, estimation of the gradient vector of the error surface used in the computation is stochastic in nature—hence the name "stochastic back-propagation learning." On the other hand, in the batch mode, the adjustments to all synaptic weights and biases are made on an epoch-by-epoch basis, with the result that a more accurate estimate of the gradient vector is utilized in the computation. Despite its disadvantages, the stochastic form of back-propagation learning is most frequently used for the training of multilayer perceptrons, particularly for large-scale problems. To achieve the best results, however, careful tuning of the algorithm is required.

Pattern Classification and Nonlinear Filtering

The specific details involved in the design of a multilayer perceptron naturally depend on the application of interest. We may, however, make two distinctions:

1. In pattern classification involving nonlinearly separable patterns, all the neurons in the network are *nonlinear*. The nonlinearity is achieved by employing a sigmoid function, two commonly used forms of which are (a) the logistic function, and (b) the hyperbolic tangent function. Each neuron is responsible for producing a hyperplane of

its own in decision space. Through a supervised learning process, the combination of hyperplanes formed by all the neurons in the network is iteratively adjusted in order to separate patterns drawn from the different classes and not seen before, with the fewest classification errors on average. For pattern classfication, the stochastic back-propagation algorithm is widely used to perform the training, particularly for large-scale problems (e.g., optical character recognition).

2. In nonlinear filtering, the *dynamic range* at the output of the multilayer perceptron should be sufficiently large to accommodate the process values; in this context, the use of linear output neurons is the most sensible choice. As for learning algorithms, we offer the following observations:

- On-line learning is much slower than batch learning.
- Assuming that batch learning is the desired choice, the standard back-propagation algorithm is slower than the conjugate gradient algorithm.

The method of nonlinear filtering, discussed in this chapter, focused on the use of a static network, exemplified by the multilayer perceptron; the input signal is applied to the multilayer perceptron through a short-term memory structure (e.g., tapped delay line or gamma filter) that provides for time, which is an essential dimension of filtering. In Chapter 15, we revisit the design of nonlinear filters for which feedback is applied to a multilayer perceptron, turning it into a recurrent neural network.

Small-scale versus Large-scale Learning Problems

Generally speaking, there are three kinds of error that can arise in the study of machine-learning problems:

1. *Approximation error*, which refers to the error incurred in the training of a neural network or learning machine, given a training sample of some finite size N.

2. *Estimation error*, which refers to the error incurred when the training of the machine is completed and its performance is tested using data not seen before; in effect, estimation error is another way of referring to generalization error.

3. *Optimization error*, the presence of which is attributed to accuracy of the computation involved in training the machine for some prescribed computing time T.

In small-scale learning problems, we find that the *active budget constraint* is the size of the training sample, which implicily means that the optimization error is usually zero in practice. Vapnik's theory of structural risk minimization is therefore adequately equipped to handle small-scale learning problems. On the other hand, in large-scale learning problems, the active budget constraint is the available computing time, T, with the result that the optimization error takes on a critical role of its own. In particular, computational accuracy of the learning process and therefore the optimization error are both strongly affected by the type of optimization algorithm employed to solve the learning problem.

NOTES AND REFERENCES

1. Sigmoid functions are "S" shaped graphs; Mennon et al. (1996) present a detailed study of two classes of sigmoids:
   - *simple sigmoids*, defined to be odd, asymptotically bounded, and completely monotone functions of one variable;
   - *hyperbolic sigmoids*, representing a proper subset of simple sigmoids and a natural generalization of the hyperbolic tangent function.
2. For the special case of the LMS algorithm, it has been shown that use of the momentum constant α reduces the stable range of the learning-rate parameter η and could thus lead to instability if η is not adjusted appropriately. Moreover, the misadjustment increases with increasing α; for details, see Roy and Shynk (1990).
3. A vector $\mathbf{w}^*$ is said to be a *local minimum* of an input—output function F if it is no worse than its *neighbors*—that is, if there exists an ε such that

$$F(\mathbf{w}^*) \leq F(\mathbf{w}) \qquad \text{for all } \mathbf{w} \text{ with } \|\mathbf{w} - \mathbf{w}^*\| < \varepsilon$$

   (Bertsekas, 1995). The vector $\mathbf{w}^*$ is said to be a *global minimum* of the function F if it is no worse than *all* other vectors—that is,

$$F(\mathbf{w}^*) \leq F(\mathbf{w}) \qquad \text{for all } \mathbf{w} \in \mathbb{R}^n$$

   where n is the dimension of $\mathbf{w}$.
4. The first documented description of the use of back propagation for efficient gradient evaluation is attributed to Werbos (1974). The material presented in Section 4.8 follows the treatment given in Saarinen et al. (1992); a more general discussion of the topic is presented by Werbos (1990).
5. Battiti (1992) presents a review of exact and approximate algorithms for computing the Hessian, with particular reference to neural networks.
6. Müller et al. (1998) have studied the application of the annealed on-line learning algorithm of Eq. (4.77) to a nonstationary blind source separation problem, which illustrates the broad algorithmic applicability of adaptive control of the learning rate due to Murata (1998). The issue of blind source separation is discussed in Chapter 10.
7. The formulation of Eq. (4.80) follows a corresponding part of the optimally annealed on-line learning algorithm due to Sompolinski et al. (1995) that deals with adaptation of the learning-rate parameter. Practical limitations of this algorithm include the need to compute the Hessian at each iteration and the need to know the minimal loss of the learning curve.
8. The universal approximation theorem may be viewed as a natural extension of the *Weierstrass theorem* (Weierstrass, 1885; Kline, 1972). This theorem states

   Any continuous function over a closed interval on the real axis can be expressed in that interval as an absolutely and uniformly convergent series of polynomials.

   Research interest in the virtues of multilayer perceptrons as devices for the representation of arbitrary continuous functions was perhaps first put into focus by Hecht-Nielsen (1987), who invoked an improved version of Kolomogorov's superposition theorem due to Sprecher (1965). Then, Gallant and White (1988) showed that a single-hidden-layer multilayer perceptron with monotone "cosine" squashing at the hidden layer and no squashing at the output behaves like as a special case of a "Fourier network"

that yields a Fourier series approximation to a given function as its output. However, in the context of traditional multilayer perceptrons, it was Cybenko who demonstrated rigorously for the first time that a single hidden layer is sufficient to uniformly approximate any continuous function with support in a unit hypercube; this work was published as a University of Illinois Technical Report in 1988 and republished as a paper one year later (Cybenko, 1988, 1989). In 1989, two other papers were published independently on multilayer perceptrons as universal approximators, one by Funahashi (1989) and the other by Hornik et al. (1990). For subsequent contributions to the approximation problem, see Light (1992b).

9. The history of the development of cross-validation is documented in Stone (1974). The idea of cross-validation had been around at least since the 1930s, but refinement of the technique was accomplished in the 1960s and 1970s. Two important papers from that era are by Stone (1974) and Geisser (1975), who independently and almost simultaneously propounded the idea of cross-validation. The technique was termed the "cross-validating method" by Stone and the "predictive sample reuse method" by Geisser.

10. Hecht-Nielsen (1995) decribes a replicator neural network in the form of a multilayer perceptron with an input layer of source nodes, three hidden layers and an output layer:

- The activation functions of neurons in the first and third hidden layers are defined by the hyperbolic tangent function

$$\varphi^{(1)}(v) = \varphi^{(3)}(v) = \tanh(v)$$

  where v is the induced local field of a neuron in those layers.
- The activation function for each neuron in the second hidden layer is given by

$$\varphi^{(2)}(v) = \frac{1}{2} + \frac{2}{2(N-1)} \sum_{j=1}^{N-1} \tanh\left(a\left(v - \frac{j}{N} \right) \right)$$

  where a is a gain parameter and v is the induced local filed of a neuron in that layer. The function $\varphi^{(2)}(v)$ describes a smooth staircase activation function with N treadles, thereby essentially quantizing the vector of the respective neural outputs into $K = N^n$, where n is the number of neurons in the middle hidden layer.
- The neurons in the output layer are linear, with their activation functions defined by

$$\varphi^{(4)}(v) = v$$

- Based on this neural network structure, Hecht-Nielsen describes a theorem showing that optimal data compression for arbitrary input data vector can be carried out.

11. The classic reference for the conjugate-gradient method is Hestenes and Stiefel (1952). For a discussion of the convergence behavior of the conjugate-gradient algorithm, see Luenberger (1984) and Bertsekas (1995). For a tutorial treatment of the many facets of the conjugate-gradient algorithm, see Shewchuk (1994). For a readable account of the algorithm in the context of neural networks, see Johansson et al. (1990).

12. The conventional form of the conjugate-gradient algorithm requires the use of a line search, which can be time consuming because of its trial-and-error nature. Møller (1993) describes a modified version of the conjugate-gradient algorithm called the scaled conjugate-gradient algorithm, which avoids the use of a line search. Essentially, the line search is replaced by a one-dimensional Levenberg–Marquardt form of algorithm. The motivation for using such methods is to circumvent the difficulty caused by nonpositive-definite Hessian matrices (Fletcher, 1987).

13. The so-called *$\mathcal{R}$-technique*, due to Pearlmutter (1994), provides an efficient procedure for computing a matrix-vector product; as such, this technique can be of practical use in computing the inverse Hessian $\mathbf{H}^{-1}$ in Eq. (4.138). The $\mathcal{R}$-technique is addressed in Problem 4.6.

14. Hubel and Wiesel's notion of "simple" and "complex" cells was first exploited in the neural network literature by Fukushima (1980, 1995) in the design of a learning machine called the *neocognitron*. This learning machine, however, operates in a self-organized manner, whereas the convolutional network described in Fig. 4.23 operates in a supervised manner using labeled examples.

15. For the origins of the universal myopic mapping theorem, see Sandberg (1991).

16. For a detailed account of the VC-dimension and the related bound on empirical risk, see the classic book on statistical learning theory by Vapnik (1998). The VC-dimension is also discussed in the books by Schölkopf and Smola (2002) and Herbrich (2002). A noteworthy comment is in order: the VC-dimension is related to Cover's separating capacity, which will be discussed in the next chapter, Chapter 5.

PROBLEMS

Back-Propagation Learning

4.1 Figure P4.1 shows a neural network involving a single hidden neuron for solving the XOR problem; this network may be viewed as an alternative to that considered in Section 4.5. Show that the network of Fig. P4.1 solves the XOR problem by constucting (a) decision regions, and (b) a truth table for the network.

4.2 Use the back-propagation algorithm for computing a set of synaptic weights and bias levels for a neural network structured as in Fig. 4.8 to solve the XOR problem. Assume the use of a logistic function for the nonlinearity.

4.3 The momentum constant α is normally assigned a positive value in the range $0 < \alpha \leq 1$. Investigate the difference that would be made in the behavior of Eq. (4.43) with respect to time t if α were assigned a negative value in the range $-1 \leq \alpha < 0$.

4.4 Consider the simple example of a network involving a single weight, for which the cost function is

$$\mathcal{E}(w) = k_1(w - w_0)^2 + k_2$$

where w_0, k_1, and k_2 are constants. A back-propagation algorithm with momentum α is used to minimize $\mathcal{E}(w)$.

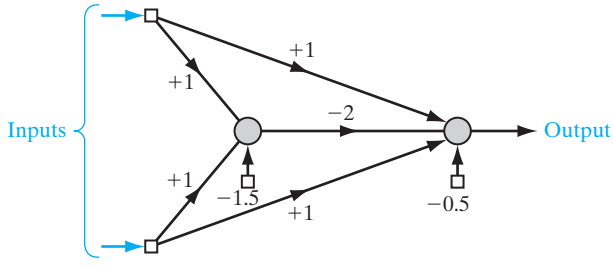

FIGURE P4.1

Explore the way in which the inclusion of the momentum constant α influences the learning process, with particular reference to the number of steps required for convergence versus α.

4.5 Equations (4.51) through (4.53) define the partial derivatives of the approximating function $F(\mathbf{w}, \mathbf{x})$ realized by the multilayer perceptron in Fig. 4.14. Derive these equations from the scenario described by the following conditions:

(a) *Cost function:*

$$\mathscr{E}(n) = \frac{1}{2}[d - F(\mathbf{w}, \mathbf{x})]^2$$

(b) *Output of neuron j:*

$$y_j = \varphi\left(\sum_i w_{ji}\, y_i\right)$$

where w_{ji} is the synaptic weight from neuron i to neuron j, and y_i is the output of neuron i;

(c) *Nonlinearity:*

$$\varphi(v) = \frac{1}{1 + \exp(-v)}$$

4.6 The $\mathscr{R}$ *technique*, developed by Pearlmutter (1994), provides a computationally fast procedure for evaluating a matrix–vector product. To illustrate this procedure, consider a multilayer perceptron with a single hidden layer; the forward-propagation equations of the network are defined by

$$\begin{aligned} v_j &= \sum_i w_{ji} x_i \\ z_j &= \varphi(v_j) \\ y_k &= \sum_j w_{kj} z_j \end{aligned}$$

$\mathscr{R}[\cdot]$ denotes an *operator* that acts on the quantity enclosed inside the brackets to produce the following results for the example network at hand:

$$\mathscr{R}[v_j] = \sum_i a_{ji} x_i, \qquad \mathscr{R}[w_{ji}] = a_{ji}$$

$$\mathscr{R}[v_j] = \varphi'(v_j)\mathscr{R}[v_j], \qquad \varphi'(v_j) = \frac{\partial}{\partial v_j}\varphi(v_j)$$

$$\mathscr{R}[y_k] = \sum_j w_{kj}\mathscr{R}[z_j] + \sum_i a_{ji} z_j, \qquad \mathscr{R}[w_{kj}] = a_{kj}$$

The $\mathscr{R}$ results are to be viewed as *new* variables. In effect, the operator $\mathscr{R}[\cdot]$ follows the ordinary rules of calculus in addition to the condition

$$\mathscr{R}[\mathbf{w}_j] = \mathbf{a}_j$$

where $\mathbf{w}_j$ is the vector of weights connected to node j and $\mathbf{a}_j$ is the associated vector resulting from application of the $\mathscr{R}$ operator.

(a) Applying the $\mathcal{R}$ technique to the back-propagation algorithm, derive expressions for the elements of the matrix–vector product **Ha**, identifying the new variables for the hidden and output neurons, the matrix **H** is the Hessian. For this application, use the multilayer perceptron described at the beginning of the problem.

(b) Justify the statement that the $\mathcal{R}$ technique is computationally fast.

Supervised Learning Issues

4.7 In this problem, we study the output representation and decision rule performed by a multilayer perceptron. In theory, for an M-class *classification problem* in which the union of the M distinct classes forms the entire input space, we need a total of M outputs to represent all possible classification decisions, as depicted in Fig. P4.7. In this figure, the vector $\mathbf{x}_j$ denotes the jth *prototype* (i.e., unique sample) of an m-dimensional random vector $\mathbf{x}$ to be classified by a multilayer perceptron. The kth of M possible classes to which $\mathbf{x}$ can belong is denoted by $\mathscr{C}_k$. Let y_{kj} be the kth output of the network produced in response to the prototype $\mathbf{x}_j$, as shown by

$$y_{kj} = F_k(\mathbf{x}_j), \qquad k = 1, 2, ..., M$$

where the function $F_k(\cdot)$ defines the mapping learned by the network from the input to the k-th output. For convenience of presentation, let

$$\begin{aligned}\mathbf{y}_j &= [y_{1j}, y_{2j}, ..., y_{Mj}]^T \\ &= [F_1(\mathbf{x}_j),\ F_2(\mathbf{x}_j), ..., F_M(\mathbf{x}_j)]^T \\ &= \mathbf{F}(\mathbf{x}_j)\end{aligned}$$

where $\mathbf{F}(\cdot)$ is a vector-valued function. The basic question we wish to address in this problem is the following:

> After a multilayer perceptron is trained, what should the optimum decision rule be for classifying the M outputs of the network?

To address this problem, consider the use of a multilayer perceptron embodying a logistic function for its hidden neurons and operating under the following assumptions:

- The size of the training sample is sufficiently large to make a reasonably accurate estimate of the probability of correct classification.
- The back-propagation algorithm used to train the multilayer perceptron does not get stuck in a local minimum.

Specifically, develop mathematical arguments for the property that the M outputs of the multilayer perceptron provide estimates of the a posteriori class probabilities.

4.8 In this problem, we revisit the adaptive control of the learning rate discussed in Section 4.10. The issue of interest is to demonstrate that the asymptotic behavior of the learning-rate parameter $\eta(n)$ in Eq. (4.85) does not converge to zero as the number of iterations increases to infinity.

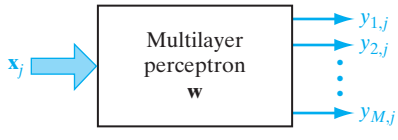

FIGURE P4.7 Block diagram of a pattern classifier for Problem 4.7.

(a) Let $\bar{\mathbf{r}}(n)$ denote the expectation of the auxiliary vector $\mathbf{r}(n)$ with respect to the example $\{\mathbf{x}, \mathbf{d}\}$. Show that if the estimator $\hat{\mathbf{w}}(n)$ is in the close vicinity of the optimal estimator $\mathbf{w}^*$, we may then write

$$\bar{\mathbf{r}}(n+1) \approx (1-\delta)\,\bar{\mathbf{r}}(n) + \delta \mathbf{K}^*(\hat{\mathbf{w}}(n) - \bar{\mathbf{w}}(n))$$

where $\bar{\mathbf{w}}(n)$ is the mean value of the estimator $\hat{\mathbf{w}}(n)$ and δ is a small positive parameter.

(b) In Heskas and Kappen (1991), it is shown that the estimator $\hat{\mathbf{w}}(n)$ is closely approximated by a Gaussian-distributed random vector. Hence, justify the following asymptotic behavior:

$$\lim_{n\to\infty} \hat{\mathbf{w}}(n) \neq \tilde{\mathbf{w}}(n)$$

What does this condition teach us about the asymptotic behavior of the learning-rate parameter $\eta(n)$?

4.9 The composition of the *minimum-description-length (MDL) criterion* is described as follows (see Eq. (2.37)):

$$\text{MDL} = (\text{Error term}) + (\text{Complexity term})$$

Discuss how the weight-decay method used for network pruning fits into the MDL formalism.

4.10 In the *optimal-brain-damage (OBD)* algorithm for network pruning, due to LeCun et al. (1990b), the Hessian $\mathbf{H}$ is approximated by its diagonal version. Using this approximation, derive the OBD procedure as a special case of the optimal-brain-surgeon (OBS) algorithm, studied in Section 4.14.

4.11 In Jacobs (1988), the following heuristics are proposed to accelerate the convergence of on-line back-propagation learning:

(i) Every adjustable network parameter of the cost function should have its own learning-rate parameter.

(ii) Every learning-rate parameter should be allowed to vary from one iteration to the next.

(iii) When the derivative of the cost function with respect to a synaptic weight has the same algebraic sign for several consecutive iterations of the algorithm, the learning-rate parameter for that particular weight should be increased.

(iv) When the algebraic sign of the cost function with respect to a particular synaptic weight alternates for several consecutive iterations of the algorithm, the learning-rate parameter for that weight should be decreased.

These four heuristics satisfy the locality constraint of the back-propagation algorithm.

(a) Use intuitive arguments to justify these four heuristics.

(b) The inclusion of a momentum in the weight update of the back-propagation algorithm may be viewed as a mechanism for satisfying heuristics (iii) and (iv). Demonstrate the validity of this statement.

Second-Order Optimization Methods

4.12 The use of a momentum term in the weight update described in Eq. (4.41) may be considered as an approximation to the conjugate-gradient method (Battiti, 1992). Discuss the validity of this statement.

4.13 Starting with the formula for $\beta(n)$ in Eq. (4.127), derive the *Hesteness-Stiefel formula*,

$$\beta(n) = \frac{\mathbf{r}^T(n)(\mathbf{r}(n) - \mathbf{r}(n-1))}{\mathbf{s}^T(n-1)\mathbf{r}(n-1)}$$

where $\mathbf{s}(n)$ is the direction vector and $\mathbf{r}(n)$ is the residual in the conjugate-gradient method. Use this result to derive the Polak–Ribière formula of Eq. (4.128) and the Fletcher–Reeves formula of Eq. (4.129).

Temporal Processing

4.14 Figure P4.14 illustrates the use of a *Gaussian-shaped time window* as a method for temporal processing, which is motivated by neurobiological considerations (Bodenhausen and Waibel, 1991). The time window associated with synapse i of neuron j is denoted by $\theta(n, \tau_{ji}, \sigma_{ji})$, where τ_{ji} and σ_{ji} are measures of *time delay* and *width* of the windows, respectively, as shown by

$$\theta(n, \tau_{ji}, \sigma_{ji}) = \frac{1}{\sqrt{2\pi}\sigma_{ji}} \exp\left(-\frac{1}{2\sigma_{ji}^2}(n - \tau_{ji})^2\right), \quad i = 1, 2, ..., m_0$$

The output of neuron j is thus defined as

$$y_j(n) = \varphi\left(\sum_{i=1}^{m_0} w_{ji} u_i(n)\right)$$

where $u_i(n)$ is the convolution of the input $x_i(n)$ and the time window $\theta(n, \tau_{ji}, \sigma_{ji})$. The requirement is for the weight w_{ji}, and time delay τ_{ji} of synapse i belonging to neuron j are all to be *learned* in a supervised manner.

This process of learning may be accomplished by using the standard back-propagation algorithm. Demonstrate this learning process by deriving update equations for w_{ji}, τ_{ji}, and σ_{ji}.

Computer Experiments

4.15 Investigate the use of back-propagation learning employing a sigmoidal nonlinearity to achieve one-to-one mappings, as described here:

1. $f(x) = \dfrac{1}{x}, \qquad 1 \le x \le 100$
2. $f(x) = \log_{10} x, \qquad 1 \le x \le 10$
3. $f(x) = \exp(-x), \qquad 1 \le x \le 10$
4. $f(x) = \sin x, \qquad 0 \le x \le \dfrac{\pi}{2}$

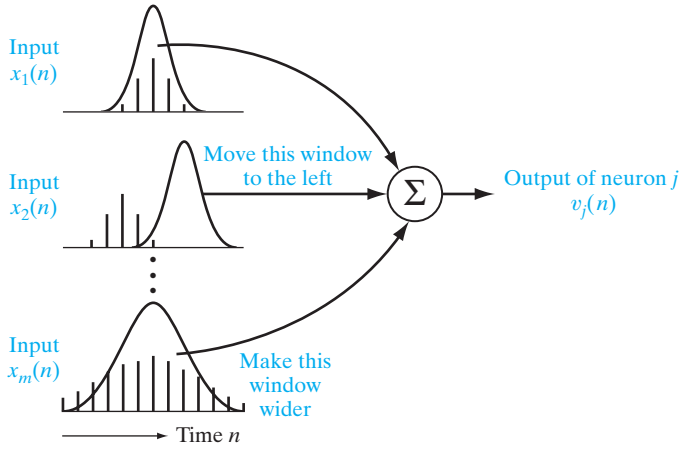

FIGURE P4.14 The figure for Problem 4.14; the instructions appended to the Gaussian windows are aimed at the learning algorithm.

For each mapping, do the following:

(a) Set up two sets of data, one for network training, and the other for testing.
(b) Use the training data set to compute the synaptic weights of the network, assumed to have a single hidden layer.
(c) Evaluate the computation accuracy of the network by using the test data.

Use a single hidden layer, but with a variable number of hidden neurons. Investigate how the network performance is affected by varying the size of the hidden layer.

4.16 Repeat the computer experiment of Section 4.7 for the MLP classifier, where the distance between the two moons is set at $d = 0$. Comment on the findings of your experiment in light of the corresponding experiment performed on the perceptron in Problem 1.6 for the same setting.

4.17 In this computer experiment, we consider a pattern-classification experiment for which the decision boundary is theoretically known. The primary objective of the experiment is to see how the design of the multilayer perceptron could be optimized experimentally in relation to the optimum decision boundary.

Specifically, the requirement is to distinguish between two *equiprobable* classes of "overlapping" two-dimensional Gaussian-distributed patterns, labeled $\mathscr{C}_1$ and $\mathscr{C}_2$. The conditional probability density functions of the two classes are

Class $\mathscr{C}_1$: $$p_{\mathbf{X}|\mathscr{C}_1}(\mathbf{x}|\mathscr{C}_1) = \frac{1}{2\pi\sigma_1^2}\exp\left(-\frac{1}{2\sigma_1^2}\|\mathbf{x}-\boldsymbol{\mu}_1\|^2\right)$$

where

$\boldsymbol{\mu}_1 = \text{mean vector} = [0, 0]^T$

$\sigma_1^2 = \text{variance} = 1$

Class $\mathscr{C}_2$: $$p_{\mathbf{X}|\mathscr{C}_2}(\mathbf{x}|\mathscr{C}_2) = \frac{1}{2\pi\sigma_2^2}\exp\left(-\frac{1}{2\sigma_2^2}\|\mathbf{x}-\boldsymbol{\mu}_2\|^2\right)$$

where

$\boldsymbol{\mu}_2 = [2, 0]^T$

$\sigma_2^2 = 4$

(a) The optimum Bayesian decision boundary is defined by the likelihood ratio test

$$\Lambda(\mathbf{x}) \underset{\mathscr{C}_2}{\overset{\mathscr{C}_1}{\gtrless}} \lambda$$

where

$$\Lambda(\mathbf{x}) = \frac{p_{\mathbf{X}|\mathscr{C}_1}(\mathbf{x}|\mathscr{C}_1)}{p_{\mathbf{X}|\mathscr{C}_2}(\mathbf{x}|\mathscr{C}_2)}$$

and λ is the *threshold* determined by the prior probabilities of the two classes. Show that the optimum decision boundary is a *circle* whose center is located at

$$\mathbf{x}_{\mathscr{C}} = \begin{bmatrix} -2/3 \\ 0 \end{bmatrix}$$

and radius $r = 2.34$.

(b) Assume the use of a single hidden layer. The requirement is to experimentally determine the optimal number of hidden neurons.

- Starting with a multilayer perceptron with two hidden neurons, and using the back-propagation algorithm with learning-rate parameter $\eta = 0.1$ and momentum constant $\alpha = 0$ to train the network, calculate the probability of correct classification for the following scenarios:

Training-sample size	Number of epochs
500	320
2,000	80
8,000	20

- Repeat the experiment, this time using four hidden neurons, with everything else remaining the same as before. Compare the results of this second experiment with those of the previous one and thereby select the network configuration, with two *or* four hidden neurons, that you consider to be the optimal choice.

(c) For the "optimal" network selection made in part (b), we now turn to experimentally find the optimal values of the learning-rate parameter η and momentum constant α. To do this, perform experiments using the following combination of parameters:

$$\eta \in [0.01, 0.1, 0.5]$$
$$\alpha \in [0.0, 0.1, 0.5]$$

Hence, determine the values of η and α that yield the best probability of correct classification.

(d) Having identified the optimum size of hidden layer and the optimum set of η and α, perform one last experiment to find the optimum decision boundary and the corresponding probability of correct classification. Compare the optimum performance so obtained experimentally against the theoretical optimum, and comment on your results.

4.18 In this problem, we use the standard back-propagation algorithm to solve a difficult nonlinear prediction problem and compare its performance with that of the LMS algorithm. The time series to be considered is created using a discrete *Volterra model* that has the form

$$x(n) = \sum_i g_i v(n-i) + \sum_i \sum_j g_{ij} v(n-i)v(n-j) + \cdots$$

where $g_i, g_{ij}, \ldots$, are the Volterra coefficients; the $v(n)$ are samples of a white, independently distributed Gaussian noise sequence; and $x(n)$ is the resulting output of the Volterra model. The first summation term is the familiar moving-average (MA) time-series model, and the remaining summation terms are nonlinear components of ever increasing order. In general, the estimation of the Volterra coefficients is considered to be difficult, primarily because of their nonlinear relationship to the data.

We consider the simple example

$$x(n) = v(n) + \beta v(n-1)v(n-2)$$

The time series has zero mean, is uncorrelated, and therefore has a white spectrum. However, the time-series samples are not independent of each other, and therefore a higher-order predictor can be constructed. The variance of the model output is given by

$$\sigma_x^2 = \sigma_\nu^2 + \beta^2\sigma_\nu^4$$

where σ_ν^2 is the white-noise variance.

(a) Construct a multilayer perceptron with an input layer of six nodes, a hidden layer of 16 neurons, and a single output neuron. A tapped-delay-line memory is used to feed the input layer of the network. The hidden neurons use sigmoid activation functions limited to the interval [0, 1], whereas the output neuron operates as a linear combiner. The network is trained with the standard back-propagation algorithm having the following description:

Learning-rate parameter	$\eta = 0.001$
Momentum constant	$\alpha = 0.6$
Total number of samples processed	100,000
Number of samples per epoch	1,000
Total number of epochs	2,500

The white-noise variance σ_ν^2 is set equal to unity. Hence, with $\beta = 0.5$, we find that the output variance of the predictor is $\sigma_x^2 = 1.25$.

Compute the learning curve of the nonlinear predictor, with the variance of the predictor output $x(n)$ plotted as a function of the number of epochs of training samples up to 2,500 epochs. For the preparation of each epoch used to perform the training, explore the following two modes:

(i) The time ordering of the training sample is maintained from one epoch to the next in exactly the same form as it is generated.

(ii) The ordering of the training sample is randomized from one pattern (state) to another.

Also, use cross-validation (described in Section 4.13) with a validation set of 1,000 samples to monitor the learning behavior of the predictor.

(b) Repeat the experiment, using the LMS algorithm designed to perform a linear prediction on an input of six samples. The learning-rate parameter of the algorithm is set equal to $\eta = 10^{-5}$.

(c) Repeat the entire experiment for $\beta = 1, \sigma_\nu^2 = 2$, and then for $\beta = 2, \sigma_\nu^2 = 5$.

The results of each experiment should reveal that initially the back-propagation algorithm and the LMS algorithm follow essentially a similar path, and then the back-propagation algorithm continues to improve, finally producing a prediction variance approaching the prescribed value of σ_x^2.

4.19 In this experiment, we use a multilayer perceptron trained with the back-propagation algorithm to perform one-step prediction on the *Lorenz attractor*. The dynamics of this attractor are defined by three equations:

$$\frac{dx(t)}{dt} = -\sigma x(t) + \sigma y(t)$$

$$\frac{dy(t)}{dt} = -x(t)z(t) + rx(t) - y(t)$$

$$\frac{dz(t)}{dt} = x(t)y(t) - bz(t)$$

where σ, r, and b are dimensionless parameters. Typical values for these parameters are $\sigma = 10, b = \frac{8}{3}$, and $r = 28$.

The specifications of the multilayer perceptron are as follows:

Number of source nodes: 20
Number of hidden neurons: 200
Number of output neurons: 1

The particulars of the data sets are as follows:

Training sample: 700 data points
Testing sample: 800 data points
Number of epochs used for training: 50

The parameters of the back-propagation algorithm are as follows:

The learning-rate parameter η is annealed linearly from 10^{-1} down to 10^{-5}.
Momentum: $\alpha = 0$

(a) Compute the learning curve of the MLP, plotting the mean-square error versus the number of epochs used to do the training.

(b) Compute the one-step prediction to the Lorenz attractor; specifically, plot the results obtained as a function of time, and compare the prediction against the evolution of the Lorenz attractor.